Synthesis and Characterization of High Performance Polymers for Gas Separation Membranes

Hailun Borjigin

Dissertation submitted to the Faculty of Virginia Polytechnic Institute and State University in partial fulfillment of the requirements for the degree of
DOCTOR OF PHILOSOPHY
In
Macromolecular Science and Engineering

James E. McGrath, Chair
Judy S. Riffle, Co-Chair
S. Richard Turner
Richey M. Davis
Alan R. Esker
Sue J. Mecham

05/05/2015
Blacksburg, VA

Keyword: Gas Separation Membrane, Thermally Rearranged Polymers, Polybenzimidazoles

Synthesis and Characterization of High Performance Polymers for Gas Separation Membranes

Hailun Borjigin

ABSTRACT

Macromolecules and Interfaces Institute,
Virginia Polytechnic Institute and State University,
Blacksburg, VA 24061, USA

This dissertation focuses on the synthesis and characterization of high performance polymers, especially polyimides, polybenzoxazoles and polybenzimidazoles for gas separation applications. An abundance of monomers and novel polymers were synthesized and fabricated into membranes.

Thermally rearranged polybenzoxazoles and their precursor polyimides were systematically studied with regard to size of pendant functional groups, thermal rearrangement conversion, and relationship of backbone structure/gas transport properties. 3,3'-Diamino-4,4'-dihydroxybiphenyl was synthesized using an economical route. *Meta* and *para* oriented polyimides with different *ortho*-functionality were synthesized and these polymers were thermally rearranged into polybenzoxazoles. The polar hydroxyl functional groups on the polyimide backbone diminished the *meta/para* isomer effect of the permeability coefficients of the polymers and only a small difference between *meta*- and *para*-oriented polyhydroxyimides in permeability coefficients was observed. The TR polybenzoxazoles derived from *meta/para*-oriented isomeric polyimides with *ortho* functionality had similar gas separation properties, especially for CO_2/CH_4 separation, and it is hypothesized that this is due to a lack of intersegmental mobility distinction between the two isomeric TR polymers. The TR polymers derived from the polyimides with acetate *ortho*-functional groups had

significantly better gas separation properties than ones derived from the precursor with hydroxyl *ortho*-functional groups.

Polybenzimidazoles were also investigated for use as gas separation membranes. Polybenzimidazoles are some of the most thermally stable polymers. However, commercial polybenzimidazoles do not have good solubility in common solvents. The solubility issue was solved by incorporating sulfonyl linkages into the polybenzimidazole backbone using a 3,3',4,4'-tetraaminodiphenylsulfone (TADPS) monomer. 3,3',4,4'-Tetraaminodiphenylsulfone was synthesized by a novel route with higher overall yield and less steps than the traditional synthetic method. The TADPS based polybenzimidazoles also demonstrated better thermal stability than commercial polybenzimidazole. The meta/para oriented isomer effect on gas transport properties is discussed. TADPS-based polybenzimidazoles exhibited H_2/CO_2 gas separation properties near or surpassing the upper bound with H_2 permeabilities from 3.6 to 5.7 Barrer and selectivities from 10.1 to 32.2 at 35 °C.

Acknowledgement

First of all, I would like to express my greatest appreciation to my late advisor Jim E. McGrath, a great scientist, professor, and friend. He not only led me into the world of polymer science but also inspired me to see and think like a scientist. I am so proud to have had such a prominent figure in polymer science as my advisor. His kindness, generosity, and guidance for his students will be always missed.

I would like to give my warmest gratitude to Judy S. Riffle who is among the finest examples of an outstanding advisor. I appreciate what she has done for me and the rest of the students from the McGrath group. Her guidance, understanding, kindness, and generosity helped me enormously to finish my education at Virginia Tech. I really enjoyed the time I worked for her. I am thankful for the rest of my committee members, Dr. S. Richard Turner, Dr. Sue Mecham, Dr. Allen Esker, and Dr. Richey Davis who have been valuable and constantly gave me their advice and support. Though not a member of my committee, I'm very thankful to Dr. Benny D. Freeman of the University of Texas-Austin for his collaboration with our research group and contribution of transport results.

The completion of my work at Virginia Tech wouldn't have been possible without the diligent work of the administrative staff in the Macromolecules and Interfaces Institute. I want to especially thank Laurie Good, Cyndy Graham, and Tammy Jo Hiner for their help in organizing and scheduling my research progress and academic requirements for my PhD degree. I would like to thank Dr. Benjamin Sundell, Dr. Jarrett Rowlett, Dr. Ali Nebipasagil, Kyle Gaines, Qiang Liu, Kevin Stevens, Wenrui Zhang, Andy Shaver, Ran Liu and the rest of the members of the McGrath/Riffle group for giving research suggestions and scientific discussion. Without your help, I wouldn't have achieved this accomplishment. I also would like to thank those of you who went

to the gym with me, played basketball with me, and spent their spare time with me though my entire graduate student life at Virginia Tech.

I would like to gratefully acknowledge the Macromolecules and Interfaces Institute and the National Science Foundation under grant numbers DMR-1126564 and AIR-1237857 which supported my graduate study at Virginia Tech.

I am really lucky to have a very supportive family including my parents Qimusurong and Shandan who are always understanding and forgiving; my brother, sister-in-law, little niece, who are always supportive and happy for what I accomplished, and my parents-in-law who are always helping me, supporting me, and understanding me. Finally, I want to say thank you to my wife and best friend, Shiqi. Thanks for her companionship no matter how depressed or excited I am. Without her I would be like a bird without wings. I am so fortunate that I met her, got to know her, and married her.

ATTRIBUTION

Chapter 3: Synthesis and Characterization of Thermally Rearranged (TR) Polymers: influence of isomeric effects on gas transport properties. Chapter 3 was submitted to Polymer.

Article in press in Polymer

Qiang Liu, B.S. (Department of Chemical Engineering) is currently a Ph.D. candidate at the University of Texas at Austin. Mr. Liu was a co-author on this paper and contributed to the gas transport property testing of the thermally rearranged polymer films.

Wenrui Zhang, B.S. (Department of Macromolecular Science and Engineering) is currently a graduate student at Virginia Tech. Mr. Zhang was a co-author on this paper and performed the initial monomer synthesis and characterization.

Kyle Gaines, B.S. (Department of Macromolecular Science and Engineering) is currently a Ph.D. candidate at Virginia Tech. Mr. Gaines was a co-author on this paper and assisted in the initial polymer synthesis.

Judy S. Riffle, Ph.D. (Department of Macromolecular Science and Engineering) was a professor at Virginia Tech. Dr. Riffle was a co-author on this paper, co-principal investigator for the grant supporting this research and contributed revisions to the final document.

Donald R. Paul, Ph.D. (Department of Chemical Engineering) is currently a professor at the University of Texas at Austin. Dr. Paul was a co-author on this paper, co-principal investigator for one of the grants supporting this research and contributed revisions to the final document.

Benny D. Freeman, Ph.D. (Department of Chemical Engineering) is currently a professor at the University of Texas at Austin. Dr. Freeman was a co-author on this paper, co-principal investigator for one of the grants supporting this research and contributed revisions to the final document.

James E. McGrath, Ph.D. (Department of Macromolecular Science and Engineering) was a professor at Virginia Tech. Dr. McGrath was a co-author on this paper, co-principal investigator for the grant supporting this research and contributed revisions to the final document.

Chapter 4: Synthesis and Characterization of Polybenzimidazoles derived from Tetraaminodiphenylsulfone for High Temperature Gas Separation Membranes

Chapter 4 was published in Polymer

Kevin A. Stevens, B.S. (Department of Chemical Engineering) is currently a Ph.D. candidate at the University of Texas at Austin. Mr. Steve was a co-author on this paper and contributed to the gas transport property testing and dynamic mechanical analysis of the polymer films.

Ran Liu, B.S. (Department of Macromolecular Science and Engineering) was a graduate student at Virginia Tech. Mr. Liu was a co-author on this paper and assisted monomer synthesis and polymer synthesis.

Joshua D. Moon, B.S. (Department of Chemical Engineering) is currently a graduate student at the University of Texas at Austin. Mr. Moon was a co-author on this paper and contributed to gas transport property testing of the polymer films.

Andrew T. Shaver, B.S. (Department of Macromolecular Science and Engineering) is a graduate student at Virginia Tech. Mr. Shaver was a co-author on this paper and performed the thermal gravimetric analysis on the polymers.

Steve Swinnea, Ph.D. (Department of Chemical Engineering) is currently a facility manager and lecturer at the University of Texas at Austin. Dr. Swinnea was a co-author on this paper and contributed to the X-ray diffraction testing of the polymers.

Benny D. Freeman, Ph.D. (Department of Chemical Engineering) is currently a professor at the University of Texas at Austin. Dr. Freeman was a co-author on this paper and contributed revisions to the final document.

Judy S. Riffle, Ph.D. (Department of Macromolecular Science and Engineering) is a professor at Virginia Tech. Dr. Riffle was a co-author on this paper and contributed revisions to the final document.

James E. McGrath, Ph.D. (Department of Macromolecular Science and Engineering) was a professor at Virginia Tech. Dr. McGrath was a co-author on this paper and principal investigator for the grant supporting this research.

Table of Contents

LIST of FIGURES

LIST OF TABLES

Chapter 1: Literature Review

1.1. Introduction

1.1.1. **Membrane Gas Separation**

Membrane gas separation is a pressure-driven process for industrial gas refining. Since Permea (now a division of Air Products) launched the first large industrial application of membrane gas separation in 1980, the use of polymeric membrane separation technology has grown into a $150 million/year business and is projected to grow to $760 million/year by 2020[1,2,3]. Current commercial membrane gas separation technologies are: 1) Air Separation 2) Hydrogen Separation 3) Natural Gas Separation 4) Other Gas Separation[2,3,4]**.** In comparison to well-established traditional separation techniques[5] such as cryogenic distillation, absorption, and pressure-swing adsorption, membrane gas separation has several advantages[4,6]. First, energy consumption, and in some cases, capital investment is lower than conventional separation processes. In addition, the necessary equipment is simple, compact, and relatively easy to operate and control. Finally, the membrane module can be easily scaled up or operated at partial capacity. However, there are also some challenges in membrane separation technology such as the trade-off correlation between the permeability and selectivity of membranes and the plasticization of linear polymer membranes, etc. [2,7,8,9], which will be discussed in greater detail in Section 1.3. In conclusion, as a new, emerging separation technology, gas separation membranes are sustainable and energy efficient, suitable for a wide variety of separation applications in the chemical industry, and are very competitive with conventional gas separation technologies.

1.1.2. History of Gas Separation Membranes

The first observation regarding gas transport through a polymer (natural rubber) was reported in 1831 by John Kearsley Mitchell[10]. Balloons were filled with hydrogen gas and then hung from the ceiling over time. It was hypothesized that hydrogen gas was somehow passing through the rubber balloon. In 1866, Sir Thomas Graham, a Scottish chemist, enriched atmospheric air from 21% to 41% oxygen using a natural rubber polymeric membrane[11,12]. Graham proposed that the permeation of gas molecules through a non-porous polymeric membrane proceeded by a solution-diffusion model mechanism, which is the commonly accepted principle for gas transport in all non-porous polymeric gas separation membranes today[3,13–15]. Over a century later, a substantial quantity of synthetic polymeric membranes and critical applications started to emerge based on Graham's principle[3,13–15].

The industrial gas separation membrane market at an industrial level has grown significantly since the 1970s as the technology improved and applications increased[1]. In 1980, Permea launched its first membrane separation plant, Prism, for hydrogen separation. Later, Cynara (Natco), Separex (UOP), GMS (Kvaerner), Generon (MG), and Medal (Air Liquide) all developed their own membrane gas separation technology and expanded the gas separation membrane market.

Over the last several decades, membrane scientists have developed new classes of materials and continue to improve existing families of gas separation membranes to discover better membranes for gas separations[7].

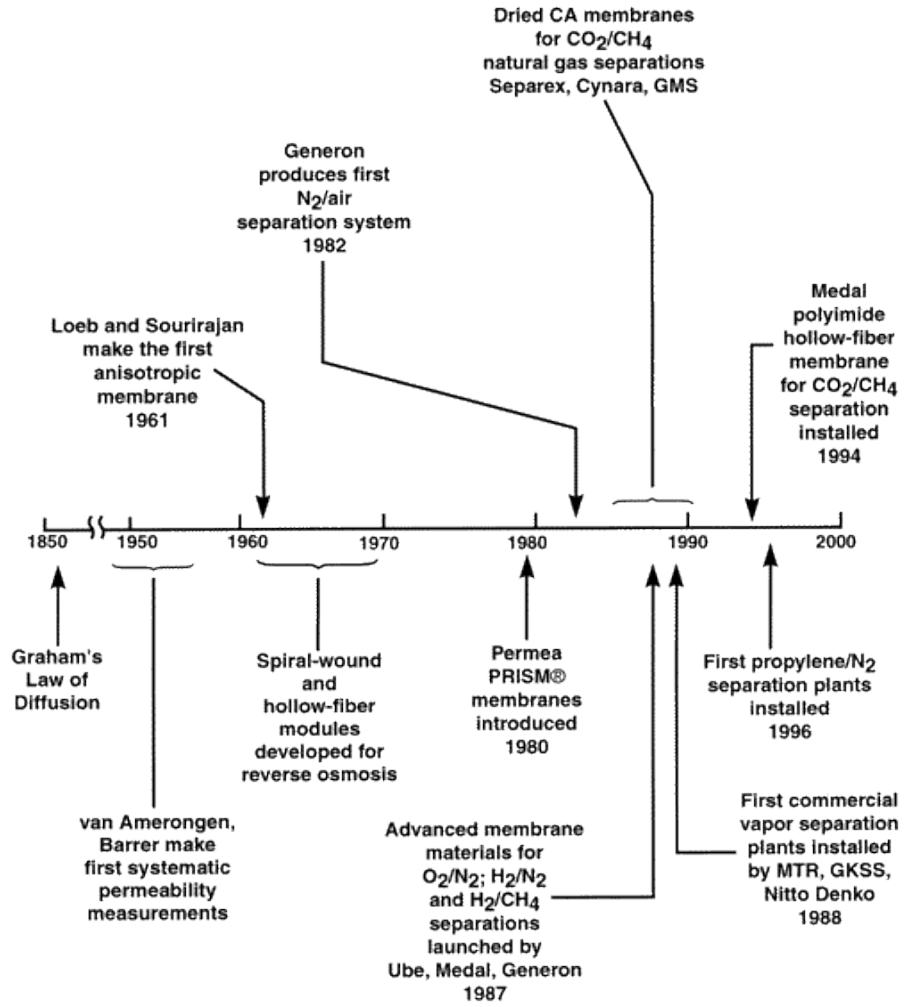

Figure 1.1 Milestones in the development of membrane gas separations. From Ind. Eng. Chem. Res. 2002, 41, 1393–1411, Baker, R. W. Future Directions of Membrane Gas Separation Technology. Used with permission of American Chemical Society, 2002.[1]

1.1.3. Principles of Membrane Gas Separation

1.1.3.1. Solution-Diffusion Mechanism and Permeability Coefficient

The mechanism of small molecule permeation through non-porous polymeric membranes was proposed as a 3-step solution-diffusion model by Sir Graham in 1866, and is commonly accepted today. In this model, small molecules first dissolve into the upstream surface of the polymeric membrane and then diffuse through the membrane to the downstream face; eventually, the molecules evaporate out of the membrane from the low pressure face. This model describes permeability as a product of two factors,

the diffusivity of a molecule through the polymer and the solubility of a molecule in the polymer. Equation 1.1 illustrates this relationship[16]:

$$P_A = S_A \times D_A \tag{1.1}$$

where D_A, the diffusivity coefficient, is a concentration-averaged, effective diffusion coefficient of gas A, characterizing the rate at which the molecule A can diffuse through the membrane[2,6,13]. The solubility coefficient,S_A, the effective sorption coefficient of gas A, is related to the amount of molecule A that can dissolve in the membrane[2,6,13]. The permeability coefficient P_A, t characterizes the flux N_A ($mol/m^2 \cdot s$) through a membrane under the pressure drop (driving force) Δp (Pa) and normalized to the unit thickness of the membrane l (m), which can be described by Equation 1.2:

$$P_A = \frac{N_A}{-\Delta p \cdot l} \tag{1.2}$$

The unit of P in the SI system is $mol/s \cdot m \cdot Pa$[2,9,13]. However, a more commonly used and accepted unit for the permeability coefficient is 1 Barrer = 10^{-10} $cm^3(STP)\ cm/cm^2 \cdot s \cdot cm \cdot Hg$[2,9]. It is important to study the contributions of diffusivity and solubility to permeability by the development of methodical, fundamental structure/property correlations to guide rational structural modifications for a current polymer family to enable optimum performance for gas separation membranes[2].

1.1.3.2. Membrane Selectivity

Permeability is an important membrane property in gas separation because it not only expresses the amount of gas that can pass through a membrane given its thickness and pressure, but it also allows for the calculation of membrane selectivity. Both of these properties are critical to the industrial performance of a membrane[2,6,9,13] since the permeability is representative of the gas throughput, and the selectivity is indicative of the separation efficiency. The selectivity of gas A over gas B for a membrane is defined

by Equation 1.3. Selectivity (or ideal selectivity: $\alpha_{A/B}$) of a membrane is a common parameter that is used to define the ability of the polymeric membrane to separate a gas pair[17,18].

$$\alpha_{A/B} = \frac{P_A}{P_B} \tag{1.3}$$

When Equations 1.1 and 1.2 combine, the permeability selectivity can be written as:

$$\alpha_{A/B} = \frac{D_A}{D_B}\frac{S_A}{S_B} \tag{1.4}$$

Therefore, the permeability selectivity becomes a product of diffusivity selectivity ($\frac{D_A}{D_B}$) and solubility selectivity ($\frac{S_A}{S_B}$). The importance of permeability and selectivity on membrane performance makes the knowledge of the diffusivity and solubility properties of a membrane fundamentally important[19–21]. Determining whether changes in permeability and selectivity occur due to changes in diffusivity or solubility allows for a greater understanding of gas transport in the membrane. An understanding of what parameters are most important in polymer transport properties will allow for more accurate prediction and effective design of new polymer structures.

1.1.3.3. Permeability-Selectivity Trade-Off Relationship

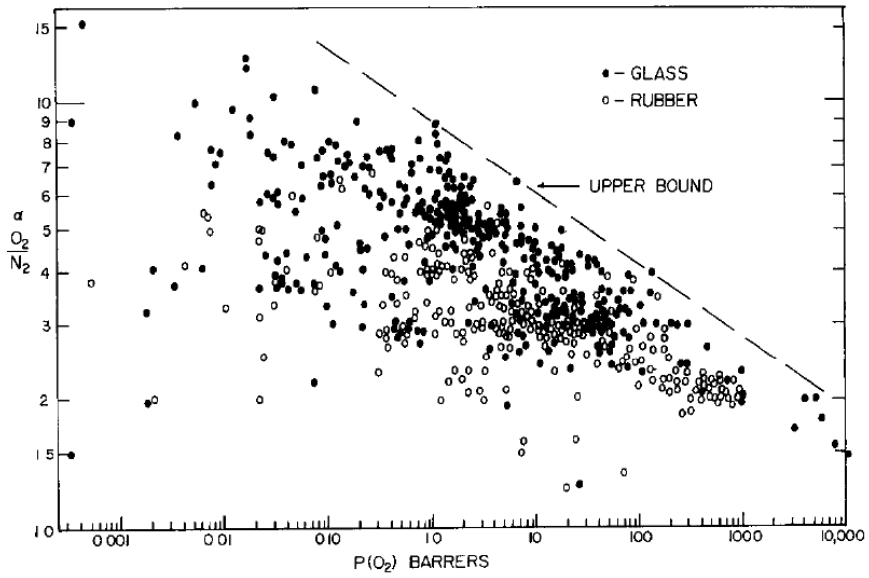

Figure 1.2 The 1991 upper bound correlation for O2/N2 separation. From J. Memb. Sci. 1991, 62, 165–185, Robeson, L. M. Correlation of Separation Factor versus Permeability for Polymeric Membranes. Used with permission of Elsevier, 1991.[22]

Structure-property relationships related to membrane gas transport properties have been considered a significant research domain since polymeric membranes were developed in the 1980s[6,8,12,13]. As many new polymers have been synthesized and many polymers have been modified to achieve enhanced gas transport properties, a trade-off between permeability and selectivity has been gradually recognized. Polymers that have higher permeability are generally less selective, while polymers that have higher selectivity are usually less permeable. In 1991, Robeson et al.[22] explained this notion quantitatively by plotting the available published transport property data of the polymers known at the time on selectivity/permeability graphs[23] (Figure 1.2). Furthermore, it is found that materials with permeability-selectivity combinations in the graph are exceptionally rare across a line termed the "upper bound." This upper bound is based on an empirical correlation between selectivity and permeability and can be described by the following equation[22]:

$$\alpha_{A/B} = \beta_{A/B}/P_A^{\lambda_{A/B}} \quad (1.5)$$

Equation 1.5 shows that as the permeability of an upper bound polymer gas A, P_A, decreases, the selectivity of the polymer for gas A over gas B increases and vice versa. $\beta_{A/B}$ and $\lambda_{A/B}$ are the front factor and upper bound slope, respectively. Both are constants for gas pairs A and B based on empirical observations initially reported by Robeson.

Although the upper bound relationship is an empirical correlation based on experimental data, the theoretical analysis by Freeman et al.[23] supported Robeson's observed empirical conclusions. By using activation energy theory, Freeman predicted the upper bound slope as:

$$\lambda_{A/B} = (\frac{d_B}{d_A})^2 - 1 = (\frac{d_B+d_A}{d_A^2})(d_B - d_A) \quad (1.6)$$

Compared to the value of the $(d_B+d_A)/d_A^2$ term, d_B-d_A has a domineering variation which yields accurate agreement between theory and experimental observation. The front factor has been analyzed further with the result of an upper bound slope, giving a relatively complicated relationship:

$$\beta_{A/B} = \frac{S_A}{S_B} S_A^{\lambda_{A/B}} \exp\{-\lambda_{\frac{A}{B}}\left[b - f\left(\frac{1-a}{RT}\right)\right]\} \quad (1.7)$$

where S_A and S_B are the gas solubility in the polymer that can be determined by correlation with the gas critical temperature, T_c, boiling point, T_b, or Lennard-Jones temperature by Equations 1.8-1.10[24].

$$lnS_A = m + 0.025T_b \quad (1.8)$$

$$lnS_A = x + 0.016T_c \quad (1.9)$$

$$lnS_A = y + 0.023(\varepsilon_A/k) \quad (1.10)$$

where *m*, *x*, and *y* have distinct values for each polymer. These relationships work for both aliphatic and aromatic polymers, with the exception of perfluorinated polymers where the values of the slope are different[25].

Constants a and b are determined by Equation 1.7, which describes the linear relationship between the activation energy of diffusion E_d and D_0.

$$lnD_{0_A} = a\frac{E_{d_A}}{RT} - b \quad (1.11)$$

The f parameter is determined by the following equation, which relates activation energy of diffusion with the diameter of the penetrating molecule.

$$E_{d_A} = cd_A^2 - f \quad (1.12)$$

The values of c and f are adaptable with respect to a specific polymer. Freeman found that the value of f for matching between the empirical upper bound and his theory is approximately 12600cal/mole[23].

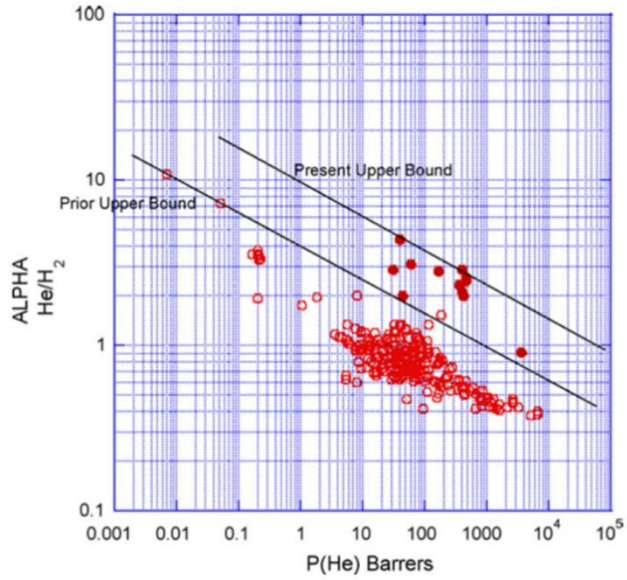

Figure 1.3 The 2008 upper bound correlation for He/H2 separation. From J. of Membr. Sci. 2008, 320, 390. Robeson, L. M. The upper bound revisited. Used with permission of Elsevier, 2008 [25]

As more novel polymers designed for gas separation membranes crossed the upper bound and therefore achieved better gas transport properties, in 2008 Robeson revised the upper bound to include them[25]. As expected, some shifts in the upper bound occurred. The significant shifts of the upper bound were mainly due to perfluorinated polymers for He/H_2 separation, which had not been investigated for gas separation prior to 1991. The superior separation property of the perfluorinated polymer is due to the solubility relationship between the gas and perfluorinated polymer being different than aliphatic or aromatic polymers.

The permeability-selectivity trade-off relationships were established based on membrane performance at 25–35°C, primarily because most permeability data in the literature were from measurements made in this temperature range. Recently, Rowe et al.[26] developed a model which indicates that the predicted upper bound behavior shifts vertically with temperature based on Freeman's theoretical framework of the trade-off relationship.

1.1.3.4. Fractional Free Volume

The free volume of polymers, which is the unoccupied space between polymer chains, has been shown to be the most significant contributor facilitating gas molecule transport in polymers. The fractional free volume (FFV), which is the fraction of free volume within the polymer, is used to estimate the free volume density of polymers[27]. FFV can be calculated by Equation 1.13:

$$FFV = \frac{V_f}{V} = \frac{V - V_0}{V} = \frac{V - 1.3\sum V_w}{V} \tag{1.13}$$

where V_f is the free volume in the polymer; V is the measured specific volume of the polymer; and V_0 is the theoretical occupied volume of the polymer chains. The value of V_0 can be assessed in many ways. A common approach by Bondi is the group contribution method where the occupied volume is estimated from Van der Waal's volume, V_w of each group in the polymer chain[28].

Generally, for gas separation polymers, the diffusion coefficient will increase with the fractional free volume of the polymer[20,27]. This is shown in Equation 1.14:

$$D = Ae^{\left(-\frac{\gamma v^*}{FFV}\right)} \tag{1.14}$$

The diffusivity coefficient is strongly related to the fractional free volume while the gas solubility coefficient is weakly dependent on the free volume of the polymers. The gas permeability often correlates with FFV. Many studies[29,30] have reported the correlation of gas permeability and FFV as

$$P = Ae^{-\frac{B}{FFV}} \tag{1.15}$$

where A and B are constants for a particular gas.

1.1.3.5. Membrane Plasticization

Many gas separation experiments show that polymeric membranes exposed to a gas at high pressure, especially CO_2, have poorer selectivity than those exposed to a gas at a low pressure[31,32]. This common phenomenon is recognized as the plasticization effect. As the pressure of a feed gas reaches a certain threshold, the free volume and chain mobility increases and results in a higher gas permeability. According to the solution diffusion mechanism equation, an increase of the gas permeability can cause an increase in the solubility coefficient, diffusivity coefficient, or both. The permeability increase due to the plasticization effect leads to the increase in the gas diffusivity coefficient[33].

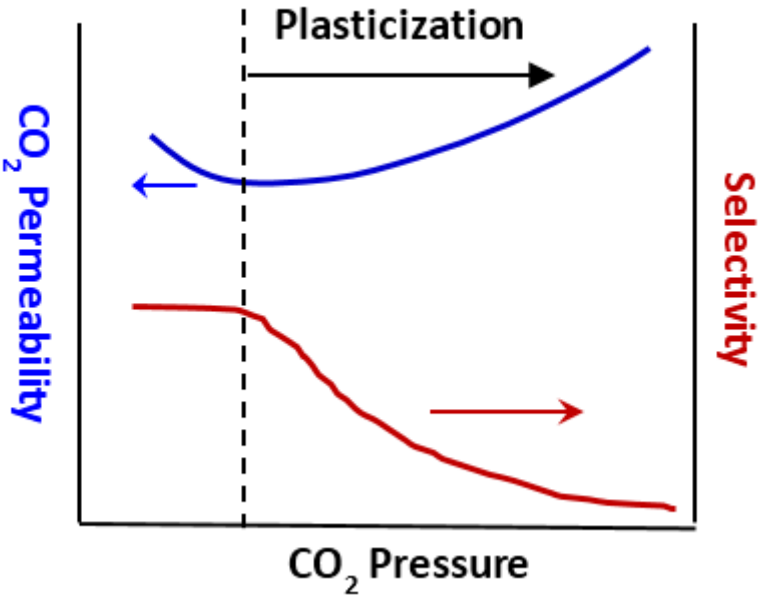

Figure 1.4 Plasticization effect in membrane gas separation

For glassy linear polymers, the plasticization effects are often observed as an initial decrease in the gas permeability with the increasing upstream pressure of the gas. Permeability begins to increase with the additional upstream pressure after plasticization occurs (Figure 1.4)[34–36]. This increase in permeability will reduce the

selectivity of the membrane for mixed gas separations, especially CH_4/CO_2 separation. The selectivity reduction in mixed gas separation polymeric membranes has been reported in many polymers such as Matrimid, cellulose acetate, etc.[33,37,34] The selectivity reduction is thought to be caused by CO_2-induced plasticization which accelerates the permeability of CH_4 more than that of CO_2[38].

Although the plasticization effect seems inevitable for linear polymers, in many studies, crosslinking linear polymer systems have been shown to reduce plasticization[37,39]. For example, crosslinked Matrimid using *p*-xylylenediamine as a crosslinker has been shown to suppress the plasticization phenomenon (Figure 1.5)[39]. However, as the degree of crosslinking increases, the permeability of the membrane will decrease due to the crosslinking modification which reduces the free volume and chain mobility[37,39]. The only known exception are the thermally rearranged (TR) polymers, which display increased permeability after crosslinking[40]. These effects will be discussed in greater detail in Chapter 3.

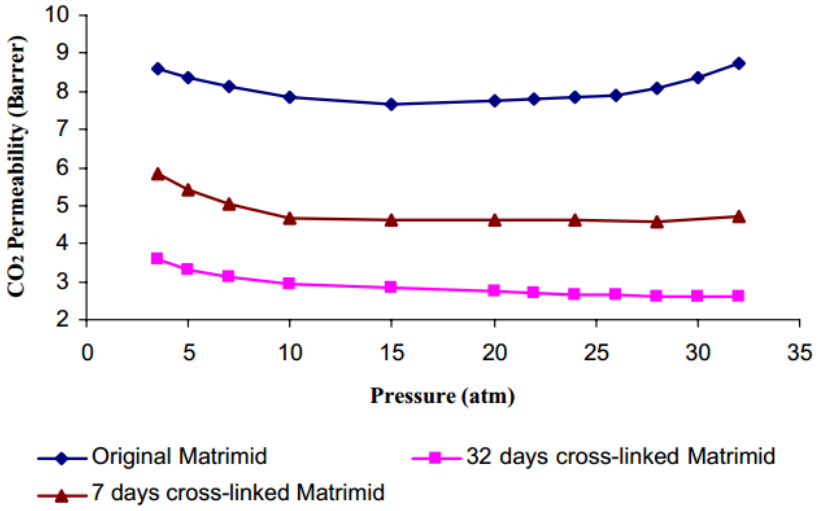

Figure 1.5 Pure CO2 permeability for untreated and crosslinked Matrimid films as a function of upstream pressure. From J. Memb. Sci. 2003, 225, 77–90, Tin, P. Effects of Cross-Linking Modification on Gas Separation Performance of Matrimid Membranes. Used with permission of Elsevier, 2003 [39]

1.2. Gas Separation Membranes

Since the first polymer membrane was used for commercial gas separation thirty years ago, several polymer membranes have been used in industrial processes for gas separations. This chapter will discuss some important commercial polymer membranes, such as polysulfone and cellulose acetate, and newly emerging polymer membranes, such as thermally rearranged polymers. Figure 2.1[2] shows the H_2/N_2 upper bound plot for some common commercial polymers.

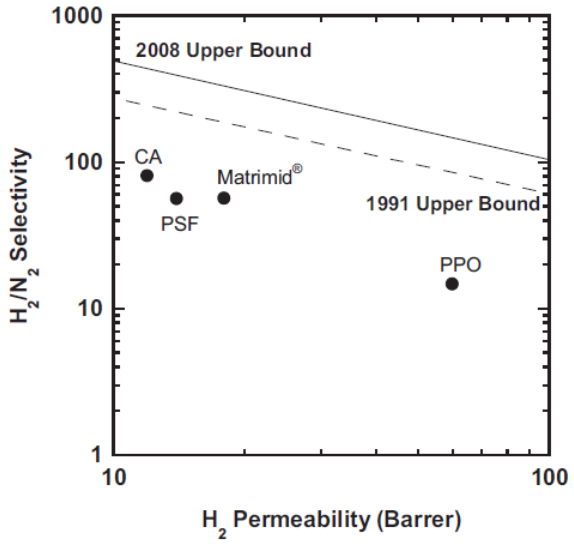

Figure 1.6 H_2/N_2 upper bound plot for representative common commercially relevant polymers. From Polymer. 2013, 54, 4729–4761, Sanders, D. F.; Smith, Z. P.; Guo, R.; Robeson, L. M.; McGrath, J. E.; Paul, D. R.; Freeman, B. D. Energy-Efficient Polymeric Gas Separation Membranes for a Sustainable Future: A Review. Used with permission of Elsevier, 2003.[2]

1.2.1. Polysulfone (PSF)

Polysulfone, with generally representative diphenylsulfone as linking groups, has been known as one of the most chemically and thermally stable engineering thermoplastics[41]. The character of the C-S-C link, which provides steric hindrance and a double bond resonance, subsequently yields the amorphous morphology and

molecular immobility. The abundance of phenylene groups provides backbone rigidity and electronic attractions due to resonating electron systems between adjacent molecules. These structural features give polysulfones ideal mechanical properties including a completely amorphous structure and high Tg, strength, good creep resistance, dimensional stability, and a high heat deflection temperature[41].

Union Carbide developed the first commercial polysulfone Udel® in the late 1960s based on the nucleophilic aromatic substitution reaction. Imperial Chemical Industry and Union Carbide also independently commercialized additional polysulfones such as Victrex®, Radel®R, and Radel®A.

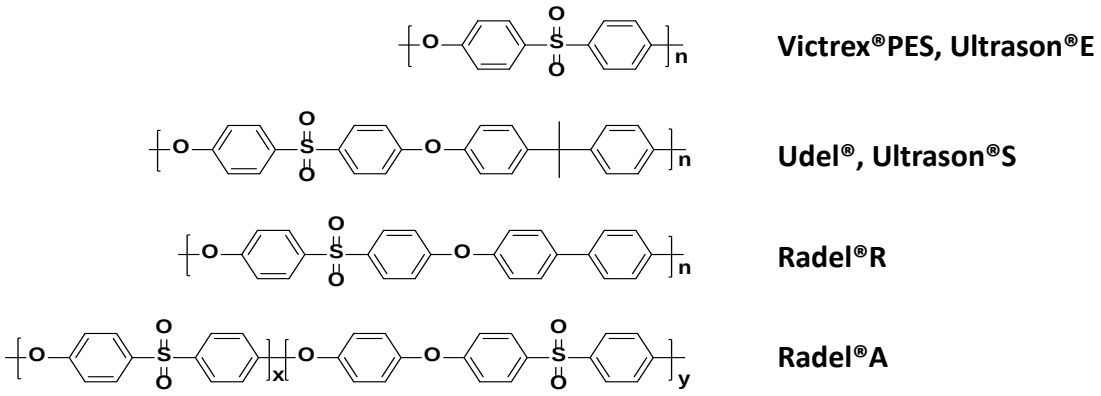

Figure 1.7 Structure of commercial polysulfones

The first polysulfone membrane used for gas separation, bisphenol A sulfone (Udel®), was develop by Monsanto in the late 1970s. Since then, the gas separation performance of these commercial polysulfones and their variants has been comprehensively studied[42–45]. For commercial polysulfones, the permeability coefficient for all gases ranks in this order: Udel®≈ Radel®R> Radel®A> Victrex®.

Substituents on phenylene rings affect the separation properties of polysulfones. Symmetric bulky substituents, such as methyl groups, bromo groups, etc., on phenyl rings of polysulfones will increases the gas permeability while the selectivity of gas pairs only changes slightly[46,47]. Asymmetric bulky substituents will decrease gas

permeability and consequently raise the selectivity of polysulfones. Polar substituents have also been shown to change the gas transport properties of polysulfones[46,48]. Nitrated polysulfones have been shown to decrease gas permeability and slightly increase selectivity for some gas pairs. Studies show that aryl-nitration does not reduce the packing density of the polysulfone while the Van der Waals volume is enlarged due to the polar nitro groups[48].

The linkages in the backbone affect the gas transport properties of polysulfones[44]. The bulkiness of the linking group can adjust the permeability of polysulfones. Replacing the isopropylidene bridging group in Udel® with a bulkier group, hexafluoro isopropylidene, will significantly increase the permeability coefficient. If the isopropylidene connector is replaced by a less bulky group, such as a methylene group, the permeability coefficient decreases[49]. These property changes from the replacement of isopropylidene bridging groups affect chain mobility, chain packing, and polymer-penetrant interactions, which in turn alters the free volume of the polysulfones[49]. Additionally, the symmetry of the phenylene linkages plays a significant role in the gas transport behavior of polysulfones. Enhanced permeability and lowered selectivity for a polysulfone can be achieved by changing from para-phenylene linkages[47] to meta-phenylene linkages. Polysulfones with meta-linkages appear to have reduced chain mobility due to molecular geometry and more efficient intermolecular packing, both of which contribute to the gas separation performance of polysulfones[47].

Polysulfones still hold part of the gas separation membrane market, especially in hydrogen and air separation[1,2]. Compared with other commercial polymers like polycarbonate, cellulose acetates, and polyimides, polysulfones are still competitive in H_2/N_2 separation but not in CH_4/CO_2 separations.

1.2.2. Polyimides (PI)

Since DuPont applied polyimide membranes to He/CH_4 separation in 1962, polyimide research related to gas separation has grown significantly and still maintains some level of interest[1]. Aromatic polyimides in general have great gas separation and physical properties, which makes them competitive gas separation membrane candidates.

The synthesis of aromatic polyimides is usually conducted by reacting aromatic dianhydride and aromatic diamine monomers through step-growth polymerization. There are several different synthesis routes that have been developed to make aromatic polyimides[50]. The classic synthesis route was invented in 1956 by Dr. A. Endrey at DuPont. This route consists of reacting the dianhydride and diamine at room temperature to form poly(amic acid). The poly(amic acid) can then be processed into a useful shape, followed by cyclodehydration of the polyamic acid to form a polyimide[51]. The details of the synthesis of polyimides will be discussed in Chapter 3.

Matrimid is a commercial polyimide that has been used for gas separation due to its excellent gas separation properties, which place it close to the upper bound. Matrimid consists of 3, 3', 4, 4'-benzophenone tetracarboxylic dianhydride, two isomeric diamine phenolindane(6-amino-1-(4-aminophenyl)-1,3,3-trimethylindane, and 5-amino-1-(4-aminophenyl)-1,3,3-trimethylindane). Among the commercialized gas separation polymers, such as Udel, cellulose acetate, etc., Matrimid has the best gas separation properties in CO_2/CH_4 separation, indicating it is close to the upper bound. However, like all of the linear polymer membranes, CO2 exposure can plasticize Matrimid, resulting in overall permeability and reduction of CO_2/CH_4 selectivity[34]. To overcome plasticization, modifications of Matrimid such as annealing and chemical crosslinking

have been studied. Although the plasticization effect can be suppressed by crosslinking, the permeability of these modified Matrimid membranes usually decreases as well[39].

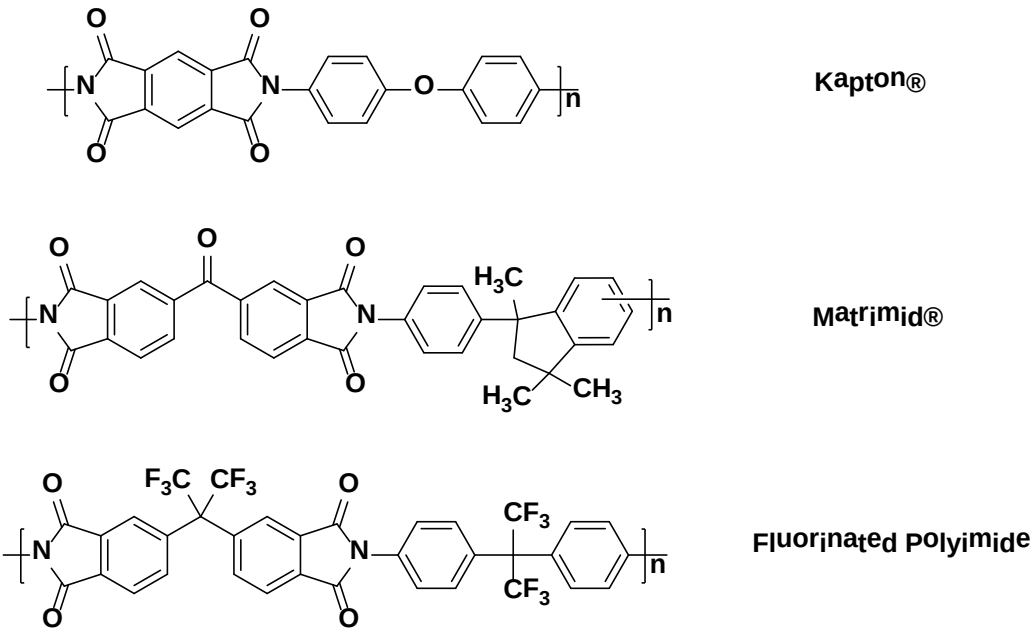

Figure 1.8 Structure of some commercial polyimides and fluorinated polyimide

Fluorinated polyimides have also received interest recently due to their excellent gas separation properties. Fluorinated polyimides generally consist of an aromatic imide moiety with hexafluoro isopropylidene linkages. The hexafluoro isopropylidene linkage decreases the chain packing efficiency due to steric hindrance and its bulkiness generates more free volume, therefore increasing permeability[2].

1.2.3. Cellulose Acetate (CA)

The abundant natural polymer, cellulose esters, a derivative of cellulose, have been used commercially for over a century[52]. The esterification of poorly soluble cellulose enables processing into various useful forms. Applications of cellulose esters include coatings, adhesives, liquid crystal displays, separation media, and biodegradable plastics[52]. Cellulose esters for gas separation membranes were developed in the 1980s.

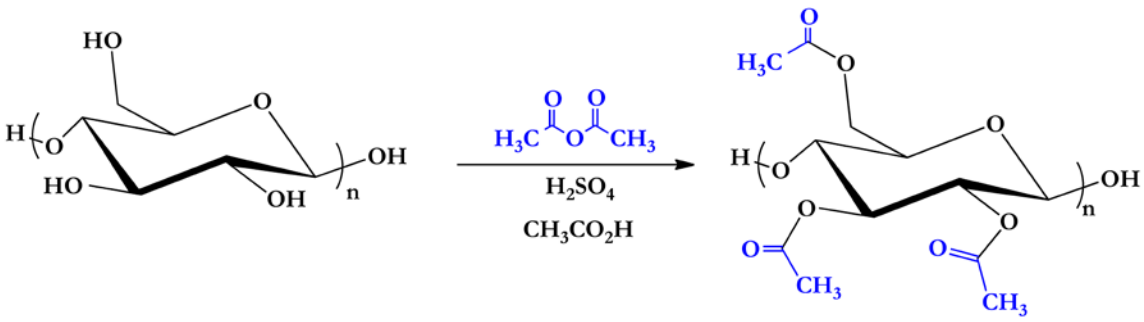

Cellulose **Cellulose Triacetate**

Figure 1.9 Acetylation of cellulose

Acetylation of cellulose using acetic anhydride or acetic acid produces cellulose acetate. Cellulose acetate, which was originally used for reverse osmosis membranes,[53] was commercialized in late 1980s for gas separation membranes, specifically natural gas separation, due to its good transport properties. Replacement of hydroxyl groups by acetate groups will reduce hydrogen bonding and crystallinity, which enables solubility in common solvents and can be processed using various established methods[52]. Cellulose acetate is characterized by its degree of acetate substituents (often referred as DS or degree of substitution). As only 3 functional groups can be converted to acetate groups in one repeating unit of cellulose, the range of DS is generally from zero to 3. The degree of acetylation has also been shown to influence gas transport properties of cellulose acetate. As the degree of acetylation of cellulose acetate increases, the permeability of cellulose for all common gases increases[54]. The rise in permeability stems from the replacement of the polar hydroxyl group with the bulky acetate group, thus reducing hydrogen bonding while decreasing the polymer density and providing the free volume polymer structure.

Cellulose acetate membrane modules are quite well-developed in industrial applications because of their abundance and affordabilityt[55]. However, CA membranes can be plasticized by CO_2 [33] which becomes a critical inherent weakness, especially for

CH_4/CO_2 separation. The plasticization decreases membrane selectivity and therefore reduces methane recovery in natural gas separation.

1.2.4. Poly (phenylene oxide) (PPO)

Poly(phenylene oxide), also known as poly(arylene ether) is a class of high performance thermoplastics with good thermo-stability and mechanical properties[41]. The ether linkages between aromatic rings provide chain flexibility and lower the glass transition temperature while increasing processibility. Moreover, the resonance of aromatic ether linkages retain stability, which contributes to its good thermal and mechanical properties.

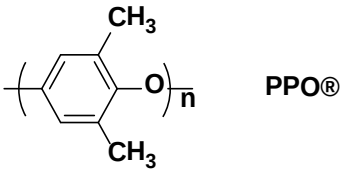

Figure 1.10 Poly(phenylene oxide)

The first commercial poly(phenylene oxide), poly(2,6-dimethyl-1,4-phenylene oxide) (PPO®) was discovered by Hay in 1959 and later commercialized by General Electric (now Sabic Innovative Plastics) and AKZO[41]. The PPO polymer can be synthesized from 2, 6-xylenol through oxidative coupling polymerization in the presence of oxygen, and catalyzed by CuCl and an amine ligand such as pyridine. The oxidative coupling reaction forms either a C-C coupling which gives a dimer (diphenoquinone) or a C-O coupling which leads to high molecular weight polymers. Therefore, minimizing the C-C coupling reaction is the key to achieving high molecular weight PPO using oxidative coupling polymerization. PPO can also be synthesized through aromatic nucleophilic substitution, Friedel-Craft reactions, and Ullman polycondensation reactions[41]. Among these various polymerization methods, oxidative

coupling polymerization has competitive advantages such as moderate reaction temperature, halogen-free monomers, and environment friendly byproducts (water)[41].

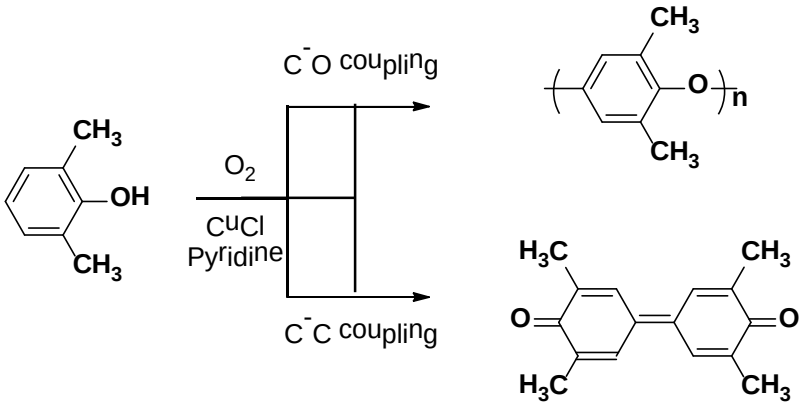

Figure 1.11 Oxidation coupling reaction

Poly phenylene oxide is also used as a gas separation membrane due its outstanding permeability (even higher than butyl rubber) as a glassy polymer[56]. Although PPO has shown high permeability, which stems from its high free volume and ease of rotation of phenyl rings due to the ether linkages, it only maintains moderate selectivity. Therefore, PPO and its derivatives such as brominated PPO, nitrated PPO, sulfonated PPO, etc. have been studied to enhance its selectivity[56–59]. Research has demonstrated that when polar functional groups are added to the PPO backbone using post-nitration, post-sulfonation, carboxylation, and esterification, the selectivity of these kinds of modified PPO is proportional to the degree of the modification[48,56,58,60]. And, of course, the permeability of these modified PPOs will also decrease. For example, a 22% carboxylated PPO has 19.5 CO_2/CH_4 selectivity while PPO only has 15.1, and carboxylated PPO also trades off its permeability for CO_2 reduced from the 42 barrer to the 22.0 barrer[56]. In addition, research shows that the permeability of PPO can be enhanced by adding non-polar bulky groups such as bromine to the PPO backbone[57]. For instance, as the degree of bromination increases from 0 to 1.06, the

CO_2 permeability increases from the 50 barrier to the 108 barrier[58]. Although the gas transport properties of PPO can be altered by a series of modifications, conducting these modifications in an economical way remains a challenge.

1.2.5. Thermally Rearranged (TR) Polymers

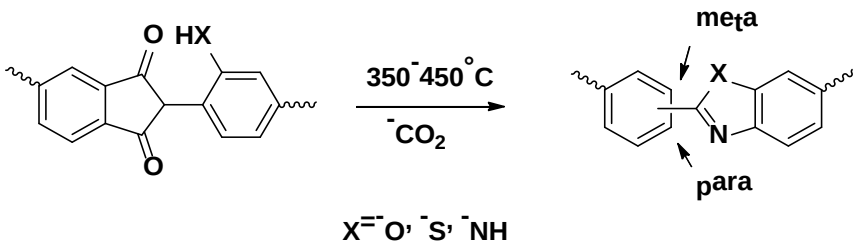

Figure 1.12 The formation of polybenzoxizoles structures from TR precursors. From Science 2007, 318, 254–258, Park, H. B.; Jung, C. H.; Lee, Y. M.; Hill, A. J.; Pas, S. J.; Mudie, S. T.; Van Wagner, E.; Freeman, B. D.; Cookson, D. J. Polymers with Cavities Tuned for Fast Selective Transport of Small Molecules and Ions. Used with permission of American Association for the Advancement of Science, 2007 [40]

The thermally rearranged (TR) polymer membrane was initially reported by Park et al.[40] which has exhibited outstanding gas separation properties, especially for CO_2/CH_4 separation. This category of materials has 4 major benefits[2,40]: high CO_2 permeability, CO_2/CH_4 selectivity (some of which have crossed Dr. Robeson's 2008 upper bound[25]), resistance to CO_2-induced plasticization, and excellent chemical resistance.

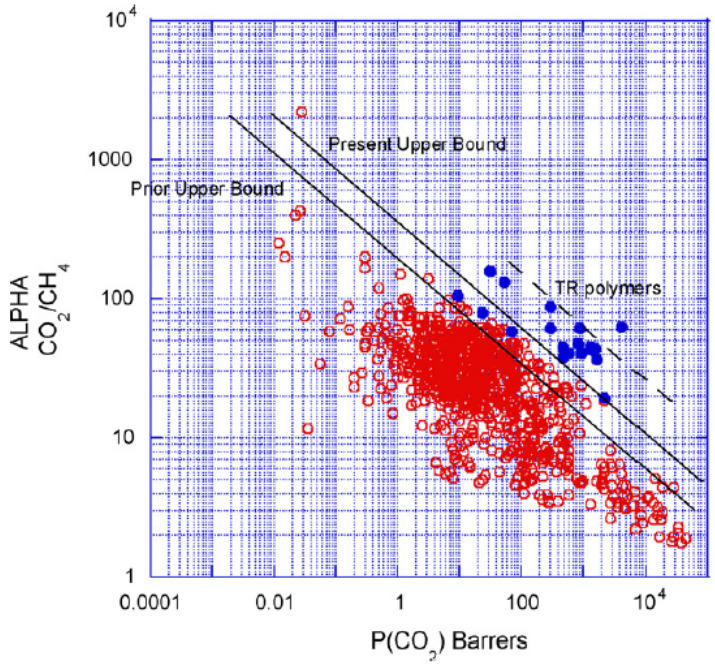

Figure 1.13 Upper bound correlation for CO_2/CH_4 separation (TR polymer in blue dots). From J. Memb. Sci. 2008, 320, 390–400, Robeson, L. M. The Upper Bound Revisited. Used with permission of Elsevier, 2008.[25]

The first TR polymer membrane introduced by Dr. Ho Bum Park[40] is derived from ortho-functionalized (-OH, -SH and -NH_2 functional groups) polyimides at an elevated temperature (from 350-450°C) in an inert atmosphere. Under such conditions, the ortho-functionalized polyimides will cyclize to form para- or meta- linked polybenzoxazole-type (or polybenzothiazole, polypyrrolone) polymers with the evolution of CO_2. Due to insolubility of the thermally rearranged polymer, it has been proposed that during the rearrangement process, not only has intramolecular cyclization occurred,[61,62] but also intermolecular reactions that lead to a crosslinked structure.

The increase in fractional free volume and a narrowing of the free volume distribution when compared with other linear polymer membranes[40], gives TR polymers a unique permeability and selectivity correlation. Positron annihilation lifetime spectroscopy and molecular modelling have been used to confirm that thermal rearrangement increases

the average size of free volume elements while also making the size distribution of these elements more uniform.[25,40] Therefore, the solubility and diffusivity of the membrane are increased during this conversion of polyimides to polybenzoxazoles. As stated previously, diffusivity plays a much larger role for gas permeability increases than solubility[63]. Hence, the fractional free volume rise with thermal rearrangement conversion is responsible for permeability enhancement.

TR polymers are promising candidates for the next generation of high-performance membrane materials for gas separation[2,25]. The practical applications could be significantly enhanced if the precursor polyimides were made from commercially available monomers and the thermal rearrangement process were performed at a more energy-efficient level.

1.2.6. Polybenzimidazole (PBI)

In the1960s, aromatic polybenzimidazoles (PBI) were initially synthesized using melt polymerization by Vogel and Marvel[64,65] at the University of Illinois, and later at DuPont. Since then, high performance polybenzimidazoles have received a great deal of attention from both academia and industry due to their impressive thermal and chemical stability[66]. In 1983, the poly[2,2′-(*m*-phenylene)-5,5′-bibenzimidazole] prepared from melt polycondensation of tetraaminobiphenyl and diphenylisophthalate was commercialized under the trade name Celazole® by Celanese.

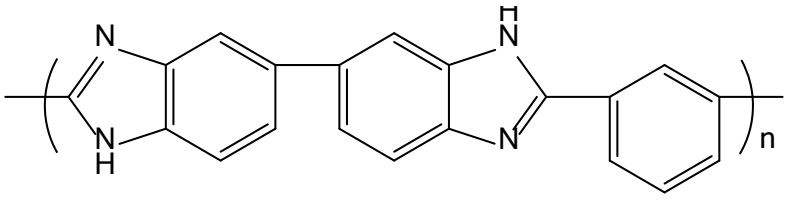

Figure 1.14 poly[2,2'-(m-phenylene)-5,5'-bibenzimidazole], Commercial PBI Celazole®

Polybenzimidazoles received significant interest in the 1960s and 1970s because of their unique properties such as good flame-retardation, high temperature stability, high glass transition temperature (>400°C), good chemical resistance, miscibility with many other polymers (polyimide, polyarylate, polyaramideimide, etc.), and high water absorption[67]. Major applications of PBI include thermally protective clothing, aircraft wall fabrics, and sealing elements in high-temperature corrosive environments[67]. However, polybenzimidazoles-related research gradually lost attention in the 1980s and 1990s due to the availability of many other high performance polymers and the high cost of polybenzimidazoles[66].

Nevertheless, polybenzimidazoles are good candidates for reverse osmosis, as well as fuel cell and gas separation membrane applications[66,68,69]. For reverse osmosis membranes, PBI membranes have comparable performance to cellulose acetate at ambient temperature and superior performance at elevated temperatures[68,70]. Acid-doped PBI membranes for fuel cell applications were also extensively investigated in the last decade[71]. Polybenzimidazole research has included changing the linkage group in PBI chains by the utilization of novel monomers and by adding pendant groups and crosslinking polybenzimidazoles to enhance the properties of PBI for fuel cell membranes[72–74]. Polybenzimidazoles have not been investigated as thoroughly for gas separation applications as they have for PEM fuel cells. Most of the research has focused on blending PBI with other polymers, the fabrication of PBI composite asymmetric membranes, and the crosslinking of PBI[75–77]. Only a few novel polybenzimidazoles have been studied for gas separation membranes besides the commercially available PBI[78,79]. Recently, Berchtold et al. reported that a PBI/zirconia/stainless steel composite membrane has outstanding gas transport properties for H_2/CO_2 separation at elevated temperatures[80].

In summary, heterocyclic PBI-based polymers are thermally stable, have a high glass transition temperature, excellent chemical resistance, and good mechanical properties. Some studies have demonstrated that PBI-based polymers have excellent size sieving ability and good potential for small molecule separations[80]. Thus, PBI-based materials are very promising candidates for gas separation membranes, especially for applications in extreme chemical and thermal environments such as syngas separation[75,80,81].

1.3. Thermally-Rearrangeable (TR-able) Polyimide Precursors

Thermally rearrangeable polyimides are a class of polymers containing ortho functionalized aromatic imide units in the polymer backbone, which are able to perform thermal rearrangements at a solid state to produce crosslinked polybenzoxazoles, polybenzothiazoles, or polypyrrolone (where the ortho functional group is O, S, or N, respectively). Additionally, research shows that aromatic polyimides synthesized by many different methods with synthetic routes can also affect their gas transport properties[82]. Therefore it is preferable to identify TR precursor polyimides by the abbreviation of the combination of dianhydride, bisaminophenol, and the synthetic route. For example, (Figure 3.1) a thermally rearrangeable polyimide made from 2,2-bis (3,4-dicarboxyphenyl) hexafluoropropane dianhydride (6FDA) and 3,3'-dihydoxy-4,4'-diaminobiphenyl (HAB) using the ester-acid route (EA) is generally named 6FDA-HAB-EA.

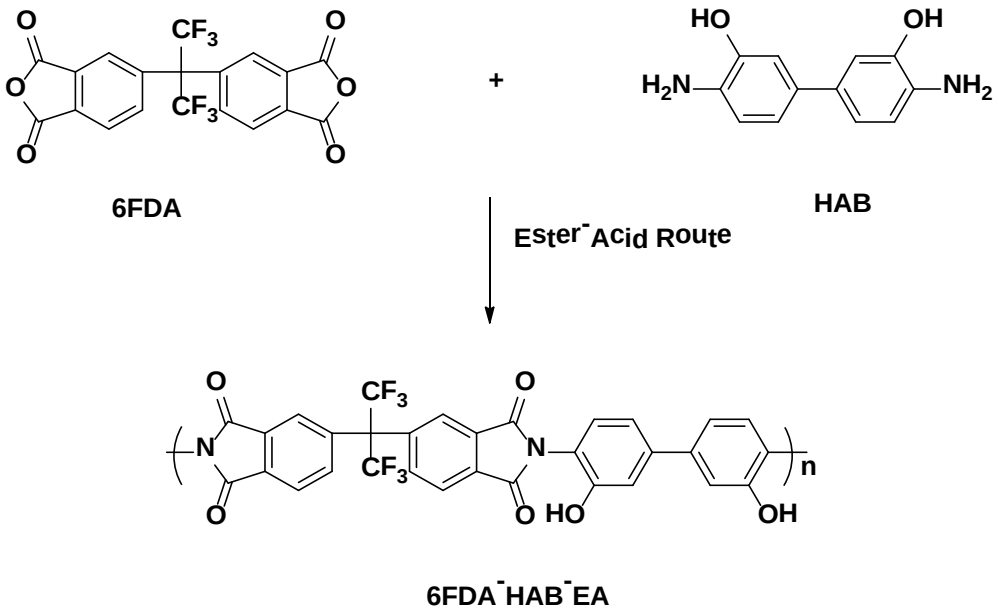

Figure 1.15 TR precursor synthesis

Preliminary research shows that not only can ortho-hydroxyl functionalized (or SH, NH_2) undergo thermal rearrangements, but some bulky groups such as acetyl and pivaloyl can also undergo thermal rearrangement[83]. Interestingly, when the functional groups are changed to acetyl and pivaloyl groups, no inert atmosphere is required for the thermal rearrangement process. Additionally, the permeability of those TR polymers derived from the polyimides with bulky functional groups increases significantly[84].

1.3.1. Synthesis of TR Precursor Polyimides

The design and the synthetic pathway of TR precursors of polyimides (ortho functionalized aromatic polyimides) are important elements in the development of the physical and gas transport properties of TR polymers. TR precursors for polyimides are commonly derived from the condensation reaction of bisaminophenols and tetracarboxylic anhydrides[40,85,86]. In general, most of the usual polyimide synthetic strategies can be applied to TR precursor polyimide synthesis. In this chapter,

fundamental aspects of common synthetic chemistry and methods used to prepare polyimides, especially TR precursor polyimide synthesis, will be discussed.

1.3.1.1. Classic Two-Step Method of Polyimide Synthesis

The invention of the classical polyimide synthetic method was pioneered at DuPont in the 1950s. This synthetic pathway allows the formation of soluble, processible polyamic acid precursors from diamine and dianhydride by the exothermic acylation of amine[87] followed by the cyclodehydration of amic acid to polyimides by various imidization methods, which will also be discussed in this chapter.

In the classic two-step method of aromatic polyimides synthesis, an aromatic diamine solution is prepared in a polar aprotic solvent such as *N*-methylpyrrolidone (NMP) and *N, N*-dimethylacetamide (DMAc), and then mixed with a tetracarboxylic dianhydride. Poly(amic acid) will be formed and typically reaches full conversion within twenty-four hours, depending on the reactivity of the two monomers at ambient temperature. The forward reaction in a dipolar solvent is a second-order reaction and the reverse reaction is a first-order reaction. Therefore, equilibrium is favored at low temperature and high monomer concentration to form high molecular weight poly(amic acid)[88]. The poly(amic acid) is soluble due its backbone flexibility and therefore can be used in solution processing. The imidization step in this synthetic method is accomplished by heating or by incorporating a chemical dehydrating agent, such as a combination of acetic anhydride and pyridine, to cyclodehydrate the poly(amic acid). A general reaction scheme of two-step polyimide synthesis is shown below:

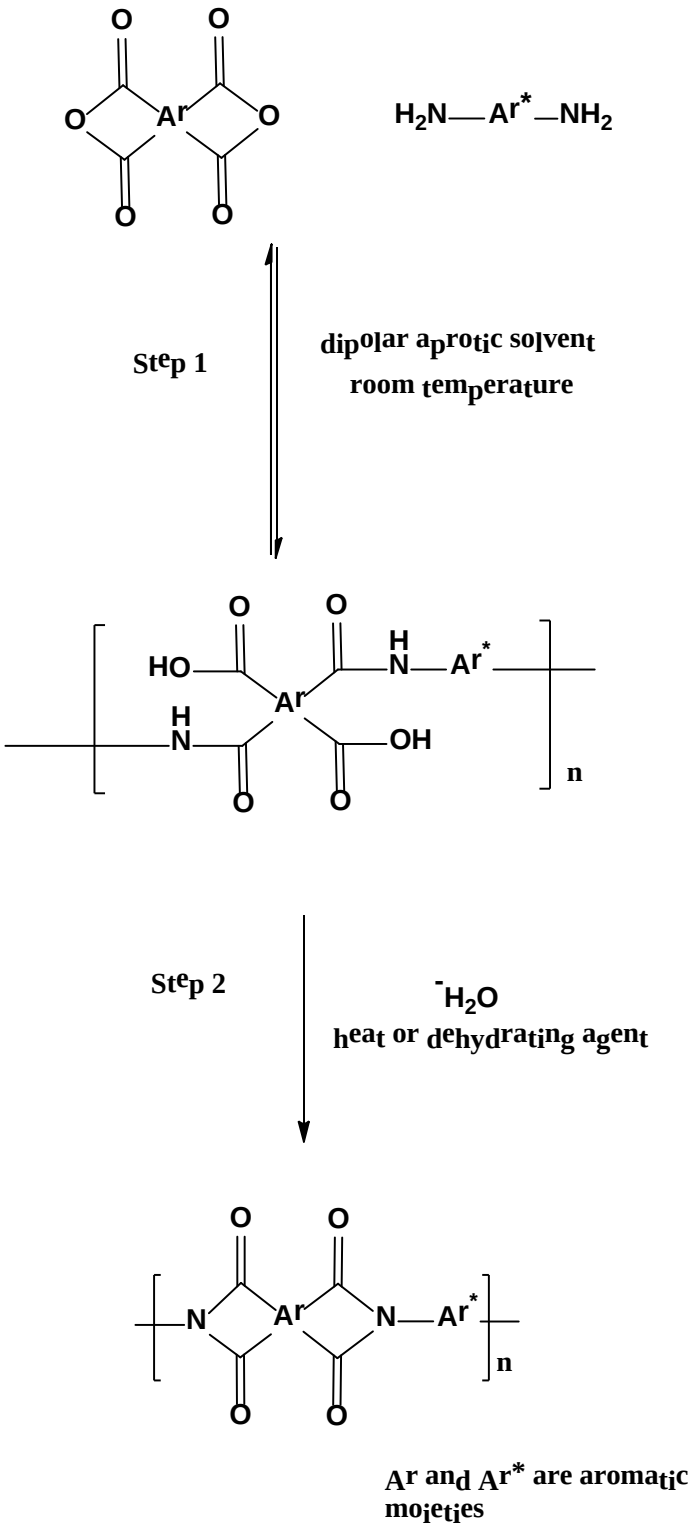

Figure 1.16 Classic two-step polyimide synthesis

1.3.1.1.1. Mechanism of polyamic acid formation

It is commonly accepted that poly(amic acid) formation consists of the aromatic amine groups with an unshared electron pair nucleophilic attacking the carbonyl group of a phthalic anhydride derived from tetracarboxylic acid anhydride groups. This forms a cyclic intermediate with a pi electron pair shifting to the oxygen, the pi electron pair on the oxygen shifts back to form a carbonyl double bond, and the C-O sigma bond breaks to open the anhydride ring[89], forming an amic acid group. In this equilibrium step, a basic solvent such as NMP will deactivate the carboxylate group due to hydrogen bonding, which will push the equilibrium forward[90]. This acylation of amine reaction is a second-order exothermic reaction. Therefore, low temperature and high monomer concentrations will favor the forward reaction to form high molecular weight poly(amic acid)[87]. The mechanism of polyamic acid formation is shown in Figure 1.17.

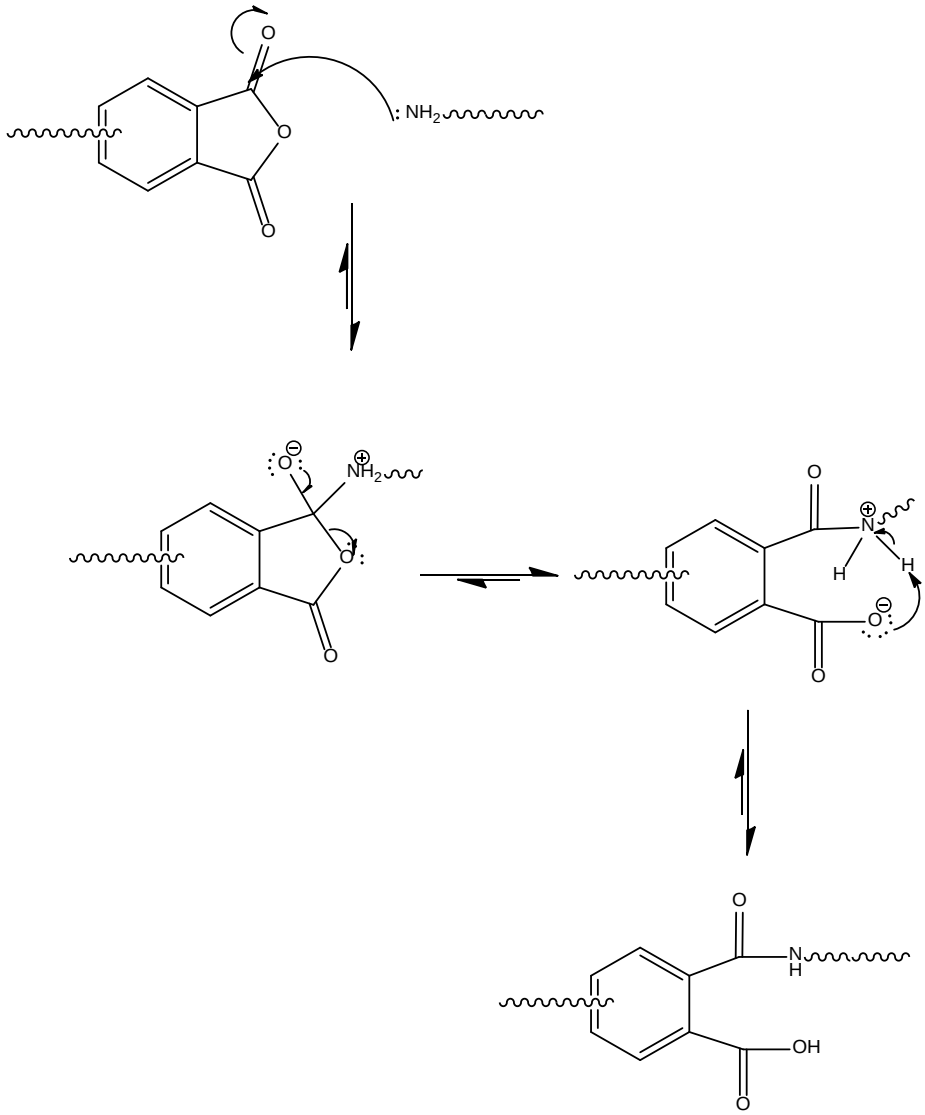

Figure 1.17 Nucleophilic mechanism of poly(amic acid) formation

1.3.1.1.2. Side reactions

The most damaging side reaction during poly(amic acid) formation is hydrolysis[91,92]. During the formation reaction, a small amount of dianhydride is always present in the equilibrium. If a trace amount of water is brought into the system from the monomers, solution, undried glassware, or is even produced by a minor side reaction, it may hydrolyze the aromatic anhydride, forming a dicarboxylic acid which is unreactive towards aromatic diamines at room temperature which effectively endcaps the polymer chains. Therefore, the imbalanced stoichiometry of dianhydride and

diamine will prevent the formation of high molecular weight polyamic acid in accordance with the Carothers' equation.

Some other minor side reactions can also occur during polyamic acid formation. A list of side reactions and their reaction rate is shown below (Table 1.1 and Figure 1.18)[50].

Table 1.1. Rate constants are estimated for typical polymerization at ca. 10 wt% concentration, i.e. 0.5 M.

Relative rate constants for side reactions during polyamic acid formation[50].

Reaction	Rate Constant(s^{-1})
Propagation(k_1)	0.1-0.5
Depropagation(k_{-1})	10^{-5}-10^{-6}
Spontaneous Imidization(k_2)	10^{-8}-10^{-9}
Hydrolysis(k_3)	10^{-1}-10^{-2}
Isoimide Formation(k_4)	_
Diamide Formation(k_5)	_
Isomerization(k_6)	_

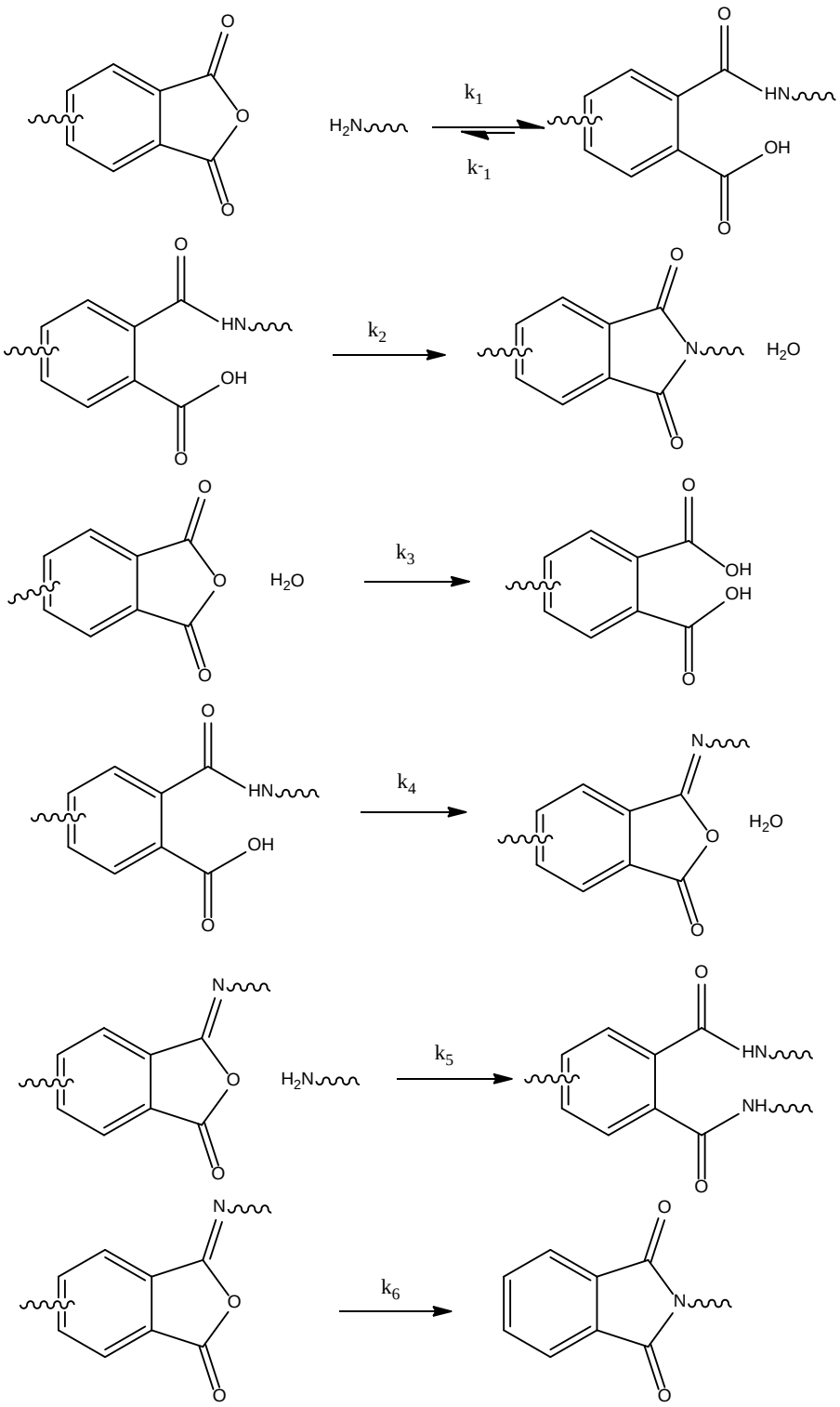

Figure 1.18 Possible side reactions during polyimide synthesis via poly(amic acid)

Although the reaction rate of these side reactions is very low compared to the acylation of amine, they may become significant when monomer reactivity is low or the concentration of the monomer is low. For example, Frost and Kesse observed that

the viscosity of an aged polyamic acid solution (made from PMDA and ODA monomers) decreases with respect to increased aging time[91]. In addition, nearly 20% of the conversion of amic acid to imide was detected by infrared spectroscopy after 119 hours.

1.3.1.1.3. Thermal or Bulk Imidization

Cyclization of the poly(amic acid) moiety into polyimide structures is achieved by gradual heating by 250°C to 350°C, depending on the T_g and thermal stability of the polymer. This is referred to as thermal imidization, also known as bulk imidization. Due to poly(amic acid) chain flexibility, they are soluble in a number of common solvents, such as NMP and DMAc, which make them available to process in a solution. The residual solvent of the processed polyamic acid is removed by gradual heating followed by cyclization which forms the polyimide in a solid state. A commonly employed thermal imidization protocol is conducted under a vacuum or nitrogen as follows: 100°C for one hour, 200°C for one hour, and 300°C for 1 ½ hours to one hour at a temperature just above Tg[50,93,94]. Although the exact mechanism is still uncertain, it is thought to proceed by a nucleophilic substitution type mechanism involving the amide nitrogen and the ortho-carboxylic acid. Two acceptable mechanisms proposed by Harris[95] are shown below:

Mechanism 1

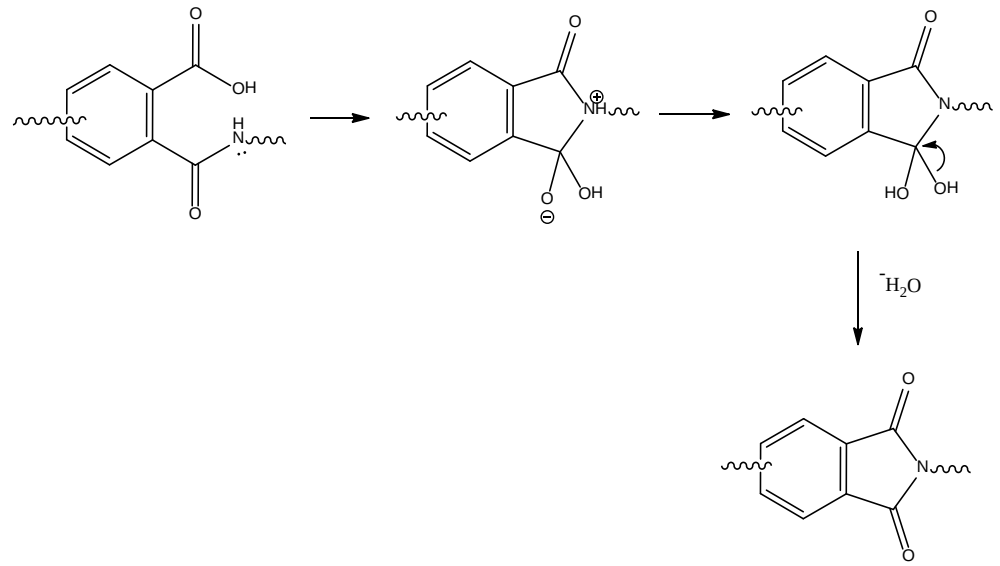

Mechanism 2

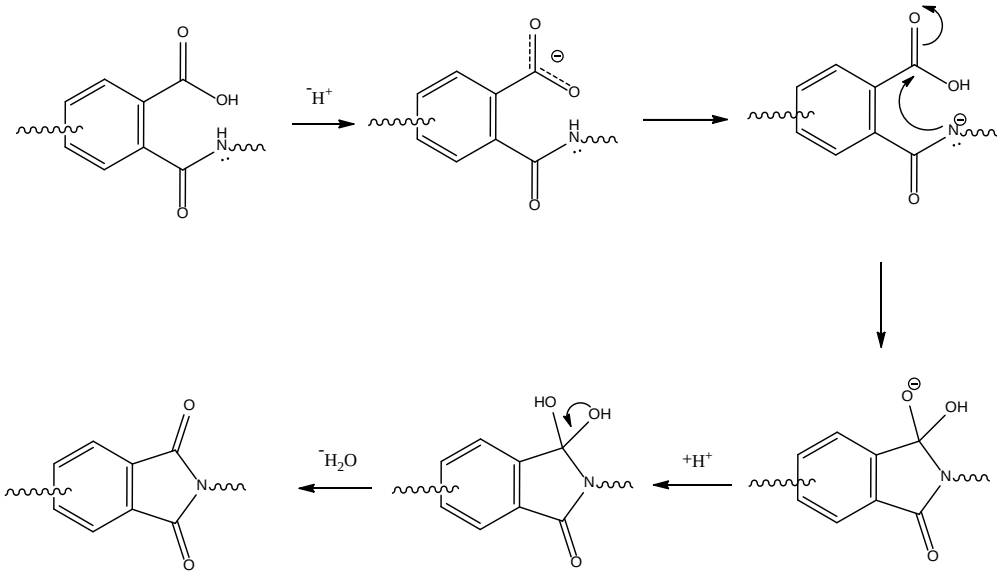

Figure 1.19 Two possible mechanisms for thermal imidization

As the rigid aromatic imide structure is formed, the Tg of the polymer increases dramatically, which results in reduced chain mobility and bond rotation[93]. Therefore, the intramolecular cyclodehydration rate decreases, which impedes complete imidization[96]. The leftover uncyclized amic acid structures are not hydrolytically stable and are considered defective sites[50]. The amic acid unit will give side reactions (Figure 1.18) and cause chain degradation (chain scission and crosslinking).

During the bulk thermal imidization, water will be generated and released as a vapor. However, the effectiveness of water release from the polymer is not well controlled. If the water is trapped in the polymer, that water will react with the amic acid unit, forming a diacid chain end which decreases the molecular weight of the polymers. In addition, the volatile water and residual solvents released during thermal imidization will cause voids and film shrinkage[91,95].

1.3.1.1.4. Chemical Imidization Method

Poly(amic acid) can be cyclized to form either a soluble or insoluble polyimide by chemical dehydration at or slightly above room temperature. There are various combinations of reagents for chemical imidization, but the common reagents are an acid anhydride (such as acetic anhydride) in the presence of a catalytical tertiary amine such as pyridine[50]. It has been shown that different reagents will show a preference for either an imide or isoimide product[50,97]. For example, acetic acid with a strong tertiary base such as triethylamine will cyclize the poly(amic acid) to a polyimide dominant product whereas a trifluoroacetic anhydride and pyridine combination will convert polyamic acid exclusively to polyisoimide[98].

The proposed mechanism of chemical imidization[50,97] indicates that in the presence of a basic tertiary amine catalyst, the polyamic acid mixes with acetic anhydride to form a poly (amic anhydride) intermediate which may tautomerize. The amide tautomer cyclizes to form an imide structure, which is the thermodynamically preferred product, while the iminol tautomer forms the kinetically preferred isoimide structure.

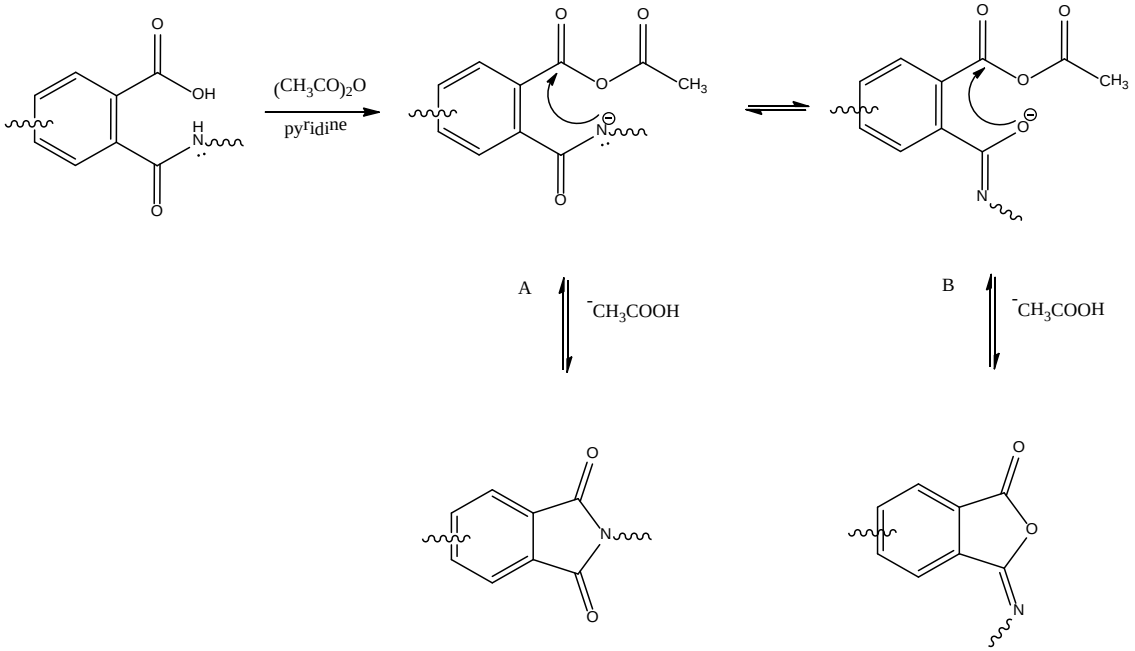

Figure 1.20 Mechanism of chemical imidization

1.3.1.1.5. Solution Imidization Method

Soluble polyimides may also be formed from poly(amic acid) in solutions under high temperature, 160°C-190°C, in the presence of an azeotropic agent. The azeotropic agent, such as *o*-dichlorobenzene or cyclohexyl pyrrolidone, is used in order to remove the water generated from the imidization to complete the polymerization[99,100].

The kinetics and mechanism for this imidization of a homogeneous system in solution have been studied by several research groups. It is suggested that the rate-determining step of the solution imidization via polyamic acid is an acid-catalyzed second-order reaction[101,102]. During solution imidization, it has been found that the viscosity of the solution initially has a significant reduction, and then increases gradually. Moreover, the viscosity reduction of solution imidization at the first step has been successfully explained by 2D-H^1 NMR, where the polyamic acid has some chain scissions and forms an anhydride and amine initially, converting to polyimides at the

end of the reaction[87]. A possible mechanism (Figure 3.6) of solution imidization has been proposed by Kim et al.[87]

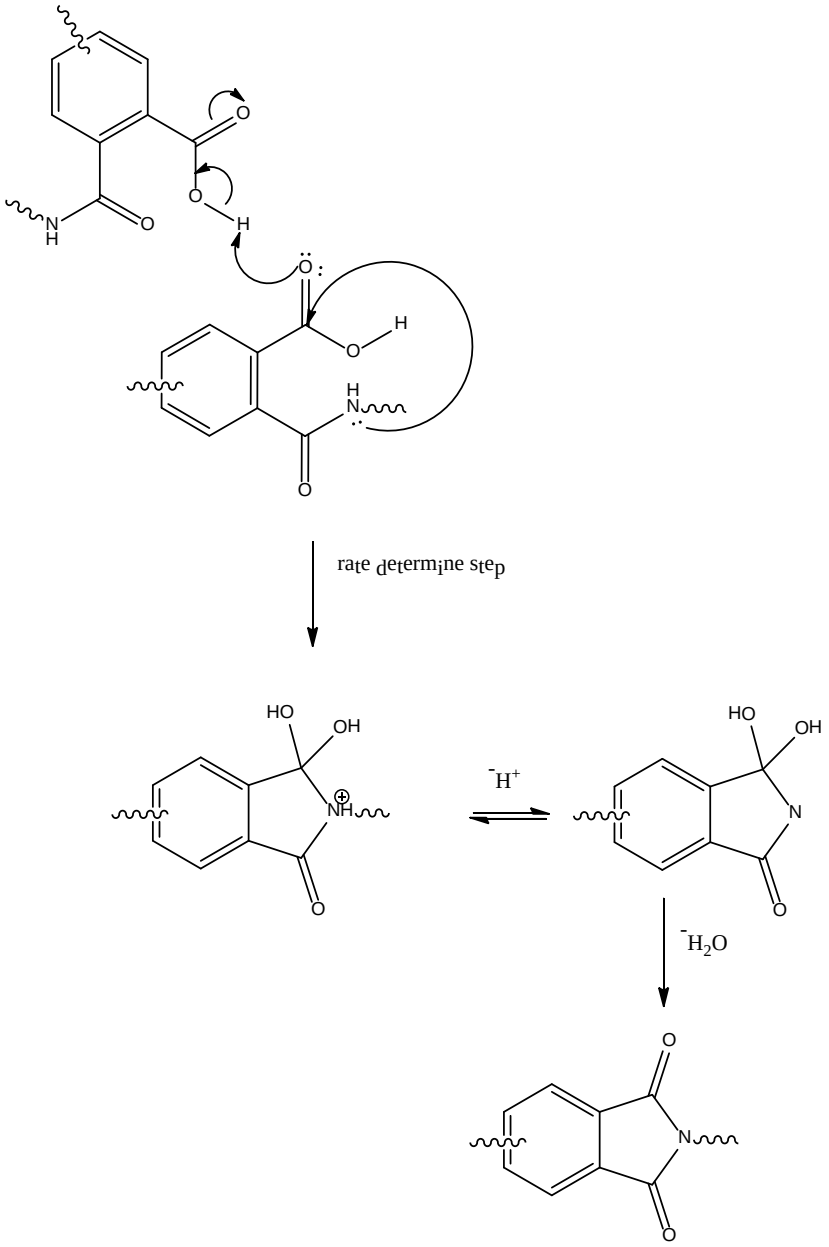

Figure 1.21 Mechanism for solution imidization

In contrast to thermal (bulk) imidization, solution imidization has advantages including complete imidization and a lower reaction temperature during the imidization process.[103] However, the solution imidization method is used in the production of soluble polyimides.

1.3.1.2. Polyimide Synthesis via the Ester-Acid Method

In the 1970s, Serafini et al.[104] from NASA introduced a method to make polyimides from dianhydrides and diamines, in which the dianhydride is modified into a diester-diacid monomer. In the ester-acid method depicted in Figure 3.7, the dianhydride monomers are initially refluxed in excess with an aliphatic alcohol such as ethanol to convert the aromatic dianhydride to the diester-diacid form. This diester-diacid formation step is usually accelerated by using an amine catalyst, such as triethylamine, as an acid acceptor. After the excess alcohol has evaporated, the diamine solution is introduced into the system in a polar aprotic solvent. The polyimide is then formed by increasing the temperature (170-185°C) in the presence of an azeotropic agent such as *o*-dichlorobenzene.

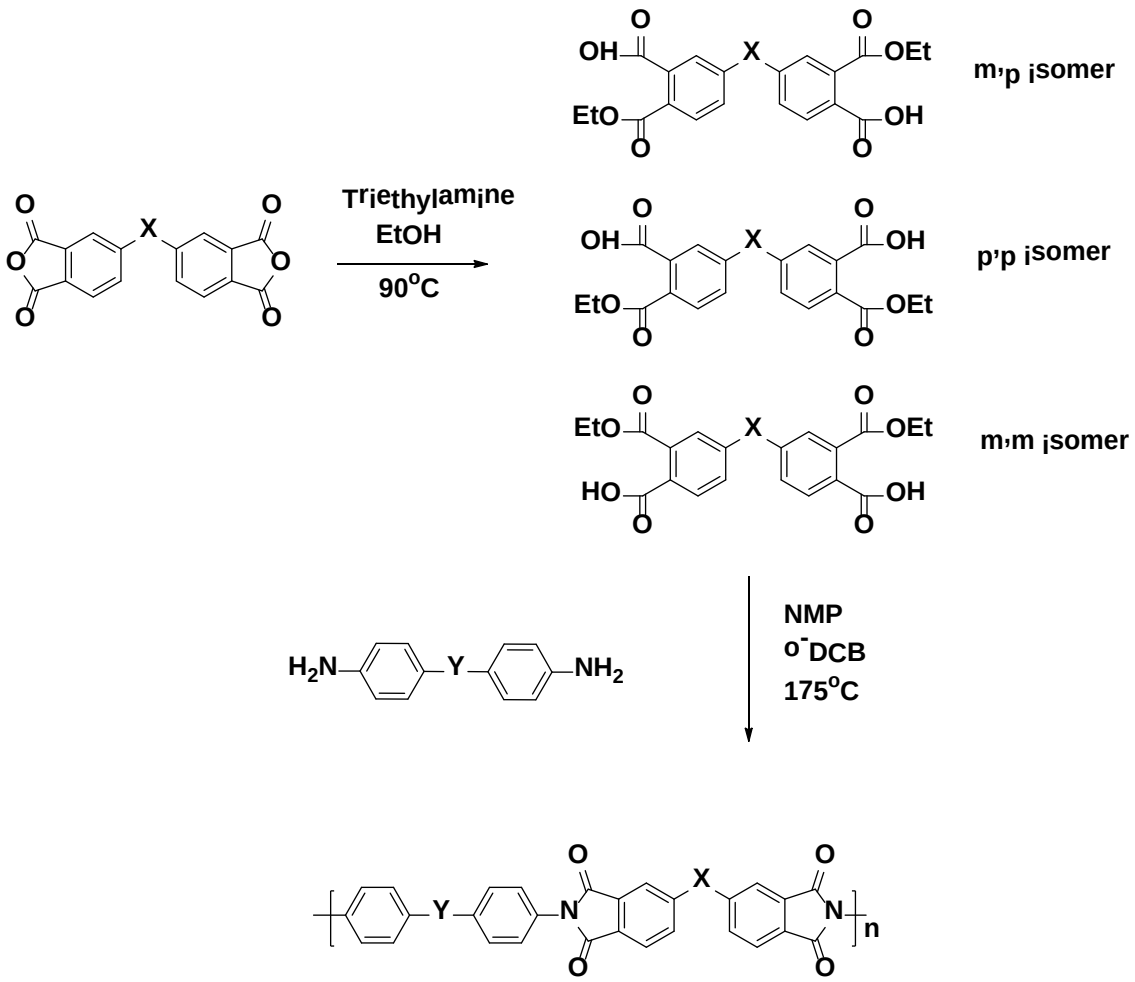

Figure 1.22 Synthesis scheme for polyimides by the ester acid route

The diester-diacid monomers that convert the dianhydrides may have up to 3 isomers depending on the symmetry of the dianhydrides, all of which are relatively more stable and soluble at an ambient temperature[105–108]. In contrast to the dianhydride, the diester-diacid monomer will maintain the stoichiometry balance with the aromatic diamines since it is no longer sensitive to moisture. Moreover, the diester-diacid monomers are not reactive with aromatic diamines at room temperature which enables the preparation of stable solutions containing both monomers[109]. In conclusion, polyimide synthesis via the ester-acid route has the following advantages over classic polyimide synthesis via poly(amic acid)s: hydrolytic stability reduces the stringent requirements for a dry

solvent and equipment, the fully soluble monomers avoid interfacial type reactions, and complete imidization occurs in a one-pot process.

1.3.1.2.1. Mechanism of polyimide synthesis via ester-acid route

Initially, polyimide synthesis by the ester-acid method was considered similar to the classical two-step polyimide mechanism. However, early studies demonstrated that the formation of polyamic acid from a diester-diacid and aromatic diamine reaction was not detectable by *in-situ* FTIR.[110] Instead, Moy et al.[109] found that diester-diacid monomers reverted back to dianhydrides at high temperatures (120-140°C) in NMP with azeotropic agents. Additionally, the model reaction conducted by Moy showed that monoethyl phthalate(ester-acid) would react with an aniline form phthalimide when refluxed with toluene at a high temperature. On the other hand, diethyl phthalate and benzoic acid undergo no reaction with an aniline under the same conditions. Thus, the suggested mechanism of imide synthesis by the ester-acid method consists of ester-acid monomers undergoing an *in-situ* formation of anhydrides, which can acylate aromatic amines, thus forming amic acid intermediates. Since *in-situ* FTIR fails to detect amic acid intermediates,[110] it is hypothesized that the amic acid intermediates have an extremely short lifetime at high temperatures, quickly progressing to imide formation or reverting back to dianhydride[109]. Hence, the concentration of amic acid is too low to be detected by FTIR.

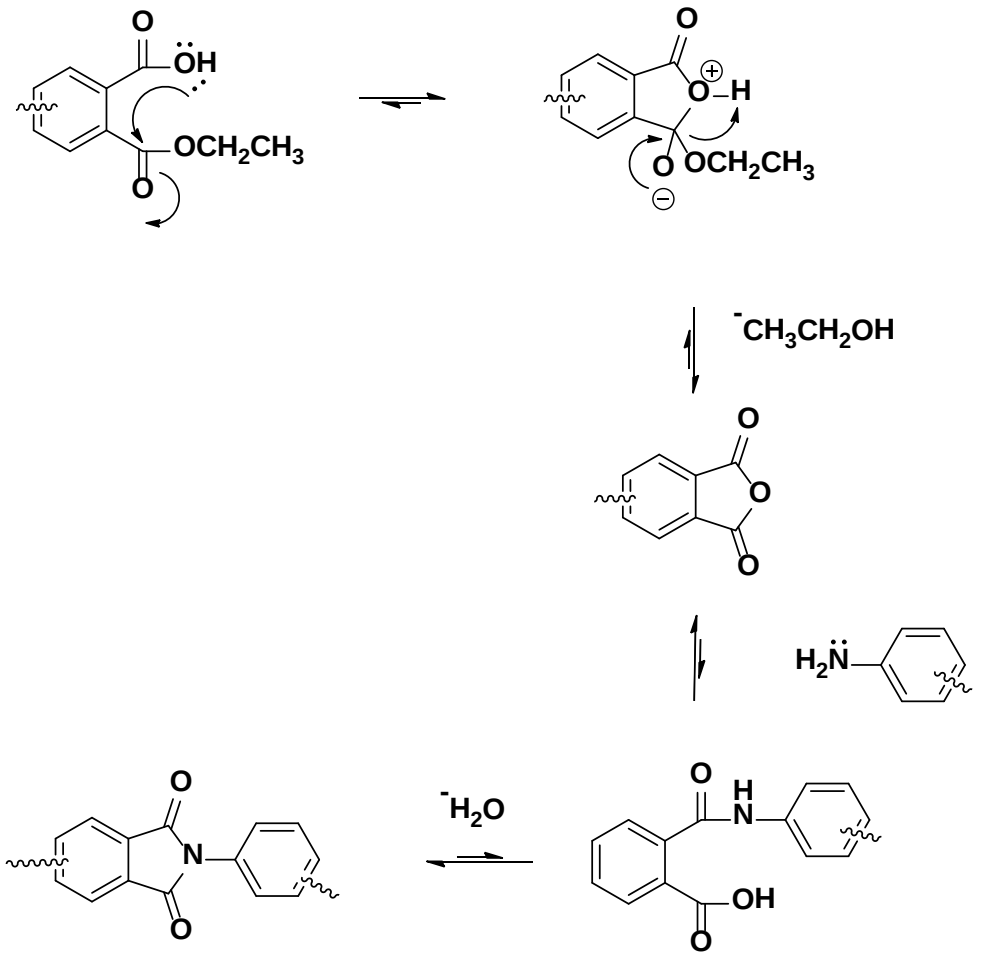

Figure 1.23 Mechanism for polyimide formation by the ester acid route109

1.3.1.3. Other Synthetic Routes to Polyimides

Besides the methods of polyimide synthesis mentioned above, various additional synthetic strategies have been reported[50]. Among these methods, many form derivatized poly(amic acid) precursors (such as alkyl ester, silyl esters, and ammonium salts) for their improved stability and solubility, and then cyclize the precursors to form polyimides. However, there are several other unique synthetic routes for polyimide synthesis.

1.3.1.3.1. Synthesis of Polyimides from Dianhydrides and Diisocyanates

The synthesis of high molecular weight polyimides made from dianhydride and diisocyanates was developed in the early 1960s, although the reaction of alkyl and aryl isocyanates with carboxylic acid anhydrides to form imides was reported roughly a century before[111]. In contrast to the synthesis of polyimides by a poly(amic acid) precursor, the preparation of polyimides from diisocyanate and dianhydride is less studied. Nevertheless, the chemistry of this synthesis route is commonly accepted to include 7-membered ring intermediates, which then proceed to form a polyimide with the release of CO_2[50].

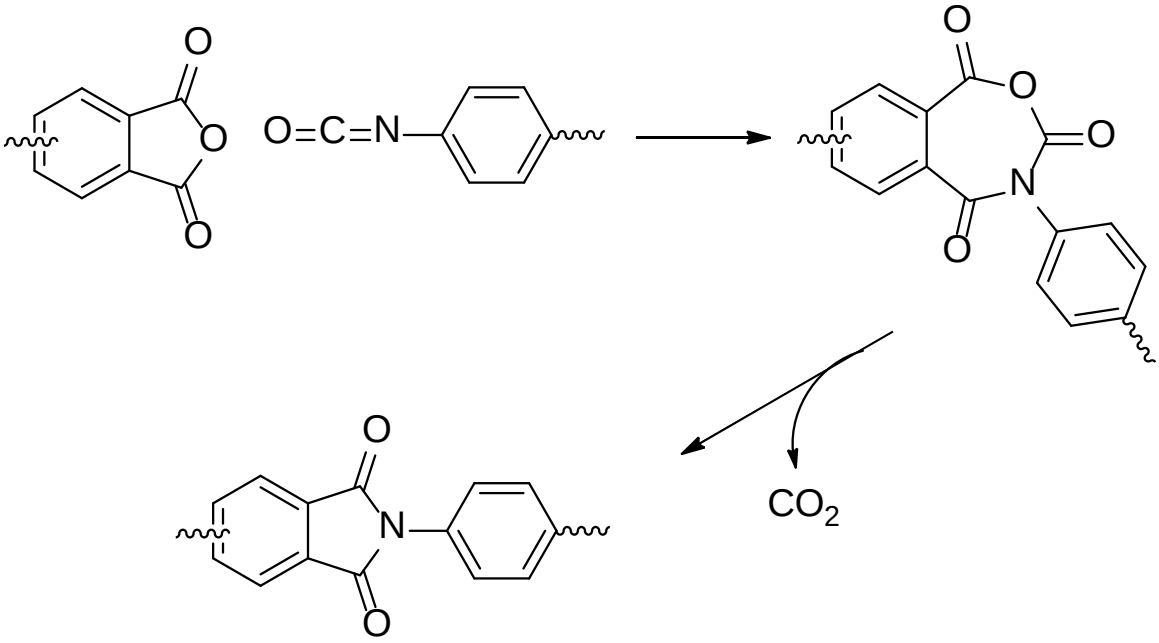

Figure 1.24 Synthesis of polyimides from diisocyanates and dianhydrides

Generally, polyimide synthesis using the diisocyanate route initially needs to be conducted at a low temperature (ca. 0°-10°C) in order to minimize the reaction of isocyanates with the solvent[112]. Then, the reaction is elevated to a higher temperature (50°-150°C) to complete the formation of polyimides and the release of CO_2. Some

studies[50,111] have reported that the addition of water or some other catalyst, such as tertiary amines, will accelerate the formation of polyimides by hydrolysis of the isocyanates and anhydrides.

Ultimately, the synthesis of polyimides by a diisocyanate route is less preferable compared to the poly(amic acid) route since the release of CO_2 acts as a boiling agent. However, this method is useful for polyimide foam preparation[51].

1.3.1.3.2. Synthesis of Polyimides by Transimidization

The transimidization method is also known as the amine-imide exchange reaction. The preparation of polyimides by this method starts with diamines and N, N'-substituted bisimide monomers[113]. Bisimide monomers initially undergo a nucleophilic attack on the carbonyl carbon to generate a poly(amic amide) intermediate[114]. This intermediate can be cyclized, which releases amines as by-products at high temperatures to form the polyimide. It is notable because during this equilibrium process, both the monoamine and the diamines can also be the leaving group.

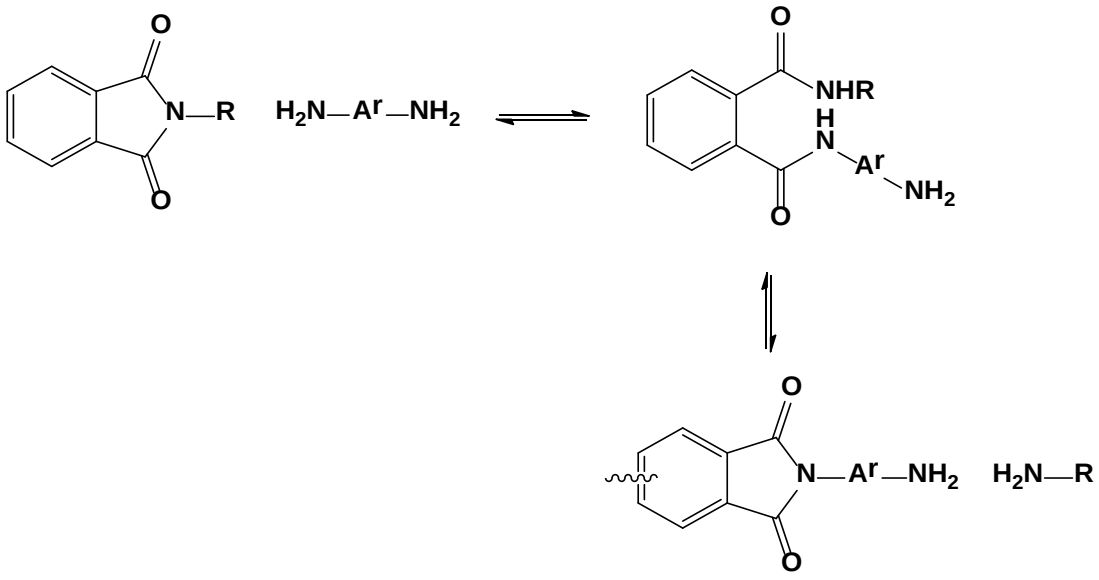

Figure 1.25 Synthesis of Polyimides by Transimidization

There are 3 main ways to achieve high molecular weight polyimides via transimidization. First, if the volatile monoamine is distilled out of the reaction, it will push the equilibrium to the right to promote polyimide formation. Second, the use of a bisimide such as 2-aminopyridine[115] releases less reactive (less basic/nucleophilic) monoamines as the leaving group, therefore hindering the reaction. Third, the use of a catalyst such as organo-metallic catalysts containing zinc, lead, or cadmium reduces the basicity/nucleophilicity of the monoamine[116] and therefore shifts the exchange reaction going forward to complete the polymerization.

1.3.2. Thermal Rearranged Polyimides

1.3.2.1. Thermal Rearrangement Process

Generally, the thermal rearrangement process occurs as the temperature reaches the glass transition temperature of the precursor polyimides. Therefore, the thermal rearrangement reaction ranges from the glass transition temperature to the temperature where the degradation occurred in the polymer membrane. For instance, Figure 3.11 shows a thermal gravimetric analysis of the HAB-6FDA-EA TR precursor. The highlighted region indicates its thermal rearrangement. The TR conversion of the membrane is controlled by the time and the temperature. For example, the low-conversion samples were held at 350°C for 60 mins., and the high-conversion samples were held at 450°C for 30 mins.

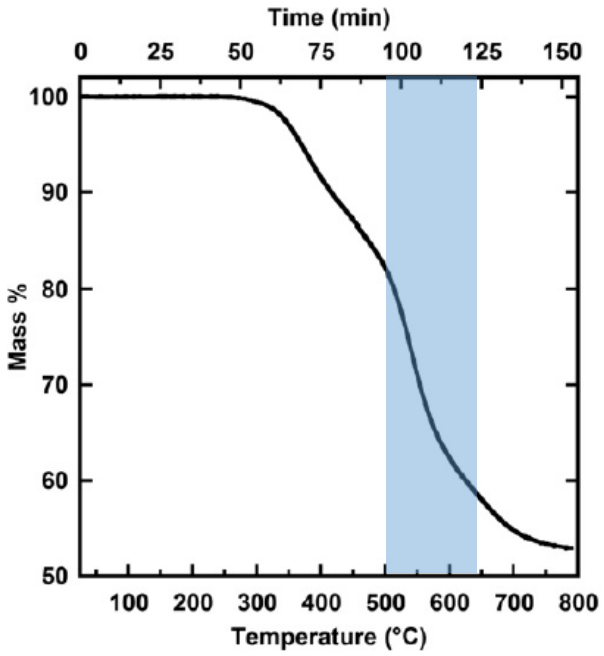

Figure 1.26 Thermal gravimetric analysis of TR precursor polyimides. From J. Memb. Sci. 2012, 409-410, 232–241, Sanders, D. F.; Smith, Z. P.; Ribeiro, C. P.; Guo, R.; McGrath, J. E.; Paul, D. R.; Freeman, B. D. Gas Permeability, Diffusivity, and Free Volume of Thermally Rearranged Polymers Based on 3,3'-Dihydroxy-4,4'-Diamino-Biphenyl (HAB) and 2,2'-Bis-(3,4-Dicarboxyphenyl) Hexafluoropropane Dianhydride (6FDA). Used with permission of Elsevier, 2012. [82]

Normally, an inert atmosphere (such as N_2, Argon, or a vacuum) is needed for the thermal conversion of TR-able polyimides. However, if the functional groups of the polyimides are ester groups (such as acetate or pivalic acetate), the thermal rearrangement can occur both in an inert atmosphere or in air. Guo et al.[84] hypothesizes that the acetate groups may protect the –OH groups from premature oxidation in air.

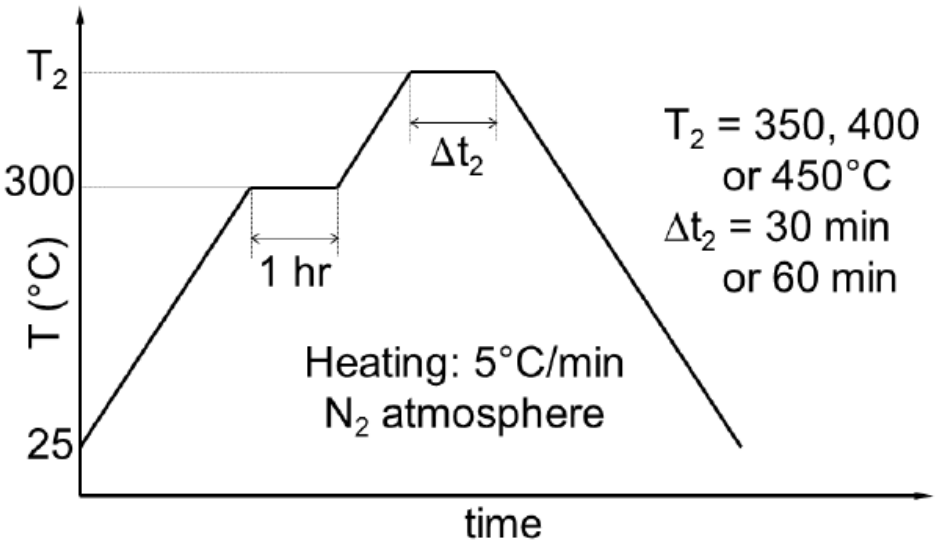

Figure 1.27 Thermal rearrangement protocol. From J. Memb. Sci. 2012, 409-410, 232–241, Sanders, D. F.; Smith, Z. P.; Ribeiro, C. P.; Guo, R.; McGrath, J. E.; Paul, D. R.; Freeman, B. D. Gas Permeability, Diffusivity, and Free Volume of Thermally Rearranged Polymers Based on 3,3'-Dihydroxy-4,4'-Diamino-Biphenyl (HAB) and 2,2'-Bis-(3,4-Dicarboxyphenyl) Hexafluoropropane Dianhydride (6FDA). Used with permission of Elsevier, 2012.[82]

The degree of the thermal rearrangement conversion of the membranes can be quantified by the weight difference between the precursors and the final TR polymer, since a significant weight loss can be detected during the thermal treatment. Therefore, the degree of conversion towards the final thermally rearranged product is usually defined as:

$$\%Conversion = \frac{Actual\ Mass\ Loss}{Theoretical\ Mass\ Loss} \times 100\% \quad (3.1)$$

The Actual Mass Loss is the weight loss that has been measured after the thermal treatment and the Theoretical Mass Loss is the expected weight loss if the imide-to-benzoxazole conversion is fully achieved.

The assessment of conversion from Equation 3.1 assumes that the actual mass loss is exclusively caused by the imide-to-benzoxazole thermal conversion shown in Figure 1.27. However, thermal degradation, particularly at high temperatures, may also occur simultaneously with the TR process to give rise to weight loss[2]. Additionally, the

conversion of the polyimide to the TR polymer could proceed by an intermolecular reaction as well as an intramolecular conversion. Furthermore, during the thermal conversion the loss of the pendant acetate groups, leaving a hydroxyl group in their place, would then undergo the thermal rearrangement to form the benzoxazole moieties, which contribute to the observed weight loss. The conversion calculation does not account for these potential situations. Thus to fully understand the molecule origins of weight loss, information from FTIR and mass spectrometry coupled with TGA is necessary to determine the final structure.

1.3.2.2. Mechanism of thermal rearrangement process of TR-able polyimides

The insolubility of TR polymers limits the number of characterization methods that can be employed. Therefore, ATR-FTIR becomes a very efficient way to study the structure of these polymers. The real mechanism of the thermal rearrangement process of ortho-functionalized polyimides is still under investigation. However, it is universally accepted that intermolecular reactions are occurring during the thermal treatment[86,117,118]. There is a commonly satisfied hypothesis that the mechanism involves intra- and inter- molecular cyclization, forming a benzoxazole structure from imide structures. Figure 3.12 shows the proposed mechanism involved in the thermal cyclization of ortho-functionalized polyimides to form polybenzoxazoles[63,119]. In this proposed mechanism, a hydroxyl-containing polyimide and a carboxyl-benzoxazole have been suggested as the intermediates. The hydroxyl-imide ring rearranged to a carboxyl-benzoxazole followed by decarboxylation in the range of 350–450 ◦C, leads to a fully aromatic benzoxazole structure. As mentioned previously, the thermal rearrangement temperature depends on the Tg of the polyimide precursors[83], as the flexibility of the precursors is strictly related to the thermal rearrangement conversion and restrictions imposed by intermolecular interactions. The intermediate state has

bulky carboxylic acid groups leading to steric hindrance and chain disruption, hence after cyclocarboxylation some free volume could be generated with a statistical combination of meta- and para- linked benzoxazole structures. The thermally rearranged polybenzoxazole chains are assumed to be much more rigid than the precursor chains, so that any physical changes after the thermal conversion would be irreversible[63].

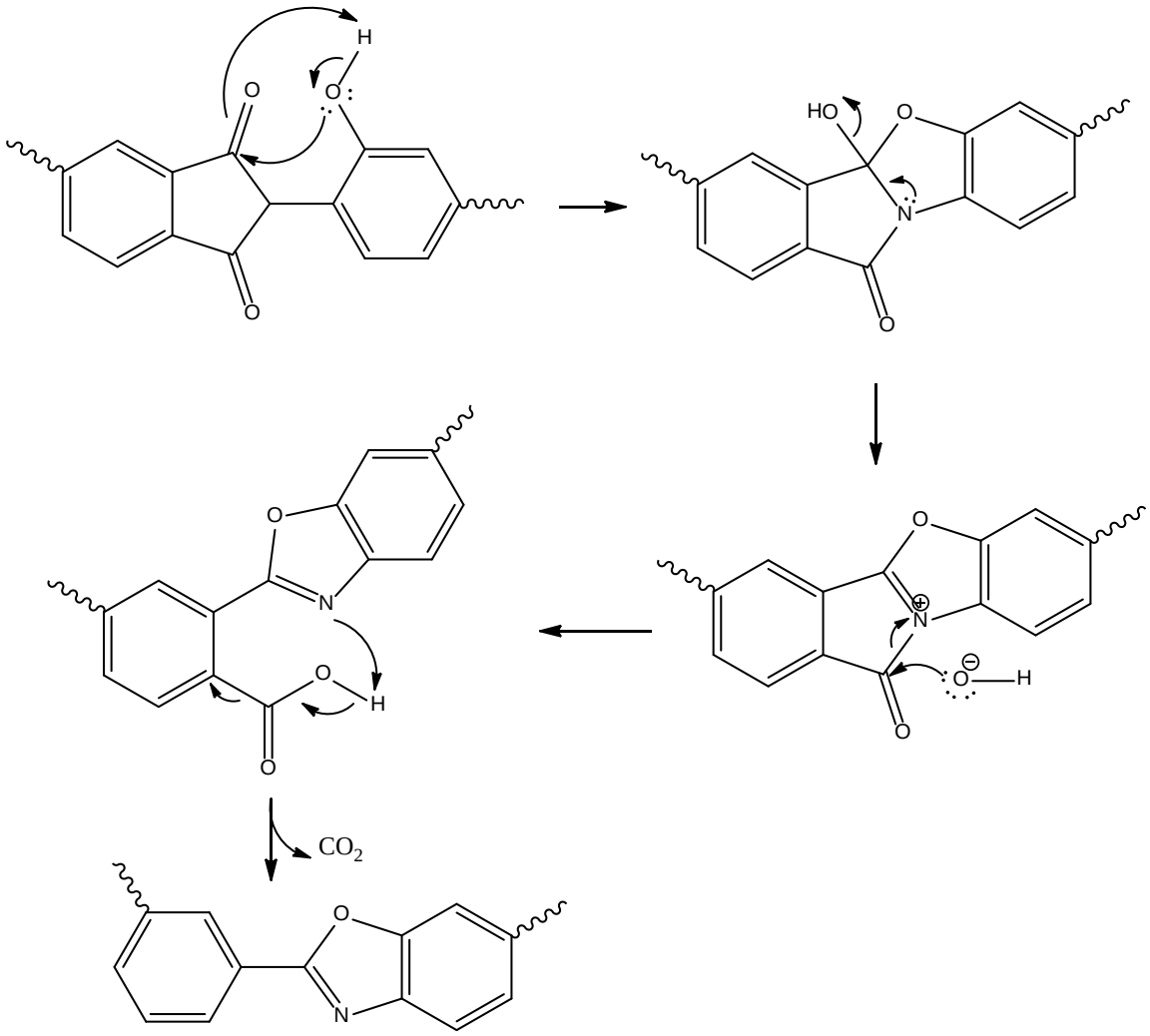

Figure 1.28 Proposed mechanism for imide to benzoxazole rearrangement. From Polymer. 2012, 53, 2783–2791Calle, M.; Chan, Y.; Jo, H. J.; Lee, Y. M. The Relationship between the Chemical Structure and Thermal Conversion Temperatures of Thermally Rearranged (TR) Polymers. Used with permission of Elsevier, 2012.[63]

1.4. Synthesis of Polybenzimidazoles

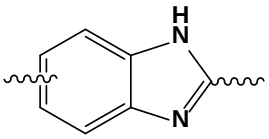

Figure 1.29 Heterocyclic benzimidazole ring

Polybenzimidazoles are a type of polymeric material which contains the heterocyclic benzimidazole ring (Figure 4.1) in their backbone chains. Aromatic polybenzimidazoles are famous for their excellent thermal stability, which was initially reported by Vogel and Marvel[65] in 1961. Research related to synthetic techniques in the field of aromatic polybenzimidazoles continued until the 1990s. In this chapter, significant aromatic polybenzimidazole synthesis techniques, including melt polymerization and solution polymerization, will be discussed.

1.4.1. Synthesis of Polybenzimidazoles by Melt Polymerization

The first reported aromatic polybenzimidazole with high molecular weight and high thermal stability was melt polymerized by Carl S. Marvel in 1961[65]. In this approach, the melt polycondensation of 3,3'-diaminobenzidine or 1,2,4,5-tetraaminobenzene with the diphenyl esters of a large number of aromatic dicarboxylic acids (such as diphenylisophthalate) was carried out by heating, under nitrogen, at temperatures gradually increasing from about 200 to 300 °C. After the melt solution had solidified, the system was continually heated for a short time under a vacuum. These initially low molecular weight solids were powdered and reheated under a high vacuum for several hours at temperatures gradually rising to 400 °C to eventually form a high molecular weight polybenzimidazole.

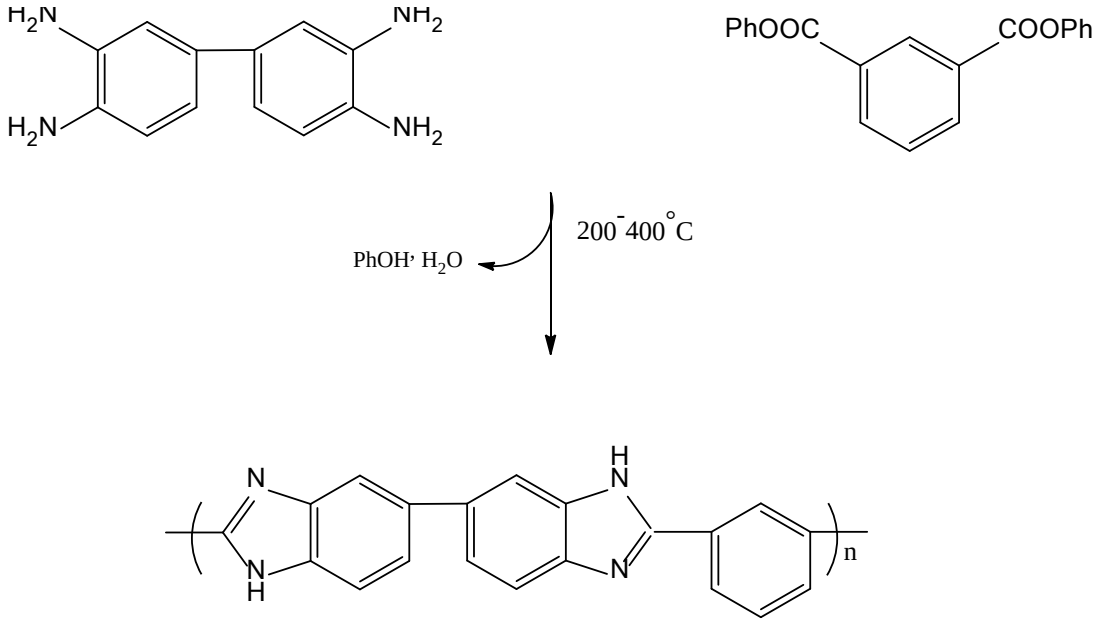

Figure 1.30 Synthesis of polybenzimidazole by melt polymerization

There are two proposed mechanisms for the melt polymerization of polybenzimidazoles.[120] Warsidlo et al.[121] postulated that during the reaction an intermediate with C=N moiety (Schiffs base-type structure) is formed and then cyclizes to a benzimidazoline, which subsequently eliminates phenol upon forming the final imidazole structure. Warsidlo observed the C=N moiety in the ultraviolet spectra during the condensation of phenyl benzoate and *o*-phenylenediamine which supports this finding. On the other hand, Gray et al.[122] postulated that a polyamic acid intermediate is formed, which then undergoes dehydration and cyclization to the imidazole. Gray et al. believes that the elimination of the weakly basic phenoxy group should be used in the initial reaction sequence and the elimination of water will occur at the end of the sequence.

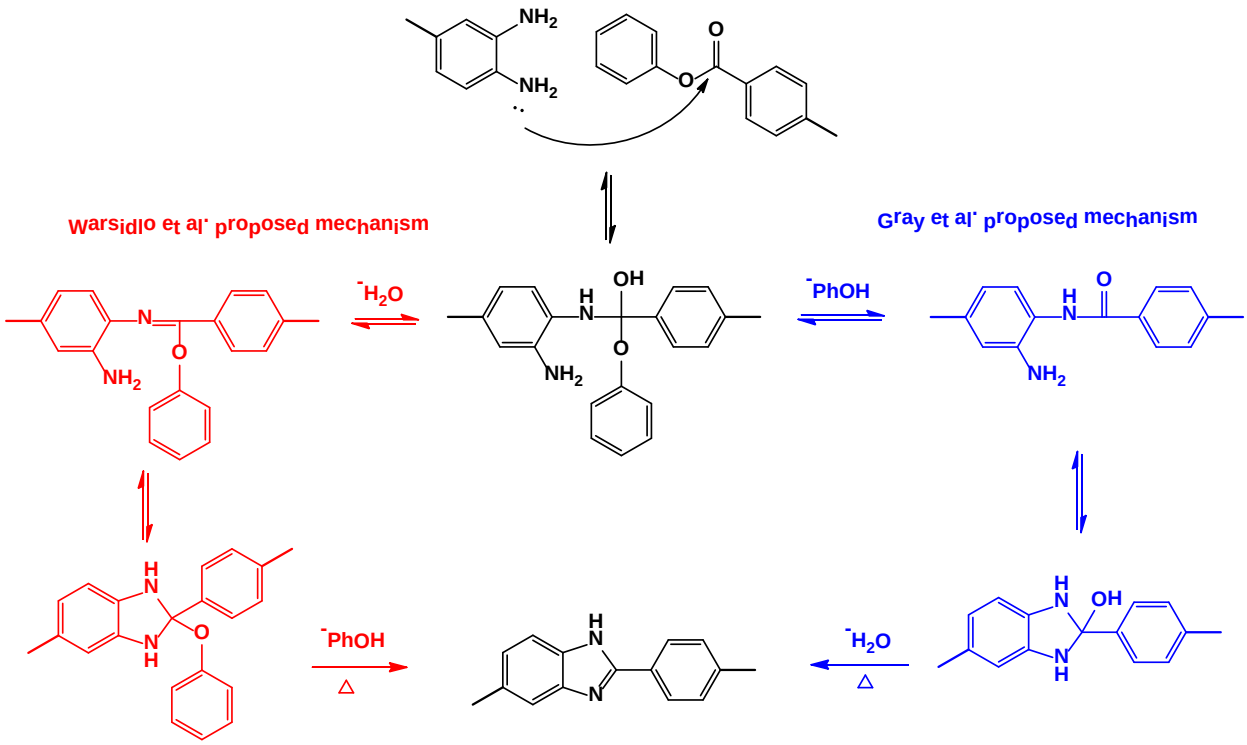

Figure 1.31 Two proposed mechanisms of polybenzimidazole formation by melt polymerization

With minor modifications, Marvel's original procedure has been further developed by himself and many others[123–127]. This procedure is still used as the principal approach for laboratory synthesis as a specialty preparation in adhesives, foam, and fiber applications, and pilot plant development manufacturing[70]. However, PBI that is produced by melt polycondensation cannot be processed by any other standard technique besides spinning and film casting, due to the lack of satisfactory solubility in non-corrosive solvents. Since this synthetic technique fails to provide well-defined fully soluble polymers to be used for the final processing, it has very limited use on the application side[70].

1.4.2. Synthesis of Polybenzimidazole in Dipolar Aprotic Solutions

In 1970, Higgins et al.[128] published procedures for the polymerization of tetramines with the bisulfite adducts of dialdehydes in polar aprotic solvents. These

polymerizations were performed at the reflux temperatures of the solvents (165-200°C). However, it is believed that the employment of dialdehydes and tetramines to form polybenzimidazole will caused branching and crosslinking due to the side reactions[120].

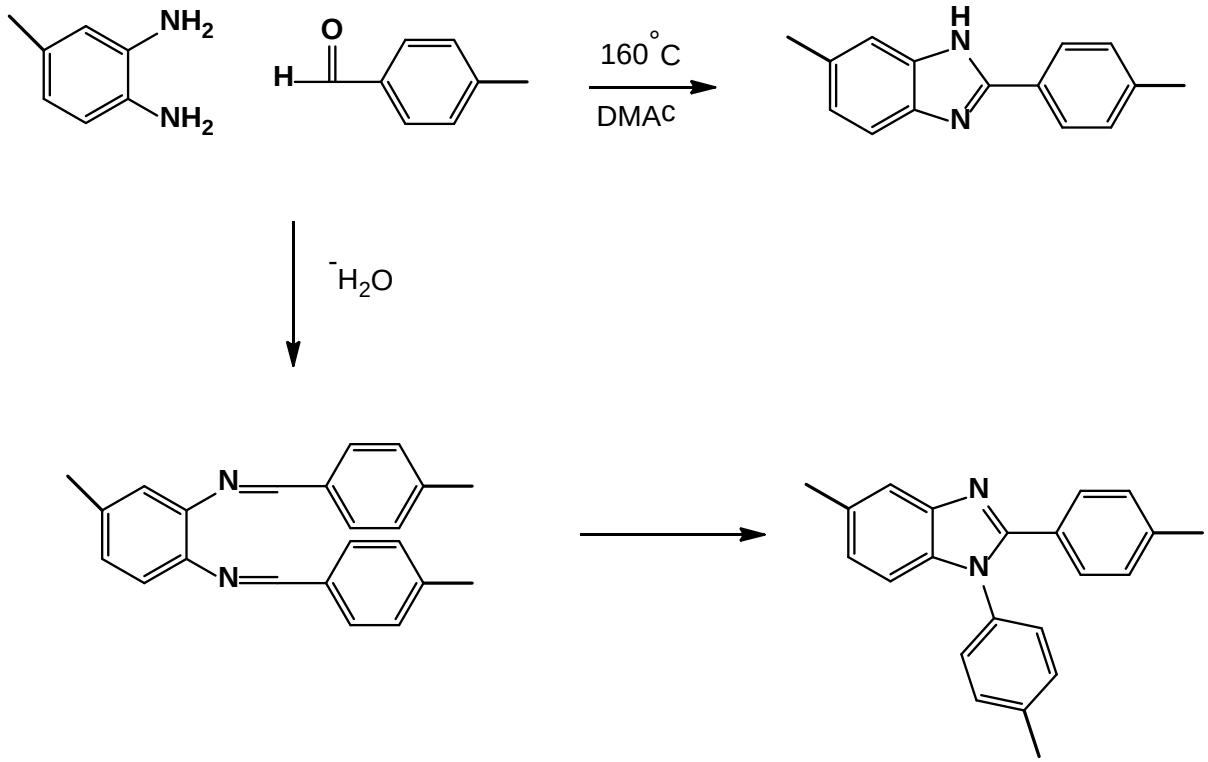

Figure 1.32 Synthesis of PBI from dialdehyde and tetramine in solution

Consequently, a patent issued by D'Alelio[129] provided for the preparation of linear polybenzimidazoles by the solution polymerization of aromatic tetramines with free dialdehydes in dipolar aprotic solvents at 100-125 °C in the presence of air. In this case, dialdehyde solution was added slowly to tetramine so that mono Schiff base structures would be dominant and di Schiff base products would be reduced to minor or negligible quantities. Therefore the mono Schiff base structures will intermediately undergo oxidative cyclodehydration[130] to form polybenzimidazoles. Hence, crosslinked structures are minimized under this procedure.

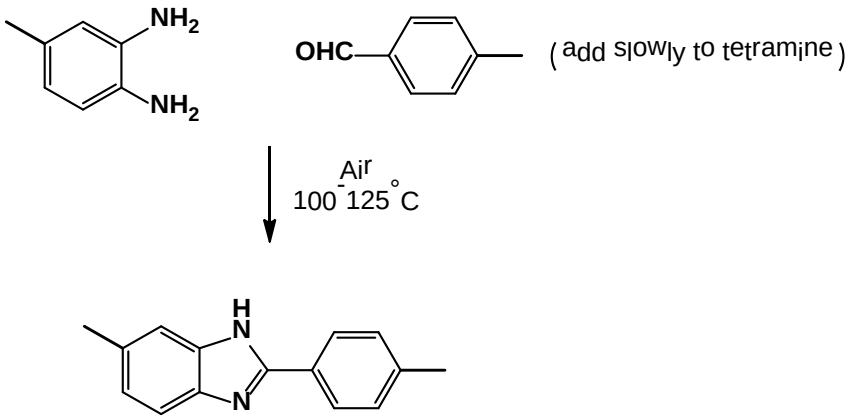

Figure 1.33 D'Alelio's approach to synthesis of PBI from dialdehyde and tetramine in dipolar aprotic solvents

Later, in 1983, Neuse et al.[131] extended the previous work on solution polymerization of PBI and reported on two-step polybenzimidazole synthesis in a dipolar aprotic solvent. In this two-step synthesis, a linear precursor polymer, polyazomethine, is formed in the first stage under controlled conditions (inert environment, -18 to +25°C). The precursor polyazomethine may afford oxidative cyclodehydration under a mild temperature (60-100°C) to eventually form a linear polybenzimidazole in solution. A general synthetic scheme of two-step polybenzimidazole synthesis is shown in Figure 4.6.

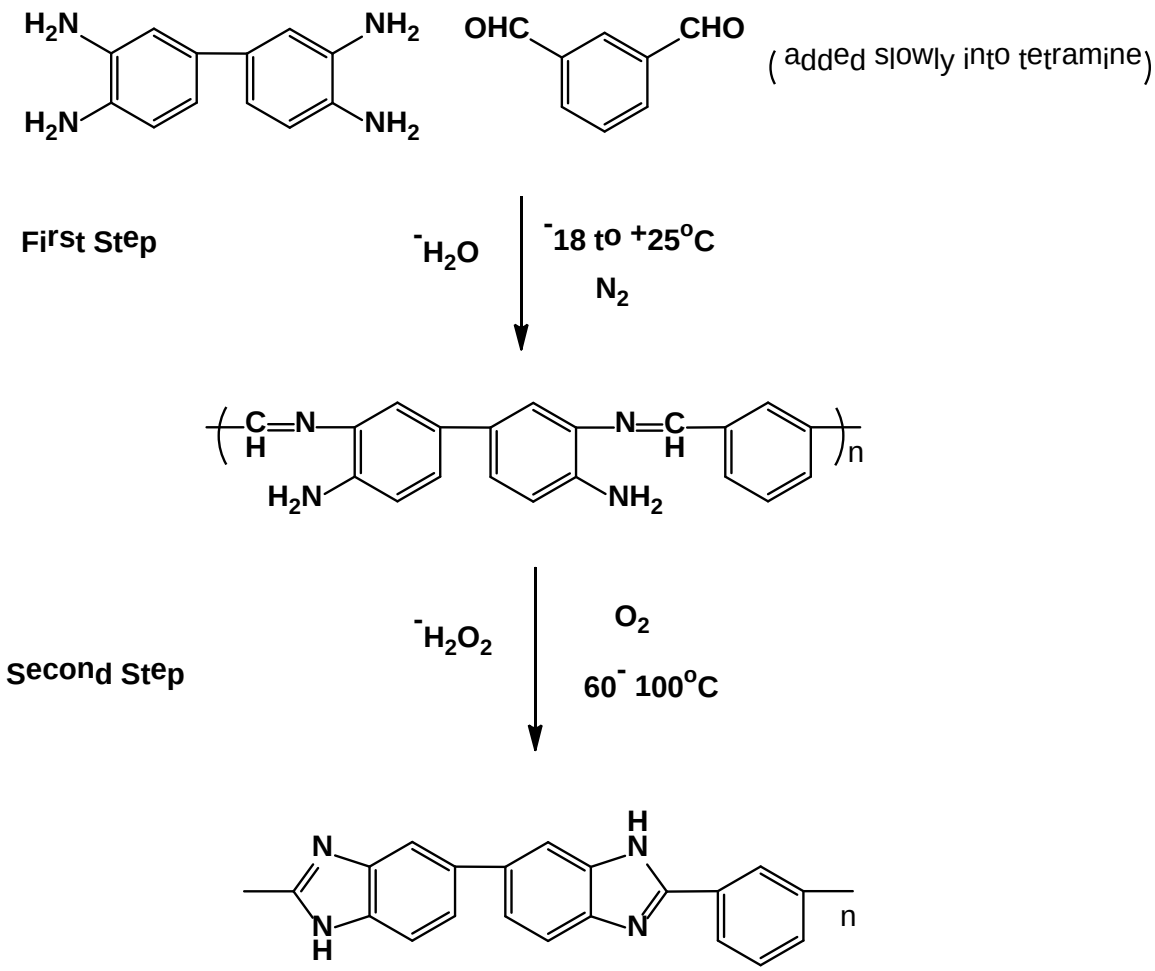

Figure 1.34 Two-step synthesis of linear PBI in DMAc

This two-step synthetic approach surpassed conventional polybenzimidazole synthesis involving melt and solid-state or poly(phosphoric acid) solution polymerization techniques while offering two significant advantages[131]. First, a soluble linear precursor can be prepared for final polybenzimidazole generation. Second, only mild conditions are necessary, which avoids exposure at high temperature and/or acidic environments in conventional PBI synthesis.

1.4.3. Synthesis of Polybenzimidazole in Acidic Solutions

In the early years of polybenzimidazoles research, Hein et al.[132] reported that 2-aryl-substituted benzimidazoles can be synthesized by the polyphosphoric acid catalyzed condensation of a carboxylic acid with an *o*-diaminobenzene. In 1963, after

Dr. Marvel published the synthesis of polybenzimidazoles by melt polymerization, Yoshio Iwakura showed that polybenzimidazoles can also be polymerized at 200°C in polyphosphoric acid as both a solvent and condensation agent[133,134]. This technique offers an advantage as tetramine monomers may be employed as stable and easy-to-handle hydrochlorides in place of the extremely air-sensitive free bases[70]. In addition, the reaction temperature (180-200°C) is much lower than the classical melt process (280-400°C). One disadvantage is that the reaction is difficult to handle due to the highly viscous nature of polyphosphoric acid[135,136]. Moreover, polyphosphoric acid tends to be incorporated into, or strongly adsorbed into, polar polymeric compounds. Therefore the removal of residue polyphosphoric acid may be an issue[137]. In spite of these challenges, this synthetic method has been extensively used for the preparation of acid-doped PBI fuel cell membranes[138].

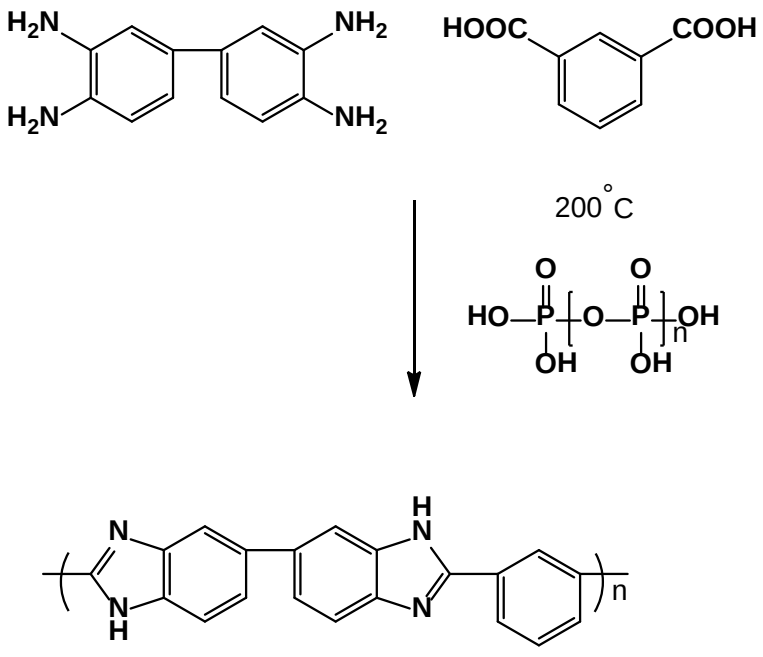

Figure 1.35 Synthesis of linear high molecular weight PBI in polyphosphoric acid.

In 1972, Eaton et al.[137] reported that a mixture of phosphorous pentoxide and methanesulfonic acid (1:10 by weight) can be used as a better alternative condensing

reagent than polyphosphoric acid. Later, Ueda et al.[136] successfully demonstrated that the polymerization of polybenzimidazoles can be achieved in a mixture of phosphorous pentoxide and methanesulfonic acid (which is also named Eaton's reagent or PPMA) at 140°C. Compared with polyphosphoric acid, the polymerization of polybenzimidazole in Eaton's reagent has obvious advantages such as the utilization of a lower temperature and the improved ease of removing any residual solvent[135,136,138]. Today, the preparation of polybenzimidazoles in Eaton's reagent (PPMA) is a commonly used approach in academic laboratories[86,140].

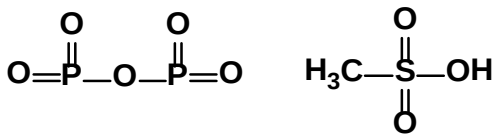

Figure 1.36 Structures of phosphorous pentoxide and methanesulfonic acid

1.5. Reference

(1) Baker, R. W. Future Directions of Membrane Gas Separation Technology. *Ind. Eng. Chem. Res.* **2002**, *41*, 1393–1411.

(2) Sanders, D. F.; Smith, Z. P.; Guo, R.; Robeson, L. M.; McGrath, J. E.; Paul, D. R.; Freeman, B. D. Energy-Efficient Polymeric Gas Separation Membranes for a Sustainable Future: A Review. *Polymer.* **2013**, *54*, 4729–4761.

(3) Stern, S. A. Polymers for Gas Separations: The next Decade. *J. Memb. Sci.* **1994**, *94*, 1–64.

(4) Koros, W. J.; Fleming, G. K. Membrane-Based Gas Separation. *J. Memb. Sci.* **1993**, *83*, 1–80.

(5) Fahrenheit, G. D.; Faraday, M.; Carnot, S. Gas Separation and Purification of Industrial Gases. In *Industrial Gas Handbook: Gas Separation and Purification*; Kerry, F. G., Ed.; 2007.

(6) Ghosal, K.; Freeman, B. D. Gas Separation Using Polymer Membranes : An Overview. *Polym. Adv. Techologies* **1994**, *5*, 673–697.

(7) Du, N.; Park, H. B.; Dal-Cin, M. M.; Guiver, M. D. Advances in High Permeability Polymeric Membrane Materials for CO_2 Separations. *Energy Environ. Sci.* **2012**, *5*, 7306–7322.

(8) Baker, R. W.; Lokhandwala, K. Natural Gas Processing with Membranes: An Overview. *Ind. Eng. Chem. Res.* **2008**, *47*, 2109–2121.

(9) Yampolskii, Y. Polymeric Gas Separation Membranes. *Macromolecules* **2012**, *45*, 3298–3311.

(10) Mitchell, J. K. On the Penetrativeness of Fluids. *J. Memb. Sci.* **1995**, *100*, 11–16.

(11) Graham, T. On the Absorption and Dialytic Separation of Gases by Colloid Septa Part I . Action of a Septum of Caoutchouc. *J. Memb. Sci.* **1995**, 27–31.

(12) Boddeker, K. W. Commentary : Tracing Membrane Science. *J. Memb. Sci.* **1995**, *100*, 65–68.

(13) Freeman, B. D.; Pinnau, I.; Park, M. Polymeric Materials for Gas Separations. In *Polymer Membranes for Gas and Vapor Separation*; ACS Symposium Series 733; American Chemical Society: Washington, DC, **1999**; pp. 1–27.

(14) Mason, E. A. From Pig Bladders and Cracked Jars to Polysulfones : An Historical Perspective on Membrane Transport. *J. Memb. Sci.* **1991**, *60*, 125–145.

(15) Wijmans, J. G.; Baker, R. W. The Solution-Diffusion Model: A Review. *J. Memb. Sci.* **1995**, *107*, 1–21.

(16) Matteucci, S.; Yampolskii, Y.; Freeman, B. D.; Pinnau, I. Transport of Gases and Vapors in Glassy and Rubbery Polymers. In *Materials Science of Membranes for Gas and Vapor Separation*; John Wiley & Sons, Ltd, **2006**; pp. 1–47.

(17) Michaels, A. S.; Parker, R. B. Sorption and Flow of Gases in Polyethylene. *J. Polym. Sci.* **1959**, *XLI*, 53–71.

(18) Fleming, G. K.; Koros, W. J. Dilation of Polymers by Sorption of Carbon Dioxide a T Elevated Pressures. 1. Silicone Rubber and Unconditioned Polycarbonate. *Macromolecules* **1986**, *19*, 2285–2291.

(19) Weinkauf, D. H.; Paul, D. R. Gas Transport Properties of Thermotropic Liquid-Crystalline Copolyesters. II. The Effects of Copolymer Composition. *J. Polym. Sci. Part B Polym. Phys.* **1992**, *30*, 837–849.

(20) Cohen, M. H.; Turnbull, D. Molecular Transport in Liquids and Glasses. *J. Chem. Phys.* **1959**, *31*, 1164–1169.

(21) Michaels, A. S.; Vieth, W. R.; Barrie, J. A. Solution of Gases in Polyethylene Terephthalate. *J. Appl. Phys.* **1963**, *34*, 1–12.

(22) Robeson, L. M. Correlation of Separation Factor versus Permeability for Polymeric Membranes. *J. Memb. Sci.* **1991**, *62*, 165–185.

(23) Freeman, B. D. Basis of Permeability/Selectivity Tradeoff Relations in Polymeric Gas Separation Membranes. *Macromolecules* **1999**, *32*, 375–380.

(24) Krevelen, D. W. Van; Nijenhuis, K. T. *Properties of Polymers*; 4th ed.; Elsevier B.V., **2009**.

(25) Robeson, L. M. The Upper Bound Revisited. *J. Memb. Sci.* **2008**, *320*, 390–400.

(26) Rowe, B. W.; Robeson, L. M.; Freeman, B. D.; Paul, D. R. Influence of Temperature on the Upper Bound: Theoretical Considerations and Comparison with Experimental Results. *J. Memb. Sci.* **2010**, *360*, 58–69.

(27) Turnbull, D.; Cohen, M. H. Free-Volume Model of the Amorphous Phase: Glass Transition. *J. Chem. Phys.* **1961**, *34*, 120–125.

(28) Bondi, A. Van Der Waals Volumes and Radii. *J. Phys. Chem.* **1964**, *68*, 441–451.

(29) Weinkauf, D. H.; Paul, D. R. Effects of Structural Order on Barrier Properties. In *Barrirer polymers and Structures*; ACS Symposium Series 423; American Chemical Society: Washington, DC, **1990**; pp. 60–91.

(30) Lee, W. M. Selection of Barrier Materials from Molecular Structure. *Polym. Eng. Sci.* **1980**, *20*, 65–69.

(31) Singh, A.; Freeman, B. D.; Pinnau, I. Pure and Mixed Gas Acetone/Nitrogen Permeation Properties of Polydimethylsiloxane [PDMS]. *J. Polym. Sci. Part B Polym. Phys.* **1998**, *36*, 289–301.

(32) Chern, R. T.; Provan, C. N. Gas-Induced Plasticization and the Permselectivity of Poly(tetrabromophenolphthalein Terephthalate) to a Mixtrue of Carbon Dioxide and Methane. *Macromolecules* **1991**, *24*, 2203–2207.

(33) Donohue, M. D.; Minhas, B. S.; Lee, S. Y. Permeation Behavior of Carbon Dioxide-Methane Mixtures in Cellulose Acetate Membranes. *J. Memb. Sci.* **1989**, *42*, 197–214.

(34) Bos, A.; Punt, I. G. M.; Wessling, M.; Strathmann, H. CO_2-Induced Plasticization Phenomena in Glassy Polymers. *J. Memb. Sci.* **1999**, *155*, 67–78.

(35) Kanehashi, S.; Nakagawa, T.; Nagai, K.; Duthie, X.; Kentish, S.; Stevens, G. Effects of Carbon Dioxide-Induced Plasticization on the Gas Transport Properties of Glassy Polyimide Membranes. *J. Memb. Sci.* **2007**, *298*, 147–155.

(36) Wind, J. D.; Sirard, S. M.; Paul, D. R.; Green, P. F.; Johnston, K. P.; Koros, W. J. Carbon Dioxide-Induced Plasticization of Polyimide Membranes: Pseudo-Equilibrium Relationships of Diffusion, Sorption, and Swelling. *Macromolecules* **2003**, *36*, 6433–6441.

(37) Wind, J. D.; Staudt-Bickel, C.; Paul, D. R.; Koros, W. J. Solid-State Covalent Cross-Linking of Polyimide Membranes for Carbon Dioxide Plasticization Reduction. *Macromolecules* **2003**, *36*, 1882–1888.

(38) Lin, H.; Freeman, B. D.; Kalakkunnath, S.; Kalika, D. S. Effect of Copolymer Composition, Temperature, and Carbon Dioxide Fugacity on Pure- and Mixed-Gas Permeability in Poly(ethylene Glycol)-Based Materials: Free Volume Interpretation. *J. Memb. Sci.* **2007**, *291*, 131–139.

(39) Tin, P. Effects of Cross-Linking Modification on Gas Separation Performance of Matrimid Membranes. *J. Memb. Sci.* **2003**, *225*, 77–90.

(40) Park, H. B.; Jung, C. H.; Lee, Y. M.; Hill, A. J.; Pas, S. J.; Mudie, S. T.; Van Wagner, E.; Freeman, B. D.; Cookson, D. J. Polymers with Cavities Tuned for Fast Selective Transport of Small Molecules and Ions. *Science* **2007**, *318*, 254–258.

(41) Guo, R.; Mcgrath, J. E. Aromatic Polyethers, Polyetherketones, Polysulfides, and Polysulfones. In *Polymer Science:A Comprehensive Reference*; Matyjaszewski, K.; Möller, M., Eds.; Elsevier B.V., **2012**; Vol. 5, pp. 377–430.

(42) Aitken, C. L.; Koros, W. J.; Paul, D. R. Gas Transport Properties of Biphenol Polysulfones. *Macromolecules* **1992**, *25*, 3651–3658.

(43) Erb, A. J.; Paul, D. R. Gas Sorption and Transport in Polysulfone. *J. Memb. Sci.* **1981**, *8*, 11–22.

(44) McHattie, J. S.; Koros, W. J.; Paul, D. R. Gas Transport Properties of Polysulphones : 2 . Effect of Bisphenol Connector Groups. *Polymer (Guildf).* **1991**.

(45) Ghosal, K.; Chern, R. T.; Freeman, B. D. Gas Permeability of Radel a Polysulfone. *J. Polym. Sci. Part B Polym. Phys.* **1993**, *31*, 891–893.

(46) Ghosal, K.; Chern, R. T.; Freeman, B. D.; Carolina, N.; Daly, W. H.; Negulescu, I. I. Effect of Basic Substituents on Gas Sorption and Permeation in Polysulfone. **1996**, 4360–4369.

(47) Aitken, C. L.; Koros, W. J.; Paul, D. R. Effect of Structural Symmetry on Gas Transport Properties of Polysulfones. *Macromolecules* **1992**, *25*, 3424–3434.

(48) Ghosal, K.; Chern, R. T. Aryl-Nitration of Poly(phenylene Oxide) and Polysulfone. Structural Characterization and Gas Permeability. *J. Memb. Sci.* **1992**, *72*, 91–97.

(49) McHattie, J. S.; Koros, W. J.; Paul, D. R. Gas Transport Properties of Polysulphones: 3. Comparison of Tetramethyl-Substituted Bisphenols. *Polymer.* **1992**, *33*, 1701–1711.

(50) Volksen, W. Condensation Polyimides: Synthesis, Solution Behavior, and Imidization Characteristics. *Adv. Polym. Sci.* **1994**, *117*, 111–164.

(51) Zhuang, H. Synthesis and Characteriation of Aryl Phosphine Oxide Containing Thermoplastic Polyimides and Thermosetting Polyimides with Controlled Reactivity, *PhD Thesis*. Virginia Tech, **1998**.

(52) Edgar, K. J.; Buchanan, C. M.; Debenham, J. S.; Rundquist, P. a; Seiler, B. D.; Shelton, M. C.; Tindall, D. Advances in Cellulose Ester Performance and Application. *Prog. Polym. Sci.* **2001**, *26*, 1605–1688.

(53) Loeb, S.; Sourirajan, S. Sea Water Demineralization by Means of an Osmotic Membrane. In *Saline Water Conversion II*; Advances in Chemistry Series 38; American Chemical Society: Washington, DC, **1963**; pp. 117–132

(54) Puleo, A. C.; Paul, D. R.; Kelley, S. S. The Effect of Degree of Acetylation on Gas Sorption and Transport Behavior in Cellulose Acetate. *J. Memb. Sci.* **1989**, *47*, 301–332.

(55) Schell, W. J.; Wensley, C. G.; Chen, M. S. K.; Venugopal, K. G.; Miller, B. D.; Stuart, J. a. Recent Advances in Cellulosic Membranes for Gas Separation and Pervaporation. *Gas Sep. Purif.* **1989**, *3*, 162–169.

(56) Story, B. J.; Koros, W. . Sorption of CO2/CH4 Mixtures in Poly(phenylene Oxide) and a Carboxylated Derivative. *J. Appl. Polym. Sci.* **1991**, *42*, 2613–2626.

(57) Chern, R. T.; Jia, L.; Shimoda, S.; Hopfenberg, H. B. A Note on the Effects of Mono- and Di-Bromination on the Transport Properties of poly(2,6-Dimethylphenylene Oxide). *J. Memb. Sci.* **1990**, *48*, 333–341.

(58) Hamad, F.; Khulbe, K. C.; Matsuura, T. Characterization of Gas Separation Membranes Prepared from Brominated Poly(phenylene Oxide) by Infrared Spectroscopy. *Desalination* **2002**, *148*, 369–375.

(59) Sridhar, S.; Smitha, B.; Ramakrishna, M.; Aminabhavi, T. M. Modified Poly(phenylene Oxide) Membranes for the Separation of Carbon Dioxide from Methane. *J. Memb. Sci.* **2006**, *280*, 202–209.

(60) Story, B. J.; Koros, W. J. Sorption and Transport of CO_2 and CH_4 in Chemically Modified Pol (phenylene Oxide). *J. Memb. Sci.* **1992**, *67*, 191–210.

(61) Park, H. B.; Han, S. H.; Jung, C. H.; Lee, Y. M.; Hill, A. J. Thermally Rearranged (TR) Polymer Membranes for CO_2 Separation. *J. Memb. Sci.* **2010**, *359*, 11–24.

(62) Yeong, Y. F.; Wang, H.; Pallathadka Pramoda, K.; Chung, T.-S. Thermal Induced Structural Rearrangement of Cardo-Copolybenzoxazole Membranes for Enhanced Gas Transport Properties. *J. Memb. Sci.* **2012**, *397-398*, 51–65.

(63) Calle, M.; Chan, Y.; Jo, H. J.; Lee, Y. M. The Relationship between the Chemical Structure and Thermal Conversion Temperatures of Thermally Rearranged (TR) Polymers. *Polymer.* **2012**, *53*, 2783–2791.

(64) Vogel, H.; Marvel, C. S. Polybenzimidazoles. II. *J. Polym. Sci. Part A* **1963**, *1*, 1532–1541.

(65) Vogel, H.; Marvel, C. S. Polybenzimidazoles, New Thermally Stable Polymers. *J. Polym. Sci.* **1961**, *50*, 511–539.

(66) Chung, T.-S. A Critical Review of Polybenzimidazoles. *J. Macromol. Sci. Part C* **1997**, *37*, 277–301.

(67) Sandor, R. B. PBI (Polybenzimidazole): Synthesis, Properties and Applications. *High Perform. Polym.* **1990**, *2*, 25–37.

(68) Model, F.; Lee, L. PBI Reverse Osmosis Membranes: An Initial Survey. In *Reverse Osmosis Membrane Research SE - 14*; Lonsdale, H. K.; Podall, H. E., Eds.; Springer US, **1972**; pp. 285–297.

(69) Li, X.; Qian, G.; Chen, X.; Benicewicz, B. C. Synthesis and Characterization of a New Fluorine-Containing Polybenzimidazole (PBI) for Proton-Conducting Membranes in Fuel Cells. *Fuel Cells* **2013**, 832–842.

(70) Neuse, E. W. Aromatic Polybenzimidazoles. Syntheses, Properties, and Applications. *Adv. Polym. Sci.* **2001**, *47*, 1–42.

(71) Xiao, L.; Zhang, H.; Scanlon, E.; Ramanathan, L. S.; Choe, E.; Rogers, D.; Apple, T.; Benicewicz, B. C. High-Temperature Polybenzimidazole Fuel Cell Membranes via a Sol-Gel Process. *Chem. Mater.* **2005**, *16*, 5328–5333.

(72) Noye, P.; Li, Q.; Pan, C.; Bjerrum, N. J. Cross-Linked Polybenzimidazole Membranes for High Temperature Proton Exchange Membrane Fuel Cells with Dichloromethyl Phosphinic Acid as a Cross-Linker. *Polym. Adv. Techologies* **2008**, *19*, 1270–1275.

(73) Mader, J. A.; Benicewicz, B. C. Sulfonated Polybenzimidazoles for High Temperature PEM Fuel Cells. *Macromolecules* **2010**, *43*, 6706–6715.

(74) Li, Q.; Jensen, J. O.; Savinell, R. F.; Bjerrum, N. J. High Temperature Proton Exchange Membranes Based on Polybenzimidazoles for Fuel Cells. *Prog. Polym. Sci.* **2009**, *34*, 449–477.

(75) Jorgensen, B. S.; Springs, J.; Young, J. S.; Espinoza, B. F. Cross-Linked Polybenzimidazole Membrane For Gas Separation. US 6,946,015 B2, **2005**.

(76) Hosseini, S. S.; Omidkhah, M. R.; Zarringhalam Moghaddam, A.; Pirouzfar, V.; Krantz, W. B.; Tan, N. R. Enhancing the Properties and Gas Separation Performance of PBI–polyimides Blend Carbon Molecular Sieve Membranes via Optimization of the Pyrolysis Process. *Sep. Purif. Technol.* **2014**, *122*, 278–289.

(77) Chung, T.; Xu, Z. Asymmetric Hollow Fiber Membranes Prepared from Miscible Polybenzimidazole and Polyetherimide Blends. *J. Memb. Sci.* **1998**, *147*, 35–47.

(78) Kumbharkar, S. C.; Karadkar, P. B.; Kharul, U. K. Enhancement of Gas Permeation Properties of Polybenzimidazoles by Systematic Structure Architecture. *J. Memb. Sci.* **2006**, *286*, 161–169.

(79) Kumbharkar, S. C.; Liu, Y.; Li, K. High Performance Polybenzimidazole Based Asymmetric Hollow Fibre Membranes for H_2/CO_2 Separation. *J. Memb. Sci.* **2011**, *375*, 231–240.

(80) Berchtold, K. A.; Singh, R. P.; Young, J. S.; Dudeck, K. W. Polybenzimidazole Composite Membranes for High Temperature Synthesis Gas Separations. *J. Memb. Sci.* **2012**, *415-416*, 265–270.

(81) Young, J. S.; Long, G. S.; Espinoza, B. F. Cross-Linked Polybenzimidazole Membrane for Gas Separation. US 6,997,971 B1, **2006**.

(82) Sanders, D. F.; Smith, Z. P.; Ribeiro, C. P.; Guo, R.; McGrath, J. E.; Paul, D. R.; Freeman, B. D. Gas Permeability, Diffusivity, and Free Volume of Thermally Rearranged Polymers Based on 3,3′-Dihydroxy-4,4′-Diamino-Biphenyl (HAB) and 2,2′-Bis-(3,4-Dicarboxyphenyl) Hexafluoropropane Dianhydride (6FDA). *J. Memb. Sci.* **2012**, *409-410*, 232–241.

(83) Guo, R.; Sanders, D. F.; Smith, Z. P.; Freeman, B. D.; Paul, D. R.; McGrath, J. E. Synthesis and Characterization of Thermally Rearranged (TR) Polymers: Influence of Ortho-Positioned Functional Groups of Polyimide Precursors on TR Process and Gas Transport Properties. *J. Mater. Chem. A* **2013**, *1*, 262.

(84) Guo, R.; Sanders, D. F.; Smith, Z. P.; Freeman, B. D.; Paul, D. R.; Mcgrath, J. E. Synthesis and Characterization of Thermally Rearranged (TR) Polymers : In Fl Uence of Ortho -Positioned Functional Transport Properties. **2013**, 262–272.

(85) Kim, S.; Han, S. H.; Lee, Y. M. Thermally Rearranged (TR) Polybenzoxazole Hollow Fiber Membranes for CO2 Capture. *J. Memb. Sci.* **2012**, *403-404*, 169–178.

(86) Calle, M.; Lozano, A. E.; Lee, Y. M. Formation of Thermally Rearranged (TR) Polybenzoxazoles: Effect of Synthesis Routes and Polymer Form. *Eur. Polym. J.* **2012**, *48*, 1313–1322.

(87) Kim, Y. J.; Glass, T. E.; Lyle, G. D.; McGrath, J. E. Kinetic and Mechanistic Investigations of the Formation of Polyimides under Homogeneous Conditions. *Macromolecules* **1993**, *26*, 1344–1358.

(88) Hodgkin, J. H. Reactivity Changes During Polyimide Formation. *J. Polym. Sci. Polym. Chem. Ed.* **1976**, *14*, 409–431.

(89) Bower, G. M.; Frost, L. W. Aromatic Polyimides. *J. Polym. Sci. Part A* **1963**, *1*, 3135–3150.

(90) Kaas, R. L. Autocatalysis and Equilibrium in Polyimide Synthesis. *J. Polym. Sci. Polym. Chem. Ed.* **1981**, *19*, 2255–2267.

(91) Frost, L. W.; Kesse, I. Spontaneous Degradation of Aromatic Polypyromellitamic Acids. *J. Appl. Polym. Sci.* **1964**, *8*, 1039–1051.

(92) Dine-Hart, R. A.; Wright, W. W. Preparation and Fabrication of Aromatic Polyimides. *J. Appl. Polym. Sci.* **1967**, *11*, 609–627.

(93) Takekoshi, T. Synthesis of Polyimides. In *Polyimides Fundamentals and Applications*; Ghosh, M. K.; Mittal, K. L., Eds.; Marcel Dekker: New York, **1996**; pp. 7–48.

(94) Snyder, R. W.; Thomson, B.; Bartges, B.; Czerniawski, D.; Painter, P. C. FTIR Studies of Polyimides: Thermal Curing. *Macromolecules* **1989**, *22*, 4166–4172.

(95) Harris, F. W. *Polyimides, Eds. D. Wilson, H. D. Stenzenberger and P. M. Hergenrother (Blackie & Son Ltd., Glasgow and London, **1990**).*

(96) Sroog, C. E. Polyimides. *J. Polym. Sci. Part C* **1967**, *16*, 1191–1209.

(97) Koton, M. M.; Kudryavtsev, V. V.; Zubkov, V. A.; Yakimanskii, A. V.; Meleshko, T. K.; Bogorad, N. N. Experimental and Theoretical Study of the Effect of Medium on Chemical Imidization. *Polymer Science U.S.S.R.*, 1984, *26*, 2839–2848.

(98) Roderick, W. R. Dehydration of N-(p-Chlorophenyl) Phthalamic Acid by Acetic and Trifluoroacetic Anhydrides. *J. Org. Chem.* **1964**, *29*, 745–747.

(99) Arnold, C. A.; Summers, J. D.; Chen, Y. P.; Bott, R. H.; Chen, D.; McGrath, J. E. Structure-Property Behaviour of Soluble Polyimide-Polydimethylsiloxane Segmented Copolymers. *Polymer.* **1989**, *30*, 986–995.

(100) Kreuz, J. a.; Endrey, a. L.; Gay, F. P.; Sroog, C. E. Studies of Thermal Cyclizations of Polyamic Acids and Tertiary Amine Salts. *J. Polym. Sci. Part A-1 Polym. Chem.* **1966**, *4*, 2607–2616.

(101) Solomin, V. A.; Kardash, I. E.; Snagovskii, I. S.; Messerle, P. E.; Zhubanov, B. A.; Pravendnikov, A. N. Kinetics of the Acylation of Amines by Aromatic and Alicyclic Carboxylic Acid Anhydrides. *Dokl. Akad. Nauk SSSR* **1977**, *236*, 139–142.

(102) Lavrov, S. V.; Ardashnikov, A. Y.; Kardash, I. Y.; Pravednikov, A. N. Cyclization of Aromatic Poly(amic Acids) to Polyimides. Cyclization Kinetics of a Model Compound of N-Phenylphthalamic Acid. *Polymer Science U.S.S.R.*, **1977**, *19*, 1212–1219.

(103) Dunson, D. L. Synthesis and Characterization of Thermosetting Polyimide Oligomers for Microelectronics Packaging, *PhD Thesis*. Virginia Tech, **2000**.

(104) Serafini, T. T.; Delvigs, P.; Lightsey, G. R. Thermally Stable Polyimides from Solutions of Monomeric Reactants. *J. Appl. Polym. Sci.* **1972**, *16*, 905–915.

(105) Farr, I. V.; Glass, T. E.; Ji, Q.; McGrath, J. E. Synthesis and Characterization of Diaminophenylindane Based Polyimides via Ester-Acid Solution Imidization. *High Perform. Polym.* **1997**, *9*, 345–352.

(106) Tan, B.; Tchatchoua, C. N.; Dong, L.; McGrath, J. E. Synthesis and Characterization of Arylene Ether Imide Reactive Oligomers and Polymers Containing Diaryl Alkyl Phosphine Oxide Groups. *Polym. Adv. Techologies* **1998**, *9*, 84–93.

(107) Moy, T. M.; DePorter, C. D.; McGrath, J. E. Synthesis of Soluble Polyimides and Functionalized Imide Oligomers via Solution Imidization of Aromatic Diester-Diacids and Aromatic Diamines. *Polymer*. **1993**, *34*, 819–824.

(108) Serafini, T. T.; Delvigs, P.; Lightsey, G. R. Thermally Stable Polyimides from Solutions of Monomeric Reactants. *J. Appl. Polym. Sci.* **1972**, *16*, 905–915.

(109) Moy, T. M.; DePorter, C. D.; McGrath, J. E. Synthesis of Soluble Polyimides and Functionalized Imide Oligomers via Solution Imidization of Aromatic Diester-Diacids and Aromatic Diamines. *Polymer*. **1993**, *34*, 819–824.

(110) Takekoshi, T.; Kochanowski, J. E.; Manello, J. S.; Webber, M. J. Polyetherimides. II. High-Temperature Solution Polymerization. *J. Polym. Sci. Polym. Symp.* **1986**, *74*, 93–108.

(111) Carleton, P. S.; Farrissey, W. J.; Rose, J. S. The Formation of Polyimides from Anhydrides and Isocyanates. *J. Appl. Polym. Sci.* **1972**, *16*, 2983–2989.

(112) Avadhani, C. V; Wadgaonkar, P. P.; Vernekar, S. P. Synthesis and Characterization of Oxyethylene Containing Diisocyanates and Polyirnides Therefrom. *J. Polym. Sci. Part A Polym. Chem.* **1990**, *28*, 1681–1691.

(113) Takekoshi, T.; Kochanowski, E. J. Method for Making Polyetherimides. US 3,850,855, **1974**.

(114) Rogers, M. E.; Glass, T. E.; Mecham, S. J.; Rodrigues, D.; Wilkes, G. L.; McGrath, J. E. Perfectly Alternating Segmented Polyimide-Polydimethyl Siloxane Copolymers via Transimidization. *J. Polym. Sci. Part A Polym. Chem.* **1994**, *32*, 2663–2675.

(115) Farr, I. V. Synthesis and Characterization of Novel Polyimide Gas Separation Membrane Material Systems, *PhD Thesis*. Virginia Tech, **1999**.

(116) Takekoshi, T.; Kochanowski, J. E. Method for Making Polyetherimides. US 3,850,855, **1974**.

(117) Fong, Y.; Wang, H.; Pallathadka, K.; Chung, T. Thermal Induced Structural Rearrangement of Cardo-Copolybenzoxazole Membranes for Enhanced Gas Transport Properties. *J. Memb. Sci.* **2012**, *397-398*, 51–65.

(118) Calle, M.; Chan, Y.; Jo, H. J.; Lee, Y. M. The Relationship between the Chemical Structure and Thermal Conversion Temperatures of Thermally Rearranged (TR) Polymers. *Polymer.* **2012**, *53*, 2783–2791.

(119) Tullos, G. L.; Powers, J. M.; Jeskey, S. J.; Mathias, L. J. Thermal Conversion of Hydroxy-Containing Imides to Benzoxazoles: Polymer and Model Compound Study. *Macromolecules* **1999**, *32*, 3598–3612.

(120) Sandor, R. B. PBI (Polybenzimidazole): Synthesis, Properties and Applications. *High Perform. Polym.* **1990**, *2*, 25–37.

(121) Wrasidlo, W.; Levine, H. H. Polybenzimidazoles. I. Reaction Mechanism and Kinetics. *J. Polym. Sci. Part A* **1964**, *2*, 4795–4808.

(122) Gray, D. N.; Shulman, G. P.; Conley, R. T. The Mechanism of Polybenzimidazole Formation by Condensation of Aromatic Tetramines and Esters and the Structure of the Resulting Polycondensates. *J. Macromol. Sci. Part A - Chem.* **1967**, *1*, 395–411.

(123) Prince, A. E.; Ridge, B. Process For The Polymerization of Aromatic Polybenzimidazoles. US 3,551,389, **1970**.

(124) Ward, B. C.; Jamison, C. E.; Rierson, Donald R., J. Improvements In Tw Stage Polybenzimidazole Process. EP 0,248,666, **1987**.

(125) Marvel, C. S.; Vogel, H. A. Polybenzimidazoles and Their Preparation. US 3,174,947, **1965**.

(126) Marvel, C. S.; Vogel, H. A. Polybenzimidazoles and Their Prepareation. US Re. 26,065, 1**966**.

(127) Levine, H. H. Fusible Polybenzimidazoles. US 3,386,969, **1968**.

(128) Higgins, J.; Marvel, C. S. Benzimidazole Polymers from Aldehydes and Tetraamines. *J. Polym. Sci. Part A-1 Polym. Chem.* **1970**, *8*, 171–177.

(129) D'Alelio, G. F. Polybenzimidazoles and Method of Preparation. US 3,763,107, **1973**.

(130) Coville, N. J.; Neuse, E. W. Oxidative Cyclodehydrogenation of Aromatic Bis(o-Aminoanils). *J. Org. Chem.* **1977**, *42*, 3485–3491.

(131) Neuse, E. W.; Loonat, M. S. Two-Stage Polybenzimidazole Synthesis via Poly(azomethine) Intermediates. *Macromolecules* **1983**, *16*, 128–136.

(132) Hein, D. W.; Alheim, R. J.; Leavitt, J. J. The Use of Polyphosphoric Acid in the Synhtesis of 2-Aryl- and 2-Alkyl-Substituted Benzimidazoles, Benzoxazoles and Benzothiazoles. *J. Am. Chem. Soc.* **1957**, *79*, 427–429.

(133) Iwakura, Y.; Uno, K.; Imai, Y. Process For Preparation of Polybenzimidazoles. US 3,313,783, **1967**.

(134) Iwakura, Y.; Uno, K.; Imai, Y. Polyphenylenebenzimidazoles. *J. Polym. Sci. Part A-1 Polym. Chem.* **1964**, *2*, 2605–2615.

(135) So, Y.-H.; Heeschen, J. P. Mechanism of Polyphosphoric Acid and Phosphorus Pentoxide-Methanesulfonic Acid as Synthetic Reagents for Benzoxazole Formation. *J. Org. Chem.* **1997**, *62*, 3552–3561.

(136) Ueda, M.; Sato, M.; Mochizuki, A. Poly(benzimidazole) Synthesis by Direct Reaction of Diacids and Tetramine. *Macromolecules* **1985**, 2723–2726.

(137) Levine, H. H. Polybenzothiazoles. In *Encyclopedia of polymer science and technology*; Mark, H. F.; Gaylord, N. G., Eds.; Wiley: New York, **1969**; Vol. 10, pp. 675–681.

(138) Hodgkin, J. H.; Liu, M. S.; Dao, B. N.; Mardel, J.; Hill, A. J. Reaction Mechanism and Products of the Thermal Conversion of Hydroxy-Containing Polyimides. *Eur. Polym. J.* **2011**, *47*, 394–400.

Chapter 2: Monomer Purification and Synthesis

2.1. Introduction

Aromatic polyimides, polybenzoxazoles, and polybenzimidazoles are classified as high performance polymers and are well-known for their thermo-stability. After extensive research and development, polyimides, polybenzoxazoles, and polybenzimidazoles all are used in commercial products. Among these polymers, polyimides have become the most widely used engineering plastics due to the low cost of available polyimides monomers and ease of polymerization[1]. Therefore, the production of low cost and novel monomers is one of the critical keys necessary for the production of next generation, economical, high performance polymers with the desired properties.

For step-growth polymerization, there are several criteria for monomers that must be met to produce high molecular linear polymers. First, monomers must be difunctional. Second, functional groups on monomers need to have high enough reactivity towards one another. Moreover, functional groups on monomers do not participate in any side reactions. Lastly, according to the Carothers equation, the monomers need to be added in a 1:1 molar stoichiometry for polymerization. Therefore, monomers must be prepared to near 100% purity, especially for AA-BB type step-growth polymerization, to ensure that high molecular weight polymers will be produced. The following section discusses the purification of commercially available monomers, as well as traditional and novel monomer synthesis.

2.2. Monomer and Reagent Purification

2.2.1. 4,4'-(Hexafluoroisopropylidene)diphthalic anhydride (6FDA)

Supplier: Air Products

Empirical Formula: $C_{19}H_6F_6O_6$

Molecular Weight (g/mol): 444.243

Melting point: 247 °C

Structure:

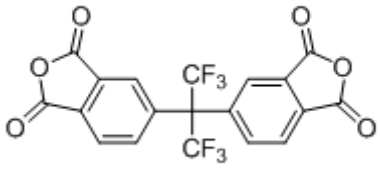

Purification: Polymer grade 6FDA was dried at ~180°C under a vacuum for at least 12 hours prior to use.

2.2.2. 3,3',4,4'-Benzophenone tetracarboxylic dianhydride (BTDA)

Supplier: Air Products

Empirical Formula: $C_{17}H_6O_7$

Molecular Weight (g/mol): 322.23

Melting point: 223 °C

Structure:

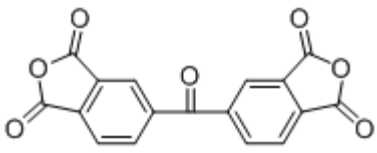

Purification: Polymer grade BTDA was dried at ~180°C under a vacuum for at least 12 hours prior to use.

2.2.3. 4,4’-(4,4’-Isopropylidenediphenoxy)bis(phthalic anhydride) (BisADA)

Supplier: Sigma Aldrich

Empirical Formula: $C_{31}H_{20}O_8$

Molecular Weight (g/mol): 520.49

Melting point: 191 °C

Structure:

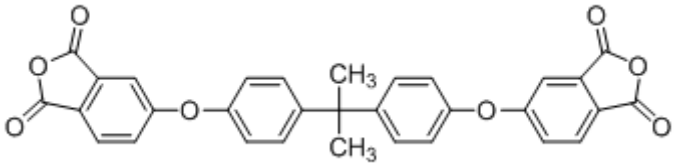

Purification: Polymer grade BisADA was dried at ~150°C under a vacuum for at least 12 hours prior to use.

2.2.4. 3,3'-Dihydroxy-4,4'-diamino-biphenyl (HAB)

Supplier: TCI America

Empirical Formula: $C_{12}H_{12}O_2N_2$

Molecular Weight (g/mole): 216.2

Melting point: 295-296°C

Structure:

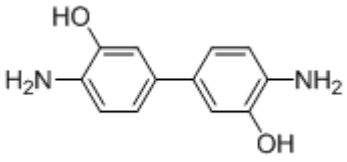

Purification: The HAB monomer (5.0 g, 23.1 mmol) was dissolved in DMAc (50 mL). After the insoluble impurities were filtered out, Methanol (50 mL) was then added in the solution.

2.2.5. 4, 4'-Biphenol

Supplier: Eastman Chemical Company

Empirical Formula: $C_{12}H_{10}O_2$

Molecular Weight (g/mole): 186.21

Melting point: 284°C

Structure:

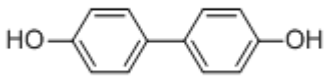

Purification: Monomer grade biphenol was used as received. If necessary, biphenol can be recrystallized from toluene. Biphenol was dried under a vacuum at 100°C for 12 hours before use in polymerization reactions or nitration reactions.

2.2.6. Bisphenol A

Supplier: Solvay

Empirical Formula: $C_{15}H_{16}O_2$

Molecular Weight (g/mole): 228.29

Melting point: 158°C

Structure:

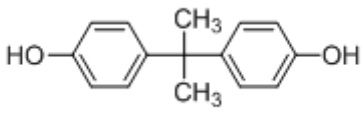

Purification: Bisphenol A was recrystallized from methanol to produce fine, needle-like, white crystals. Bisphenol A was dried under a vacuum at 100°C for 12 hours before use in polymerization reactions.

2.2.7. 4,4'-Dichlorodiphenyl sulfone (DCDPS)

Supplier: Solvay

Empirical Formula: $C_{12}H_8Cl_2O_2S$

Molecular Weight (g/mole): 287.16

Melting point: 143°C

Structure:

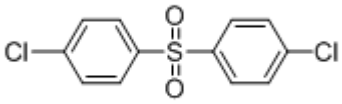

Purification: DCDPS was recrystallized from toluene to produce large, white crystals that were pulverized prior to drying. DCDPS was dried under a vacuum at 100°C for 12 hours before use in polymerization reactions.

2.2.8. 4,4'-Dichlorobenzophenone (DCBP)

Supplier: Solvay

Empirical Formula: $C_{13}H_8Cl_2O$

Molecular Weight (g/mole): 251.11

Melting point: 144-147°C

Structure:

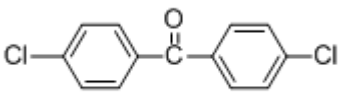

Purification: DCBP was dried at ~100°C under a vacuum for at least 12 hours prior to use.

2.2.9. Isophthalic acid (IPA)

Supplier: Amoco

Empirical Formula: $C_8H_6O_4$

Molecular Weight (g/mole): 166.14

Melting point: 347°C

Structure:

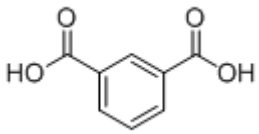

Purification: IPA was recrystallized from methanol to produce large, white crystals. IPA was dried under a vacuum at 100°C for 12 hours before use in polymerization reactions.

2.2.10. Terephthalic acid (TPA)

Supplier: Eastman

Empirical Formula: $C_8H_6O_4$

Molecular Weight (g/mole): 166.14

Melting point: 300°C

Structure:

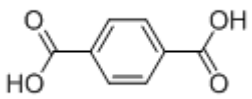

Purification: TPA was washed from methanol and then dried under a vacuum at 100°C for 12 hours before use in polymerization reactions.

2.2.11. Terephthaloyl chloride (TPC)

Supplier: TCI America

Empirical Formula: $C_8H_4Cl_2O_2$

Molecular Weight (g/mole): 203.02

Melting point: 81.5-83 °C

Structure:

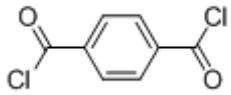

Purification: TPC was recrystallized from n-hexane. TPC was then dried under a vacuum at 50°C for 12 hours before use in polymerization reactions.

2.2.12. Isophthaloyl chloride (IPC)

Supplier: TCI America

Empirical Formula: $C_8H_4Cl_2O_2$

Molecular Weight (g/mole): 203.02

Melting point: 43-44°C

Structure:

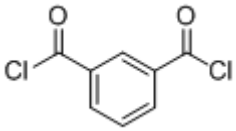

Purification: IPC was recrystallized from n-hexane. IPC was then dried under a vacuum at room temperature for 12 hours before use in polymerization reactions.

2.3. Monomer Synthesis

2.3.1. 3,3'-dinitro-4,4'dihydroxylbiphenyl

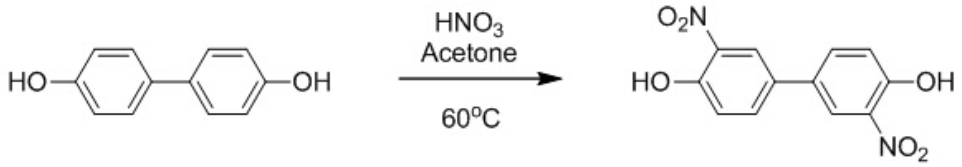

Figure 2.1. Preparation of crosslinked polybenzimidazoles using epoxy end capped polypropylene oxide

Molecular Weight: 276.2 g/mol

Experiment: Excess 4,4'-biphenol(12.2g, 65.5 mmol) and 250mL of Acetone were added to a 500-mL, 3-necked flask equipped with a condenser, mechanical stirrer, and addition funnel. The reaction mixture was stirred at 60°C until complete solubilization of 4,4'-biphenol. 11.9 grams of 69.3% Nitric acid (131.0 mmol) was added drop-wise via the addition funnel. Upon completion of the addition, the solution was stirred for 6 hours at 60°C. The final heterogeneous solution containing yellow precipitant was washed with copious acetone. The product was then filtered and dried in *vacuo* at 80°C with 87% yield. The ^{1}H-NMR spectrum is shown below.

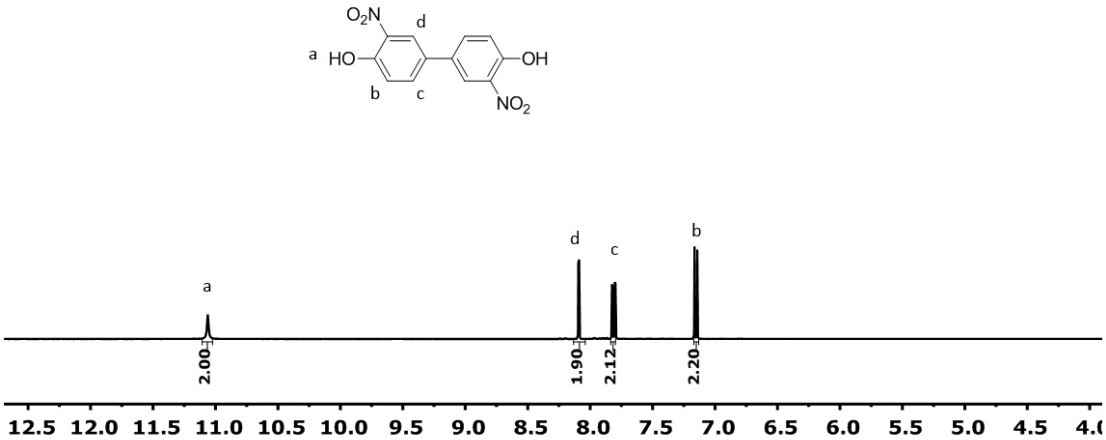

Figure 2.2. 1H NMR of 3,3'-dinitro-4,4'-dihydroxybiphenyl

2.3.2. 3,3’-diamino-4,4’dihydroxylbiphenyl

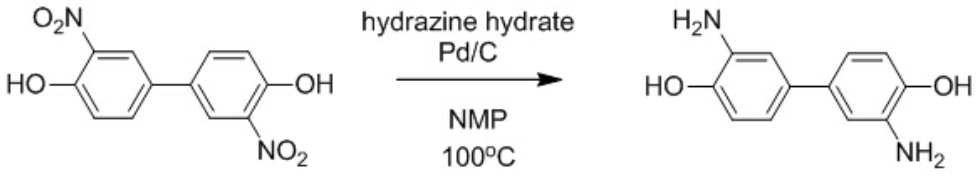

Figure 2.3. Synthesis of 3,3’-diamino-4,4’-dihydroxybiphenyl (m-HAB)

Molecular Weight: 216.24 g/mol

Experiment: 3,3’-dinitro-4,4’-dihydroxyl biphenyl(11.6g, 42.0mmol), 1.1g Pd/C, and 200ml NMP were added to a 500-mL, 3-necked flask equipped with a condenser, mechanical stirrer, and addition funnel. The reaction mixture was heated in a thermocouple regulated oil bath to 100^{o}C and stirred. 24mL of hydrazine hydrate (7M excess) was then added drop-wise. After completion of the addition, the solution was stirred and refluxed for 12 hours at 100^{o}C. The reaction mixture was then hot-filtered through Celite. 200ml methanol was slowly added into the hot-filtered solution. The product started to crystallize upon cooling. White crystals were filtered and washed with water. The final product was dried in *vacuo* at 100°C overnight with 81% yield. The ^{1}H-NMR spectrum is shown below.

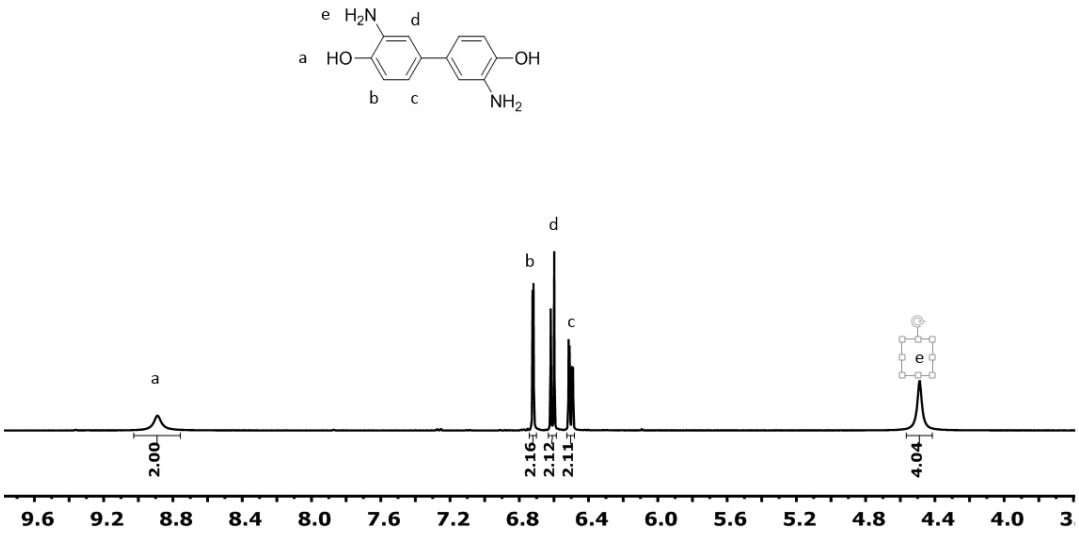

Figure 2.4. [1]H NMR of 3,3'-diamino-4,4'-dihydroxybiphenyl (m-HAB)

2.3.3. 4,4'-Methylenebis(2,6-dimethylphenol) (Tetramethyl bisphenol F, TMDPF)

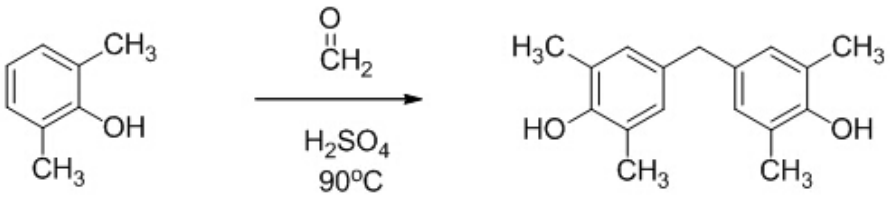

Figure 2.5. Synthesis of 4,4'-methylenebis(2,6-dimethylphenol) (TMBPF)

Molecular Weight: 256.34 g/mol

Experiment: The synthesis of 4,4'-methylenebis(2,6-dimethylphenol), hereafter referred to as tetramethyl bisphenol F (TMBPF), was adapted from a traditional synthesis of a phenolformaldehyde resin[2]. Excess 2,6-xylenol (245.58 mmol, 30.00 g) was added to a 250-mL, 3-necked flask equipped with a condenser, mechanical stirrer, and addition funnel. The 2,6-xylenol was heated in a thermocouple regulated oil bath to 90°C and stirred as it began to melt. Sulfuric acid (0.5 g, 5.10 mmol) was added very

slowly via the addition funnel, which changed the reaction solution to a dark pink color. The addition funnel was rinsed with DI water to ensure that all of the acid catalyst was transferred into the reaction flask. Formalin (37% by mass formaldehyde in H_2O, 9.16 mL, 123mmol) was added slowly via the addition funnel over the course of several hours. As the product continued to form, the reaction mixture transformed from a liquid to a solid. The crude product was removed from the flask and filtered using an aspirator and washed with copious amounts of hot DI water. The crude product was dried at 70°C and was recrystallized from MeOH to obtain white crystals. The melting point of the recrystallized solid was 177°C, which was in the range of reported literature values. Figure 2.13 shows the 1H-NMR spectrum of tetramethyl bisphenol F.

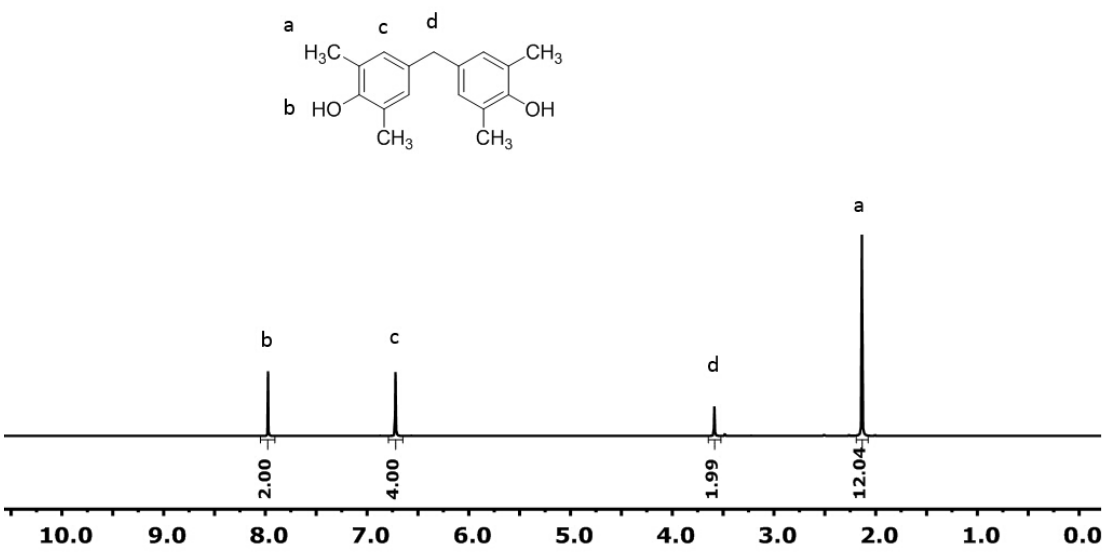

Figure 2.6. ^{1}H NMR of 4,4'-methylenebis(2,6-dimethylphenol) (TMBPF)

2.3.4. bis(4-hydroxy-3,5-dimethylphenyl)methanone (Tetramethyl Dihydroxyl Benzophenone, TMDHBP)

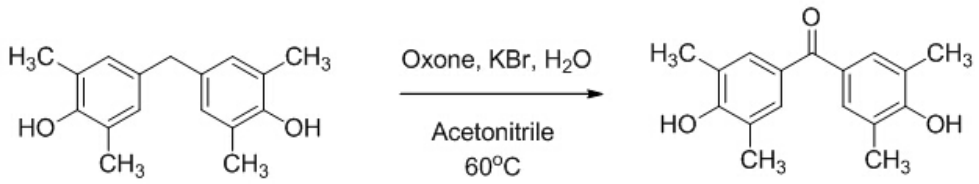

Figure 2.7. Synthesis of bis(4-hydroxy-3,5-dimethylphenyl)methanone (TMDHBP)

Molecular Weight: 270.32 g/mol

The synthesis of bis(4-hydroxy-3,5-dimethylphenyl)methanone, hereafter referred to as tetramethyl dihydroxyl benzophenone, was adapted from the novel synthesis of a ketone group from a methylene group[3]. Tetramethyl bisphenol F (10.00grams, 3.90mmol), Oxone (52.82grams, 7.80mmol, 2.2 equivalent), KBr (5.11grams, 4.3mmol, 1.1 equivalent), and 10ml deionized water were introduced into a 500ml, 2-neck flask, equipped with a condenser and mechanical stirrer.The reaction mixture was heated in a thermocouple regulated oil bath to 60°C and stirred for 6 hours. The crude product was filtered and was recrystallized from DI water to obtain brown, needle-like crystals. The melting point of the recrystallized solid was 116°C. Figure 2.14 and Figure 2.15 show the 1H-NMR and 13C-NMR spectra of tetramethyl dihydroxyl benzophenone.

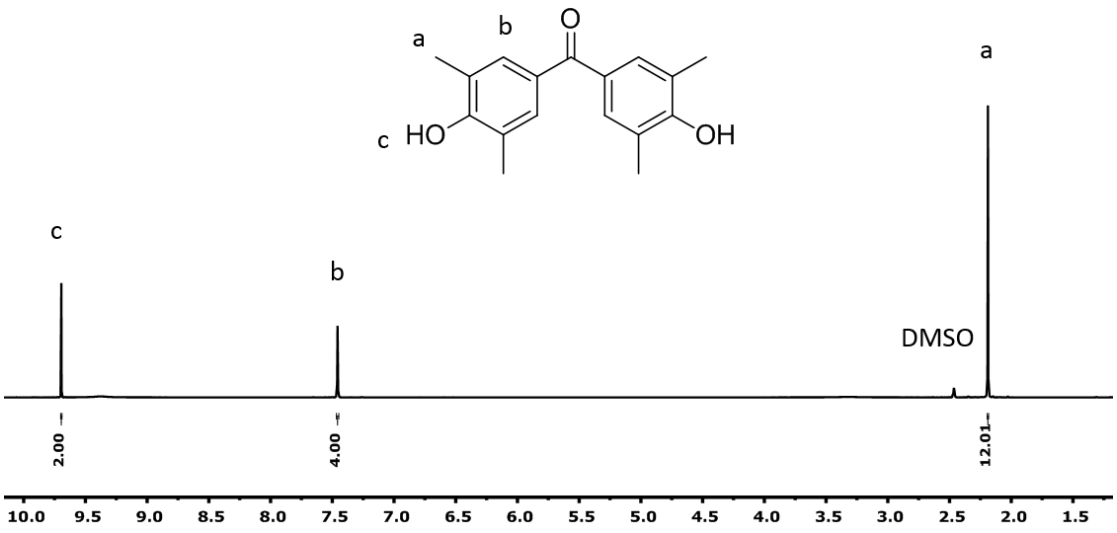

***Figure 2.8. ^{1}H NMR of bis(4-hydroxy-3,5-dimethylphenyl)methanone (TMDHBP*)**

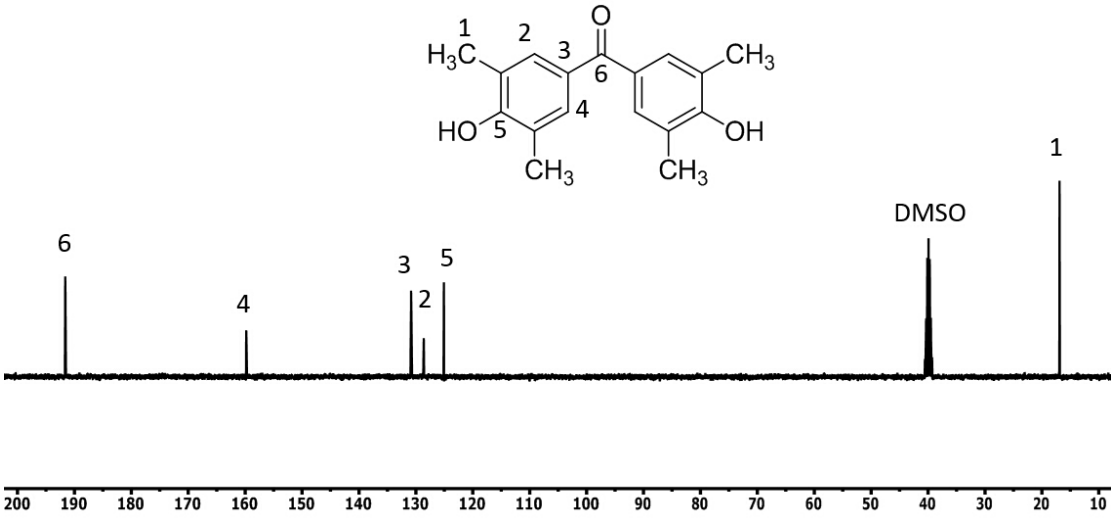

Figure 2.9. ^{13}C NMR of bis(4-hydroxy-3,5-dimethylphenyl)methanone (TMDHBP)

2.3.5. 4,4'-Methylenebis(2,6-dimethylanline) (Methylene Bis(dimethylanline), MBDMA)

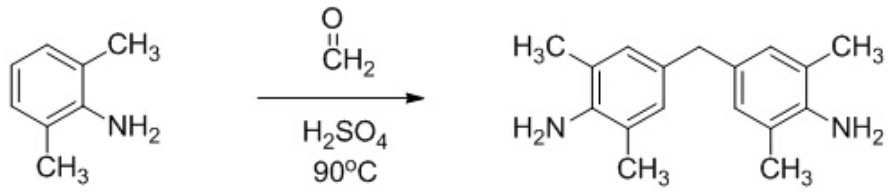

Figure 2.10. Synthesis of 4,4'-methylenebis(2,6-xylidine) (MBXD)

Molecular Weight: 254.37 g/mol

Experiment: The synthesis of 4,4'-methylenebis(2,6-xylidine), hereafter referred to as MBXD, was adapted from the traditional synthesis of a phenol-formaldehyde resin[2]. Excess 2,6-xylidine (259.70 mmol, 31.47 g) was added to a 250-mL, 3-necked flask equipped with a condenser, mechanical stirrer, and addition funnel. The 2,6-dimethylaniline was heated in a thermally regulated oil bath to 90°C and stirred. Sulfuric acid (0.5 g, 5.10 mmol) was added very slowly via the addition funnel, which made the reaction solution opaque. Formalin (37% by mass formaldehyde in H_2O, 9.68 mL, 130 mmol) was added slowly via the addition funnel over the course of several hours; during this time, the reaction solution turned orange. As more of the product continued to form, the color changed from orange to a dark maroon and the reaction mixture transformed from a liquid to a viscous liquid/partial solid. The addition funnel was removed and replaced with a 24/40 joint stopper. The reaction was allowed to stir for an additional 2.5 hours. The oil bath was heated to 110°C and the mixture was stirred for four hours. After this last stage of the reaction, the mixture was cooled to room temperature to yield a crude murky brown solid. The solid was extracted with DI water (700 mL) and diethyl ether (700 mL), which were transferred to a separation funnel.

Most of the product was contained in the organic layer, which was collected and set aside. The aqueous layer was washed with methylene chloride (200 mL), which was also collected and contained crude product. After sitting overnight, much of the organic phase had evaporated leaving crude product in the form of yellow-brown crystals. Methylene chloride also evaporated in the second organic layer which yielded darker, less pure product. The crude product was recrystallized from MeOH to obtain white crystals. Figure 2.16 shows the 1H-NMR spectrum of MBXD.

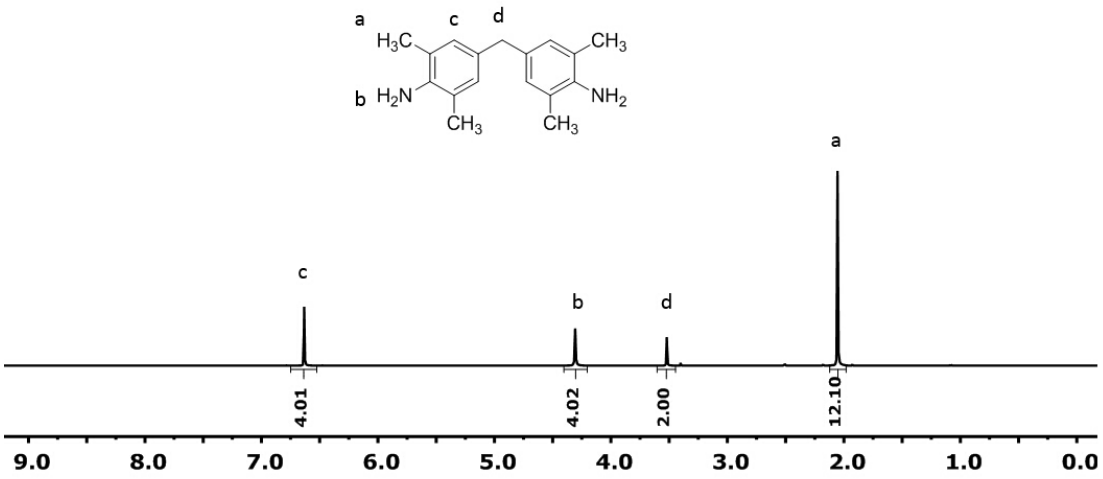

Figure 2.11. ^{1}H NMR of 4,4'-methylenebis(2,6-xylidine) (MBXD)

2.3.6. 3,3'-dinitro-4,4'-dichlorodiphenylsulfone (DNDCDPS)

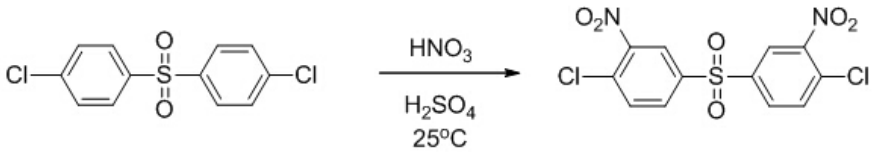

Figure 2.12. Synthesis of 3,3'-dinitro-4,4'-dichlorodiphenylsulfone (DNDCDPS)

Molecular Weight: 377.16 g/mol

Excess 4,4'-dichlorodiphenylsulfone (100.5 mmol, 28.75 g) and 290mL of 96% H_2SO_4 were added to a 500-mL, 3-necked flask equipped with a condenser, mechanical stirrer,

and addition funnel. The reaction mixture was stirred at room temperature until complete solubilization of 4,4'-dichlorodiphenylsulfone. 69.3% nitric acid (201.0 mmol, 18.28 g) was added drop-wise via the addition funnel. Upon completion of the addition, the solution was stirred for 6 hours at room temperature. The final heterogeneous solution containing pale yellow precipitant was poured into 2 L of deionized water and $NaHCO_3$ was added till the solution reached a pH of 7. Then the crude product was filtered and dried in *vacuo* at 100°C. Finally, the product was recrystallized from acetic acid to obtain a 92% yield. The ^{1}H-NMR spectrum is shown in Figure 2.17.

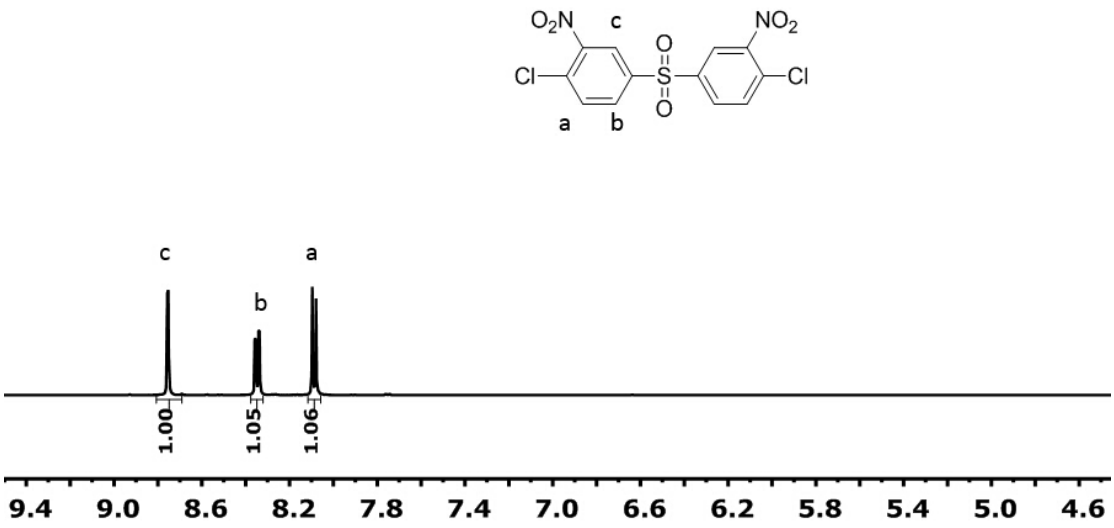

Figure 2.13. ^{1}H NMR of 3,3'-dinitro-4,4'-dichlorodiphenylsulfone (DNDCDPS)

2.3.7. 3,3'-dinitro-4,4'-diaminodiphenylsulfone (DNDADPS)

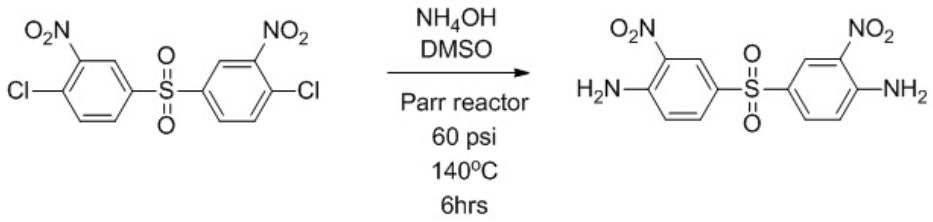

Figure 2.14. Synthesis of 3,3'-dinitro-4,4'-diaminodiphenylsulfone (DNDADPS)

Molecular Weight: 338.30 g/mol

DNDCDPS (125.1 mmol, 21.80 g), NH4OH (312.7 mmol, 39.13g) and 300mL DMSO were added into a 500 mL pressure reactor equipped with heating coils and an overhead stirrer. The reactor was then pressurized to 60 psi and heated to 140 °C. After 16 hours, the reaction mixture was precipitated in deionized water. The yellow precipitant was filtered, washed with copious amounts of water, and dried in *vacuo* at 80℃. A 90% yield of product was obtained. Figure 2.18 shows the ^{1}H-NMR spectrum.

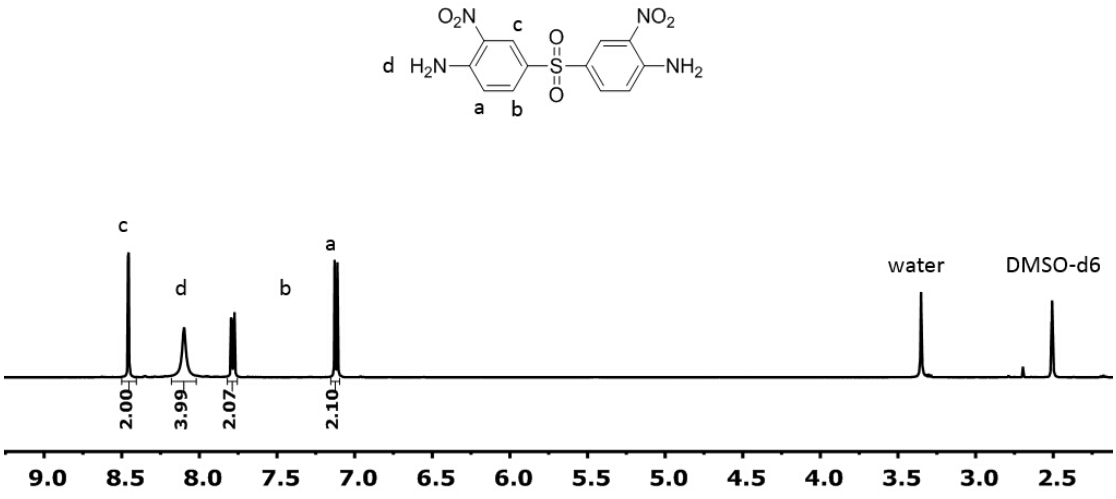

Figure 2.15. ^{1}H NMR of 3,3'-dinitro-4,4'-diaminodiphenylsulfone (DNDADPS)

2.3.8. 3,3',4,4'-tetraaminodiphenylsulfone (TADPS)

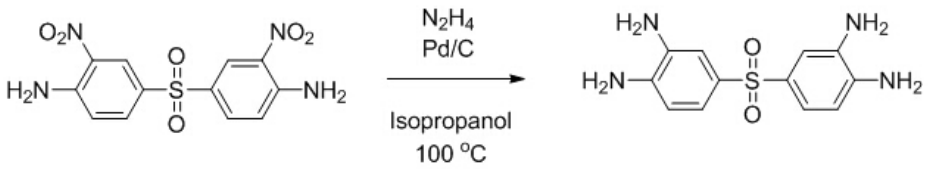

Figure 2.16. Synthesis of 3,3',4,4'-tetraaminodiphenylsulfone (TADPS)

Molecular Weight: 278.33 g/mol

DNDADPS (21.3 mmol, 10.46g), 1.05g Pd/C, and 700ml isopropanol were added to a 1000-mL, 3-necked flask equipped with a condenser, mechanical stirrer, and addition funnel. The reaction mixture was heated in a thermocouple regulated oil bath to 100°C and stirred. 37.95g of hydrazine hydrate (7M excess) was then added drop-wise. After completion of the addition, the solution was stirred and refluxed for 48 hours at 100°C. The reaction mixture was then hot-filtered through Celite. The product started to crystalize from the filtrate upon cooling. The light grey lustrous crystals were filtered off and washed with water. The final product was dried in *vacuo* at 100°C overnight with a 62% yield. The ^{1}H-NMR spectrum is shown below.

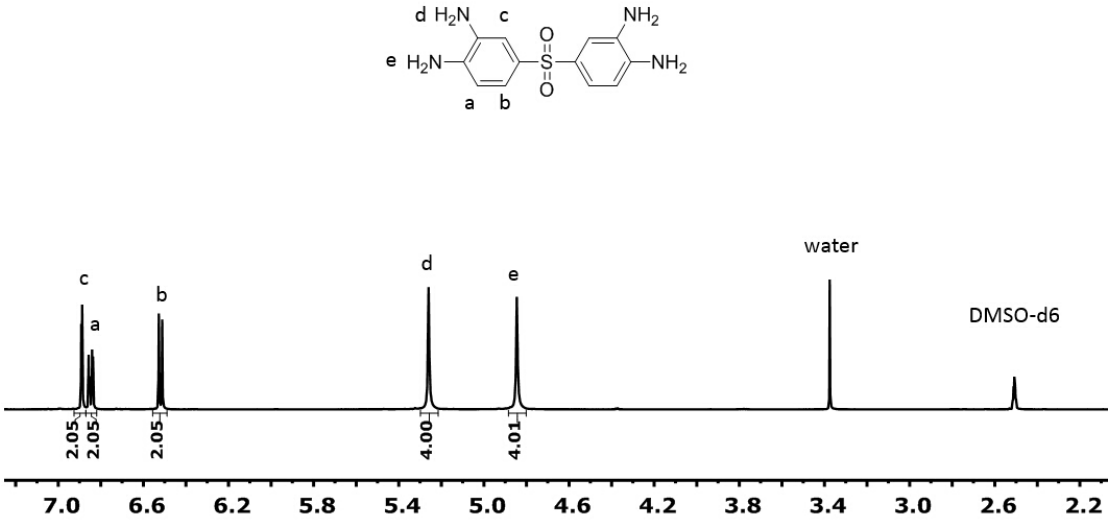

Figure 2.17. ^{1}H NMR of 3,3',4,4'-tetraaminodiphenylsulfone (TADPS)

2.3.9. 3,3’-dinitro-4,4’-dianilinodiphenylsulfone (DNDAnDPS)

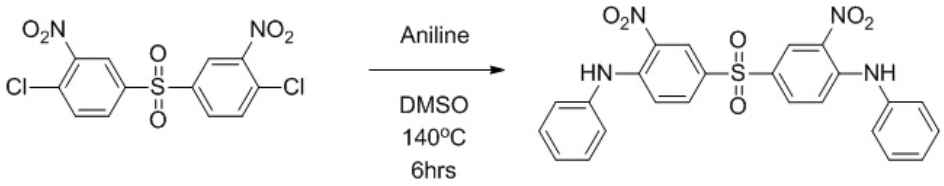

Figure 2.18. Synthesis of 3,3’-dinitro-4,4’-dianilinodiphenylsulfone (DNDAnDPS)

Molecular Weight: 490.49 g/mol

DNDCDPS (125.1 mmol, 21.80 g) and 300mL DMSO were added into a 500 mL 3-necked flask equipped with a condenser, magnetic stirrer, and addition funnel. The reaction mixture was heated in a thermocouple regulated oil bath to 140^{o}C and stirred. Aniline (312.75 mmol, 28.51 mL) was then added into the mixture drop-wise. After completion of the addition, the reaction mixture was refluxed at 140 ^{o}C for 16 hours. The mixture was then poured into 2L of deionized water. The yellow precipitant was filtered, washed with copious amounts of water, and dried in *vacuo* at 80℃. A 90% yield of product was obtained. Figure 2.20 shows the 1H-NMR spectrum.

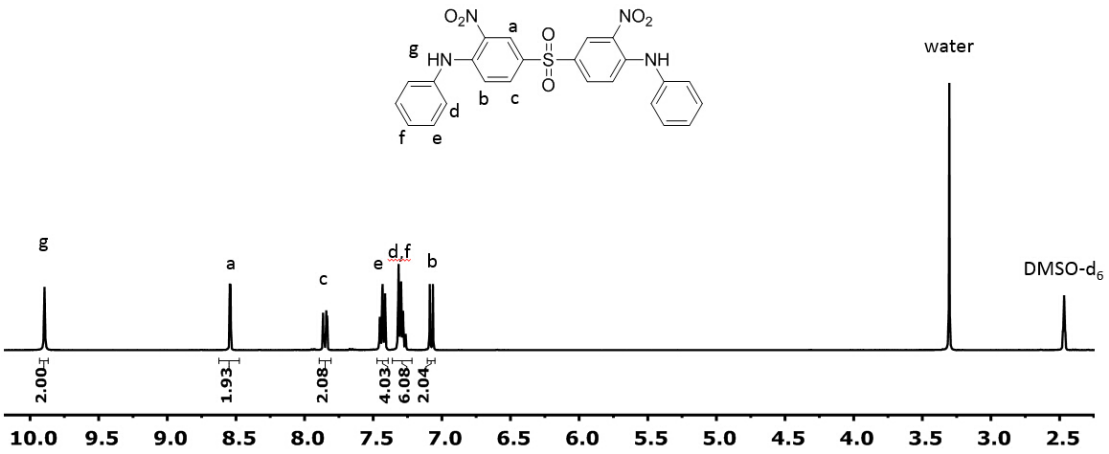

Figure 2.19. ^{1}H NMR of 3,3'-dinitro-4,4'-dianilinodiphenylsulfone (DNDAnDPS

2.3.10. 3,3'-diamino-4,4'-dianilinodiphenylsulfone (DADAnDPS)

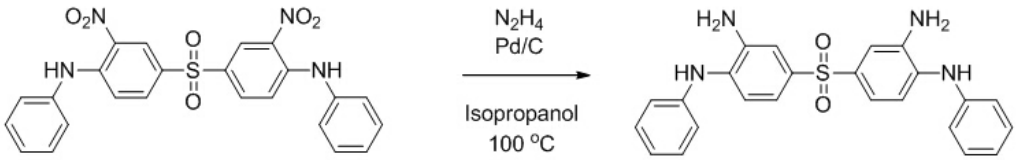

Figure 2.20. Synthesis of 3,3'-diamino-4,4'-dianilinodiphenylsulfone (DADAnDPS)

Molecular Weight: 430.52 g/mol

DNDAnDPS (21.3 mmol, 9.17g), 1.00g Pd/C, and 700ml isopropanol were added to a 1000-mL, 3-necked flask equipped with a condenser, mechanical stirrer, and addition funnel. The reaction mixture was heated in a thermocouple regulated oil bath to 100°C and stirred. 9.0g of hydrazine hydrate (~3M excess) was then added drop-wise. After completion of addition, the solution was stirred and refluxed for 24 hours at 100°C. The reaction mixture was then hot-filtered through Celite. The product started to crystalize from the filtrate upon cooling. The light pink lustrous crystals were filtered off and

washed with water. The final product was dried in *vacuo* at 100°C overnight with a 60% yield. The ^{1}H-NMR spectrum is shown in Figure 2.21.

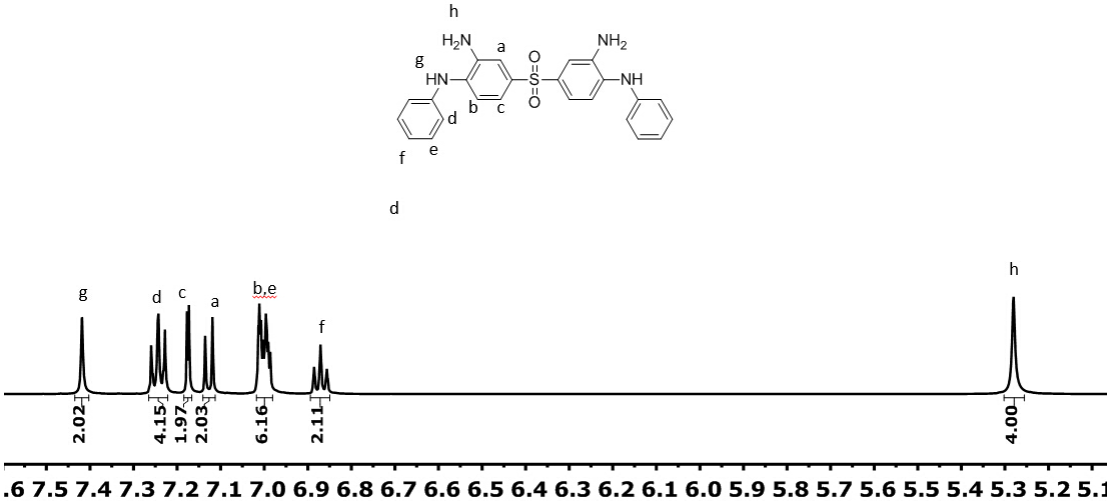

Figure 2.21. ^{1}H NMR of 3,3'-diamino-4,4'-dianilinodiphenylsulfone (DADAnDPS)

2.4. Reference

(1) Dunson, D. L. Synthesis and Characterization of Thermosetting Polyimide Oligomers for Microelectronics Packaging, *PhD Thesis*. Virginia Tech, **2000**.

(2) Moore, J. A. *Macromolecular Syntheses*; Moore, J. A., Ed.; Col. 1.; John Wiley & Sons, Inc.: New York, **1977**; Vol. 9.

(3) Yin, L.; Wu, J.; Xiao, J.; Cao, S. Oxidation of Benzylic Methylenes to Ketones with Oxone–KBr in Aqueous Acetonitrile under Transition Metal Free Conditions. *Tetrahedron Lett.* **2012**, *53*, 4418–4421.

Chapter 3: Synthesis and Characterization of Thermally Rearranged (TR) Polymers: influence of isomeric effects on gas transport properties

Hailun Borjigin[1], Qiang Liu[2], Wenrui Zhang[1], Kyle Gaines[1], Judy S. Riffle[1], Donald R. Paul[2],
Benny D. Freeman[2] and James E. McGrath[1]

1. Department of Chemistry, Macromolecules and Interfaces Institute, Virginia Tech,
325 Stanger Street, 133 Kelly Hall,
Blacksburg, VA 24061, USA
2. Department of Chemical Engineering, Texas Materials Institute, Center for Energy and Environmental Research, The University of Texas at Austin, 10100 Burnet Road, Bldg. 133, Austin, TX 78758, USA

Article in press, Polymer

3.1. Abstract

Isomeric polyhydroxyimides based on 3,3'-diamino-4,4'-dihydroxybiphenyl (*m*-HAB) or 3,3'-dihydroxy-4,4'-diaminobiphenyl (*p*-HAB) with 2,2-bis(3,4-dicarboxyphenyl)hexafluoropropane dianhydride (6FDA) were prepared via an ester-acid monomer. The polyhydroxyimides were then acetylated using acetic anhydride to change the *ortho*-functional groups on the polymer chains. These *ortho*-functional polyimides were used as precursors for thermal rearrangement (TR) to polybenzoxazoles for gas separation membranes. The permeability coefficients of TR polymers significantly improved as the *ortho*-functional polyimides converted to polybenzoxazoles. The influence of *meta* and *para* isomeric monomers on the gas transport properties of the resulting TR polybenzoxazoles were studied. In addition, gas permeation properties show a dependency on the size of the *ortho*-functionality of the polyimide precursors.

3.2. Introduction

Natural gas processing is by far the largest industrial gas separation application.[1] Separation of CO_2 from natural gas is one of the treatments required to meet pipeline specifications.[1,2] Membrane gas separation as a refinery technology has become crucial for natural gas refinery processes.[1,3] In comparison to conventional separation technology, membrane gas separation has several advantages including lower energy consumption, smaller capital investment, and enhanced ease of operation.[4–6] However, to maximize the productivity and efficiency of membrane separation technology, it still must overcome several challenges. These include the trade-off relationship between permeability and selectivity of polymeric membranes that limit the productivity of membrane gas separation.[2] In addition, CO_2-induced plasticization is encountered with most of the commercial membrane gas separation processes.[2] Plasticization, in general, will decrease the selectivities of polymeric membranes.[7,8] Designing a polymeric membrane that has both high permeability and high selectivity is one of the challenges for membrane gas separation.

Recently, a novel family of gas separation membranes known as thermally rearranged (TR) polymers, has attracted both academic and industrial attention.[9–12] TR polymers are derived from polyimides with *ortho*-positioned functional groups that are treated at high temperatures (350-450 °C) in an inert atmosphere. During the thermal rearrangement process, polyimides with *ortho*-positioned functional groups undergo decarboxylation and rearrange inter- and intra-molecularly to form crosslinked polybenzoxazoles. These TR polymer membranes possess a combination of high permeability and high selectivity and have good resistance to CO_2-induced plasticization due to their crosslinked structures.[9,13] Sanders *et al.* reported that TR polymers with higher gas permeabilities can be prepared from polyimides with various

ortho-positioned functionalities including acetate or pivalate groups.[14] Guo *et al.* demonstrated that the reaction temperature required for thermal rearrangement is related to the glass transition temperatures of the TR precursor polyimides.[15] However, relationships between the isomeric structures of the TR polymers and gas transport properties have not been extensively studied. For linear polymer membranes, gas separation properties can often be significantly manipulated by incorporating different isomeric structures.[16,17] For example, *meta*-linked polysulfone exhibited higher selectivity and correspondingly lower permeability than *para*-linked polysulfone.[16] The same phenomenon has also been found for polyimide membranes. For example, Coleman *et al.* compared *meta* and *para*-linked fluorinated polyimides and found that their permeability was greatly decreased when the *para*-connected diamine was replaced by a *meta* isomer.[17] Both studies concluded that the decreased permeability was attributed to the higher chain packing efficiency in the *meta*-linked polymer than in the *para*-linked analog. As a result, a higher chain packing efficiency led to a *meta*-linked polymer with a lower fractional free volume and therefore a lower permeability.

Recently, Comesaña-Gándara *et al.* reported a study on isomer effects of TR polymers and precursors and showed that the *meta*-linked linear polyhydroxyimide had a higher permeability than the *para*-linked linear polyhydroxyimide. After TR conversion, the polybenzoxazole derived from the *meta*-linked linear polyhydroxyimide also had significantly higher permeability than the TR polymer from the *para*-linked polyhydroxyimide.[18] This result is interestingly different from previously-reported gas transport properties on isomeric *meta/para*-linked linear polymers.[17,19] Nevertheless, the isomeric *meta/para* effects on gas transport properties may not hold true for TR polybenzoxazoles due to the inter- and intra-molecular reactions that occur during thermal rearrangement. As more of the benzoxazole

structure forms, the TR polymers may lose their structural identity related to *meta*- and *para*- linkages that existed in the precursors. Moreover, the crosslinking that occurs during thermal rearrangement makes the isomeric *meta/para* effects on gas transport properties less predictable.

In this paper, two isomeric thermally rearrangeable polyimides (*meta*- and *para*-linked TR precursors) based on 4,4'-dihydroxy-3,3'-diaminobiphenyl (*m*-HAB) and 3,3'-dihydroxy-4,4'-diaminobiphenyl (*p*-HAB) with 2,2'-bis-(3,4-dicarboxyphenyl)hexafluoropropane dianhydride (6FDA) and with different *ortho*-functional groups (hydroxyl and acetate) and their corresponding TR polymers are described. Synthesis, characterization, film preparation, and pure gas permeability/selectivity of the *meta/para* linked TR polyimide precursors and TR polybenzoxazoles are reported. Relationships of structure to gas transport properties of the isomeric *meta/para* linkages and *ortho*-functional groups of the TR polymers are discussed.

3.3. Experimental

3.3.1. Materials

4,4'-biphenol, palladium on carbon, triethylamine, pyridine, acetic anhydride, calcium hydride (CaH_2), anhydrous *o*-dichlorobenzene and hydrazine hydrate were purchased from Sigma-Aldrich and used as revived. Nitric acid, acetone, isopropanol, methanol and ethanol were purchased from Spectrum Chemical and used as received. Dimethylacetamide (DMAc) and N-Methyl-2-pyrrolidone (NMP) were purchased from Fisher. NMP used as a reaction solvent was dried with CaH_2, distilled under reduced pressure and stored under 3Å molecular sieves before use. 3,3'-dihydroxy-4,4'-diamino-biphenyl (*p*-HAB) was purchased from TCI. The *p*-HAB was recrystallized in

a mixture of DMAc and methanol, and dried in *vacuo* at 80 °C before use. 2,2'-bis-(3,4-dicarboxy-phenyl) hexafluoropropane dianhydride (6FDA) was kindly provided by Air Products and dried in *vacuo* at 160 °C before use.

3.3.2. Synthesis of 3,3'-diamino-4,4'-dihydroxybiphenyl(*m*-HAB) monomer

3,3'-Diamino-4,4'-dihydroxybiphenyl, hereafter referred to as *m*-HAB, was prepared according to a modified literature method.[20]

Synthesis of 3,3'-dinitro-4,4'-dihydroxyybiphenyl. Excess 4,4'-biphenol (12.2 g, 65.5 mmol) and 250 mL of acetone were added to a 500-mL three-necked flask equipped with a condenser, mechanical stirrer and addition funnel. The reaction mixture was stirred at 60 °C until the 4,4'-biphenol completely dissolved. Nitric acid (11.9 g of 69.3% nitric acid, 131.0 mmol) was added dropwise via the addition funnel. Upon completion of addition, the solution was stirred for 6 h at 60 °C. The final heterogeneous mixture containing a yellow precipitant was washed with copious acetone. The product was filtered and dried in *vacuo* at 80 °C. Yield 87%.

Synthesis of 3,3'-diamino-4,4'-dihydroxybiphenyl. 3,3'-Dinitro-4,4'-dihydroxybiphenyl (11.6 g, 42.0 mmol), 1.1 g of Pd/C and 200 mL of NMP were added to a 500-mL three-necked flask equipped with a condenser, mechanical stirrer and addition funnel. The reaction mixture was heated in a thermocouple-regulated oil bath to 100 °C and stirred. Hydrazine hydrate (24 mL, 290 mmol) was added dropwise. After complete addition, the solution was stirred and refluxed for 12 h at 100 °C. The reaction mixture was hot-filtered through Celite. Methanol (200 mL) was slowly added into the filtered solution. The product started to crystallize upon cooling. White crystals were filtered and washed with water. The product was dried in *vacuo* at 100 °C overnight. Yield 81%. The monomer degrades before melting.

3.3.3. Synthesis of *m*-HAB-6FDA polyhydroxyimides via an ester acid monomer

. The *m*-HAB-6FDA polyimide was synthesized via an ester-acid method according to a modified literature process.[21] 6FDA (7.0407 g, 15.9 mmol) was introduced into a 3-necked flask equipped with a mechanical stirrer, N_2 inlet, thermometer, reverse Dean-Stark trap and reflux condenser. Then, 50 mL of absolute ethanol (856 mmol) and 3 mL of triethylamine (21.5 mmol) were introduced, and the Dean-Stark trap was filled with ethanol. A stirring, thermocouple-regulated, oil bath was used to heat the reaction to 90 °C. The mixture was refluxed with stirring for 1 h. Once a clear solution was obtained, the trap was drained. When distillation of ethanol ceased, the trap was again drained and refilled with *o*-dichlorobenzene. *m*-HAB (3.4268 g, 15.9 mmol) was introduced followed by 35 mL of NMP and 9 mL of *o*-dichlorobenzene (~4/1, v/v) to produce a solids content of ~30% wt/v. The mixture was heated at 180 °C for 10 h, allowed to cool, and then precipitated in methanol. The polyhydroxyimide was dried in *vacuo* at 180 °C overnight. Yield 98%.

3.3.4. Synthesis of *p*-HAB-6FDA polyhydroxyimides via an ester acid monomer

The *p*-HAB-6FDA polyhydroxyimide was synthesized in the exact manner as the *m*-HAB-6FDA polymer, except *p*-HAB was used instead of *m*-HAB.

3.3.5. Acetylation of *m*-HAB-6FDA polyhydroxyimide to form a *m*-polyacetylimide (*m*-HAB-6FDA-Ac)

Acetylation of the *m*-HAB-6FDA polyhydroxyimide was conducted according to a modified literature method.[13] The acetylated *m*-HAB-6FDA polyacetylimide is hereafter referred to as *m*-HAB-6FDA-Ac. The *m*-HAB-6FDA polyhydroxyimide (4.00

g, 6.4 hydroxyl eq) and 20 mL of NMP were introduced into a 3-necked flask equipped with a mechanical stirrer, N_2 inlet, and a condenser. Once the polymer was fully dissolved, acetic anhydride (38.4 mmol, 3.63 mL) and pyridine (37.2 mmol, 3 mL) were added to the solution. The mixture was heated to 50 °C, and maintained at that temperature for 24 h with continuous stirring and a N_2 purge. The resulting viscous solution was cooled to room temperature, and precipitated by slowly dripping the solution into stirring methanol (1 L). The *m*-polyacetylimide (*m*-HAB-6FDA-Ac) was dried in *vacuo* at 180 °C overnight. Yield 99%.

3.3.6. Acetylation of *p*-HAB-6FDA polyhydroxyimide to form a *p*-polyacetylimide (*p*-HAB-6FDA-Ac)

Acetylation of *p*-HAB-6FDA was conducted in the exact manner as the *m*-HAB-6FDA-Ac, except *p*-HAB-6FDA was used instead of *m*-HAB-6FDA.

3.3.7. Film preparation

The polyhydroxyimide was dissolved in DMAc or NMP (~7%, w/v) and filtered through a 0.45 μm Teflon syringe filter to remove any dust and particulates. The filtered solution was sonicated for 15 min to degas the solution, then it was cast onto a dry glass plate (cleaned with acetone) and dried initially with an infrared lamp at approximately 60 °C for 24 h to remove most of the solvent and form a film. The film was soaked in deionized water for 24 h to remove residual solvent, then dried in *vacuo* at 180 °C for at least 24 h.

3.3.8. Thermal Rearrangement of Polyimides Films

The polyhydroxyimide and polyacetylimide films were converted to their corresponding polyimide-polybenzoxazole TR polymer films via thermal rearrangement using a Carbolite tube furnace (Model# HZS 12/600) under a N_2 atmosphere with a purge rate of 900 mL/min. In this study, the polyhydroxyimide films were first heated at 5 °C/min to 300 °C and held at that temperature for 1 h under N_2 protection, and then heated to a desired TR temperature (350 or 400 °C) at 5 °C/min and held at that temperature for either 30 or 60 min.

3.3.9. Structural Characterization

^{1}H- NMR analysis was performed on a Varian Inova spectrometer operating at 400 MHz. All spectra were obtained from 15% (w/v) 1 mL solutions in DMSO-d_6. Fourier Transform Infrared Spectroscopy with attenuated total reflectance (FTIR-ATR) was performed to observe acetylation of the polyhydroxyimides and to measure the conversion of thermal rearrangement to form polyimide-polybenzoxazoles. The FTIR-ATR spectra were recorded on an FTIR spectrometer (Bruker Tensor 27) equipped with an ATR attachment with a horizontal diamond crystal. The resolutions of the spectra were 4 cm-1 and 32 background scans were performed. A small amount of polymer film was placed on the diamond crystal and the FTIR spectrum was measured with 32 scans. All measurements were performed at ambient temperature. Intrinsic viscosities of the polymers were measured with a Canon-Ubbelohde viscometer using 1.0, 0.67, 0.50 and 0.40 g/dL polymer solutions in NMP at 35 °C.

Size exclusion chromatography (SEC) was conducted on HAB-6FDA-Ac polyacetylimides to measure molecular weight distributions. The solvent was DMAc that was distilled from CaH_2 and that contained dry LiCl (0.1 M). The column set

consisted of 3 Agilent PLgel 10-μm Mixed B-LS columns 300x7.5 mm (polystyrene/divinylbenzene) connected in series with a guard column having the same stationary phase. The column set was maintained at 50 °C. An isocratic pump (Agilent 1260 infinity, Agilent Technologies) with an online degasser (Agilent 1260), autosampler and column oven was used for mobile phase delivery and sample injection. A system of multiple detectors connected in series was used for the analyses. A multi-angle laser light scattering (MALLS) detector (DAWN-HELEOS II, Wyatt Technology Corp.), operating at a wavelength of 658 nm, a viscometer detector (Viscostar, Wyatt Technology Corp.), and a refractive index detector operating at a wavelength of 658 nm (Optilab T-rEX, Wyatt Technology Corp.) provided online results. The system was corrected for interdetector delay and band broadening. Data acquisition and analysis were conducted using Astra 6 software from Wyatt Technology Corp. Validation of the system was performed by monitoring the molar mass of a known molecular weight polystyrene sample by light scattering. The accepted variance of the 21,000 g/mole polystyrene standard was defined as 2 standard deviations (11.5% for Mn and 9% for Mw) from a set of 34 runs.

3.3.10. Thermal Analysis

The polyimide films were characterized by thermogravimetric analysis (TGA) and differential scanning calorimetry (DSC). TGA scans were conducted using a TA Instruments Q500 thermogravimetric analyzer under an air atmosphere. A heating rate of 10 °C min^{-1} was employed to 700 °C. Differential scanning calorimetry was performed using a Perkin-Elmer DSC6000. The glass transition temperatures of the polyimide samples were heated from 25 to 300 °C with a heating rate of 10 °C min^{-1} under a N_2 atmosphere.

3.3.11. Pure Gas Transport Properties Measurement

The pure gas permeabilities of H_2, CH_4, N_2, O_2, and CO_2 through the polymers were measured using a constant-volume/variable-pressure method at 35 °C with feed pressures up to around 17 atm.[9] In this method, the polymeric membrane was enclosed inside a stainless steel Millipore filter holder (Millipore, Billerica, MA, USA) and the test gas was allowed to permeate through the membrane into a known downstream volume. The pressure increase of the collected permeate gas in the downstream volume was monitored using a pressure transducer. The linear slope of the pressure rise versus time provided the permeation rates of penetrating gases. Hence the gas permeabilities were calculated by equation 1:

$$P_A = \frac{Vl}{P_0 RTA}\left(\frac{dp}{dt}\right) \qquad (1)$$

where V is the downstream volume, l is film thickness, P_0 is the upstream pressure, R is the gas constant, T is absolute temperature, A is film area, and dp/dt is the rate of pressure change as the gas permeated into the closed downstream volume.

Permeabilities are commonly reported in units of Barrer, defined by equation 2:

$$1\ Barrer = 10^{-10}\ \frac{cm^3(STP)\cdot cm}{cm^2\cdot s\cdot cmHg} \qquad (2)$$

The ideal selectivity (pure-gas selectivity), α, was determined by taking the ratio between the pure gas permeabilities of the gas pair under study:

$$\alpha_{A/B} = P_A/P_B \quad (3)$$

3.4. Results and Discussion

3.4.1. Synthesis and Structure Characterization of 3,3'-diamino-4,4'-dihydroxylbiphenyl(*m*-HAB) monomer

Synthesis of 3,3'-diamino-4,4'-dihydroxybiphenyl was conducted in two steps starting from 4,4'-biphenol, which is a commonly used monomer for various commercial polymers such as polysulfone, poly(arylene ether ketone) and polycarbonate.[22] 4,4'-Biphenol was nitrated in an aromatic electrophilic substitution reaction to form 3,3'-dinitro-4,4'-biphenol, and this was followed by reduction of the nitro groups with hydrazine hydrate in the presence of Pd/C as the catalyst. The product was recrystallized in a mixture of NMP and methanol to give the monomer with a high yield. The structure of the final product, 3,3'-diamino-4,4'-dihydroxybiphenyl, was confirmed by ^{1}H NMR (Figure 3.1).

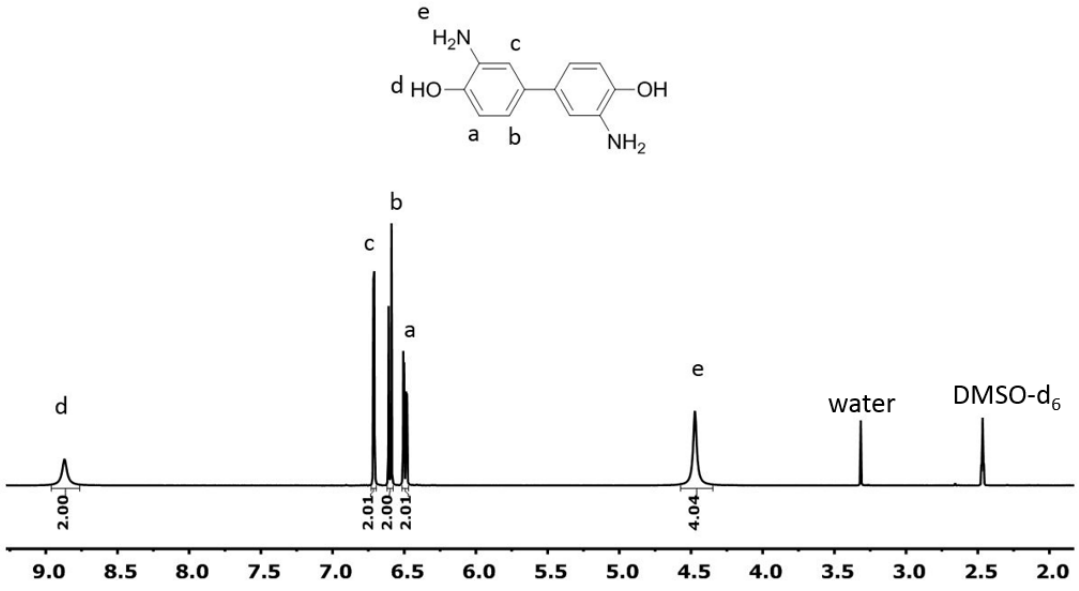

Figure 3.1. ^{1}H NMR spectrum confirms the structure of the m-HAB monomer.

3.4.2. Synthesis and Structure Characterization of isomeric TR precursors.

The isomeric *meta*- and *para*-HAB-6FDA polyhydroxyimides were synthesized via a diester-diacid monomer in a manner similar to previously described procedures.[13,15] In the diester-diacid method (Figure 3.2), the hydrolytically unstable dianhydride monomer was first reacted with an alcohol at low temperature to form a hydrolytically-stable diester-diacid monomer. Then, the aminophenol monomer was introduced and the temperature was elevated to produce the polyhydroxyimide in a one-step process. The diester-diacid monomer is less reactive than the corresponding dianhydride. Our objective was to avoid any reaction of the *ortho*-hydroxyl group with the very reactive dianhydride during imide formation. The structural differences between the two isomeric polyhydroxyimides, *meta*- and *para*-HAB-6FDA, were confirmed by ^{1}H NMR (Figure 3.4). Previous studies have demonstrated that the pendent functional groups affect the transport properties of TR polymers.[13] For example, TR polymers that were prepared from *ortho*-acetate functional polyimides had significantly higher permeabilities than the TR polymers that were prepared from *ortho*-hydroxyl functional polyimides. In order to compare the isomer effect and the bulky pendent group effect on the TR polymers, the two isomeric polyhydroxyimides were post-acetylated using acetic anhydride and a weak base as the catalyst to form the corresponding isomeric polyacetylimides, *meta*- and *para*-HAB-6FDA-Ac (Figure 3.5). Since the *meta*- and *para*-HAB-6FDA-Ac polyacetylimides were chemically modified from the initial polyhydroxyimides (*meta*- and *para*-HAB-6FDA), any effects of different molecular weights or possible isoimide structures resulting from different synthetic methods were avoided. Acetylation of the isomeric polyhydroxyimides was confirmed by ^{1}H NMR and FT-IR (Figures 3.3 and 3.9). Molecular weights of these polyimides were estimated by intrinsic viscosities and SEC (Table 3.1). Lower intrinsic viscosities were observed

for the acetylated polyimides as compared to the polyhydroxyimides due to lack of hydrogen bonding interactions. SEC of the polyacetylimides quantitatively substantiated high molecular weight, and these results are shown in Figure 3.3 and Table 3.1.

Table 3.1. Molecular weights of meta and para-HAB-6FDA ortho-functional polyimides

	m-HAB-6FDA	*p*-HAB-6FDA	*m*-HAB-6FDA-Ac	*p*-HAB-6FDA-Ac
[η]	1.33	1.58	0.93	1.04
M_n (10^{-3} g/mol)	-	-	44	41
M_w (10^{-3} g/mol)	-	-	112	92
PDI	-	-	2.6	2.2

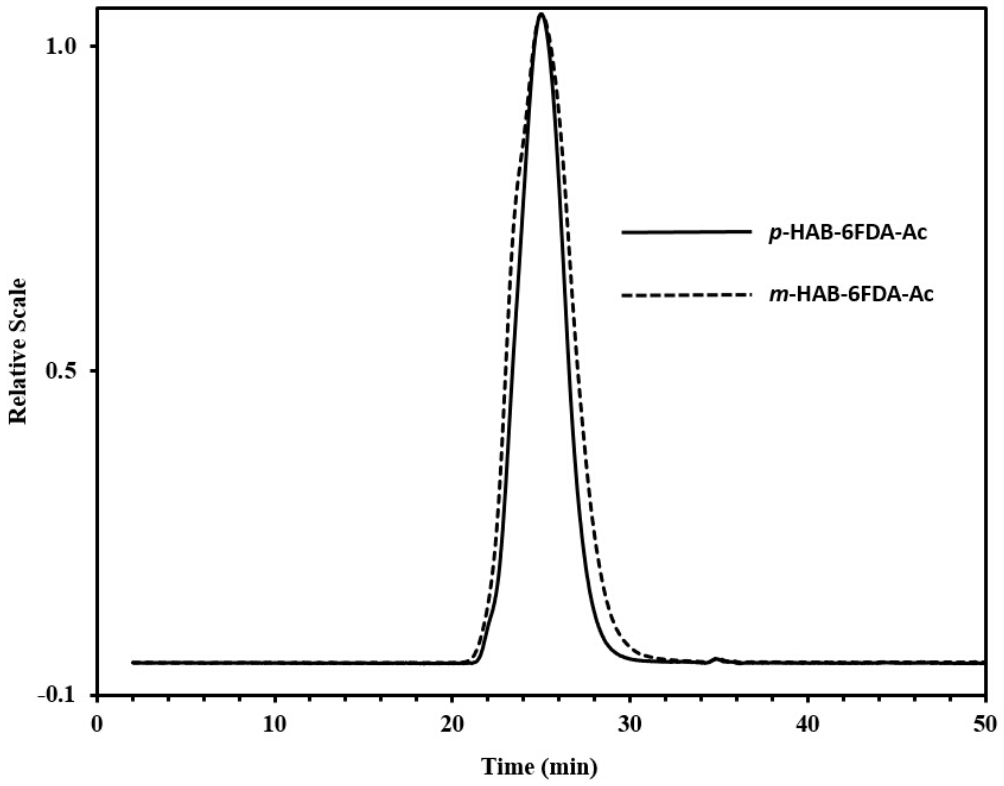

Figure 3.2. Light scattering SEC chromatograms of para and meta-HAB-6FDA-Ac

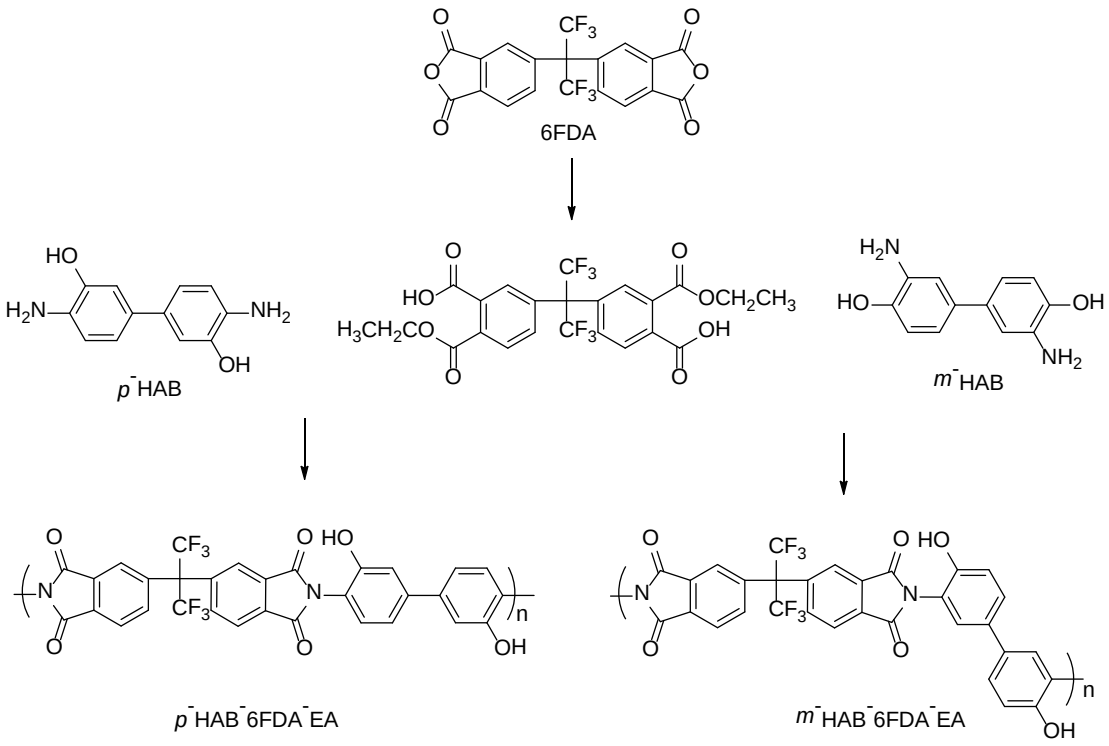

Figure 3.3. Synthesis of para and meta HAB-6FDA polyimides via the ester-acid method

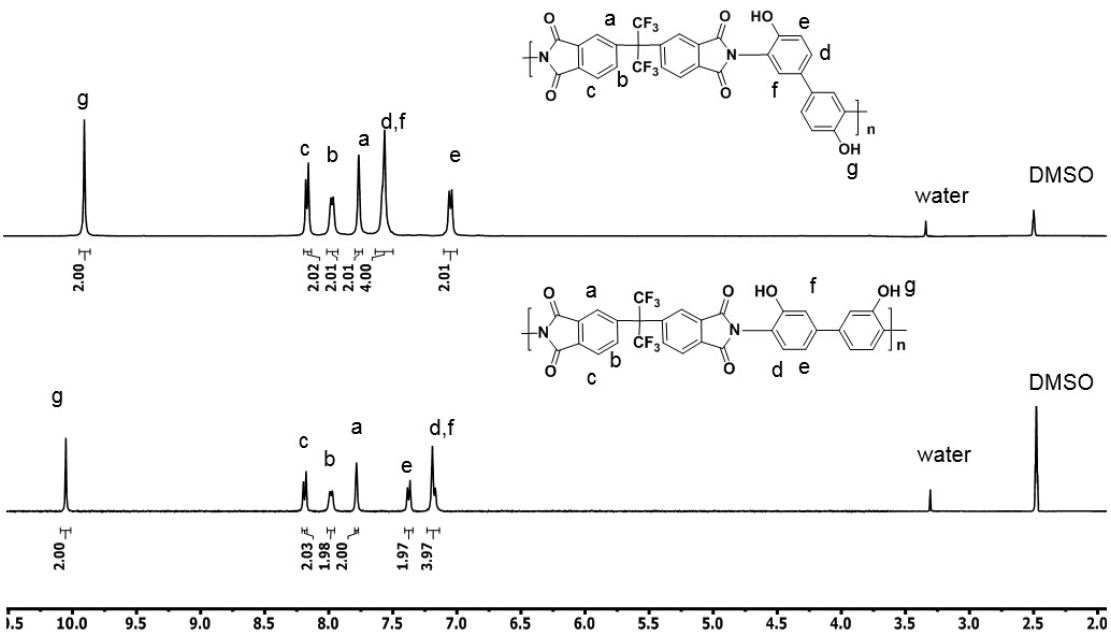

Figure 3.4. ^{1}H NMR spectra confirms the structures of meta and para HAB-6FDA-EA polymers.

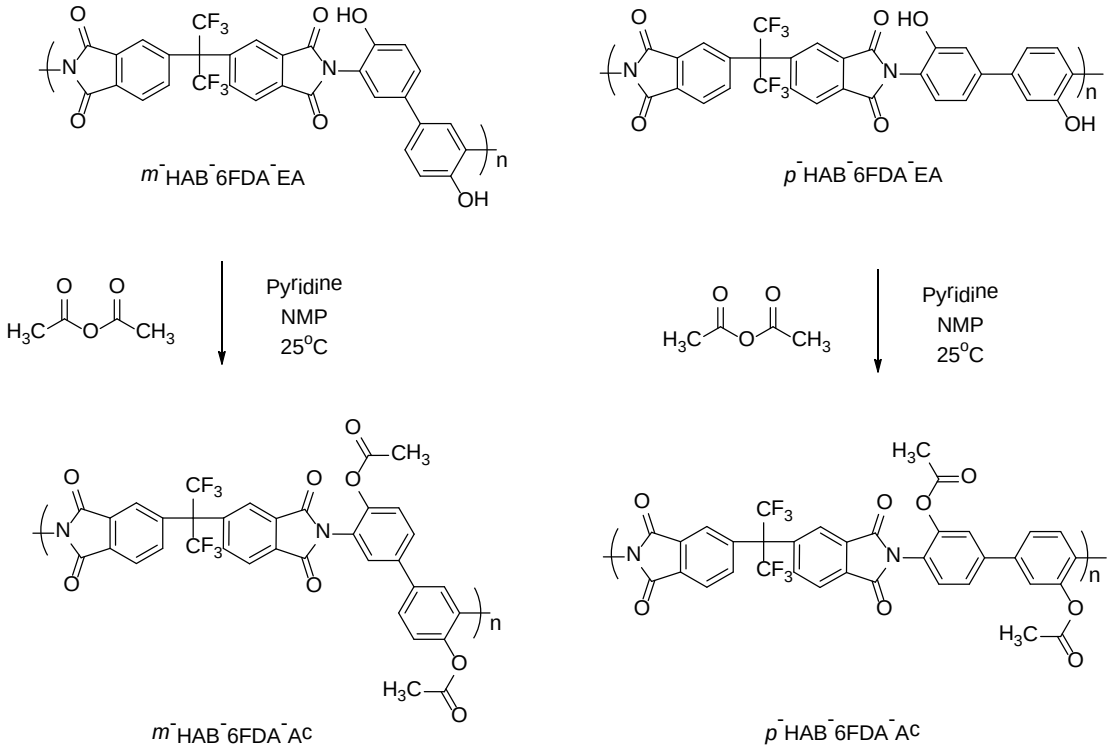

Figure 3.5. Acetylation of meta and para HAB-6FDA poly(hydroxyimide)s

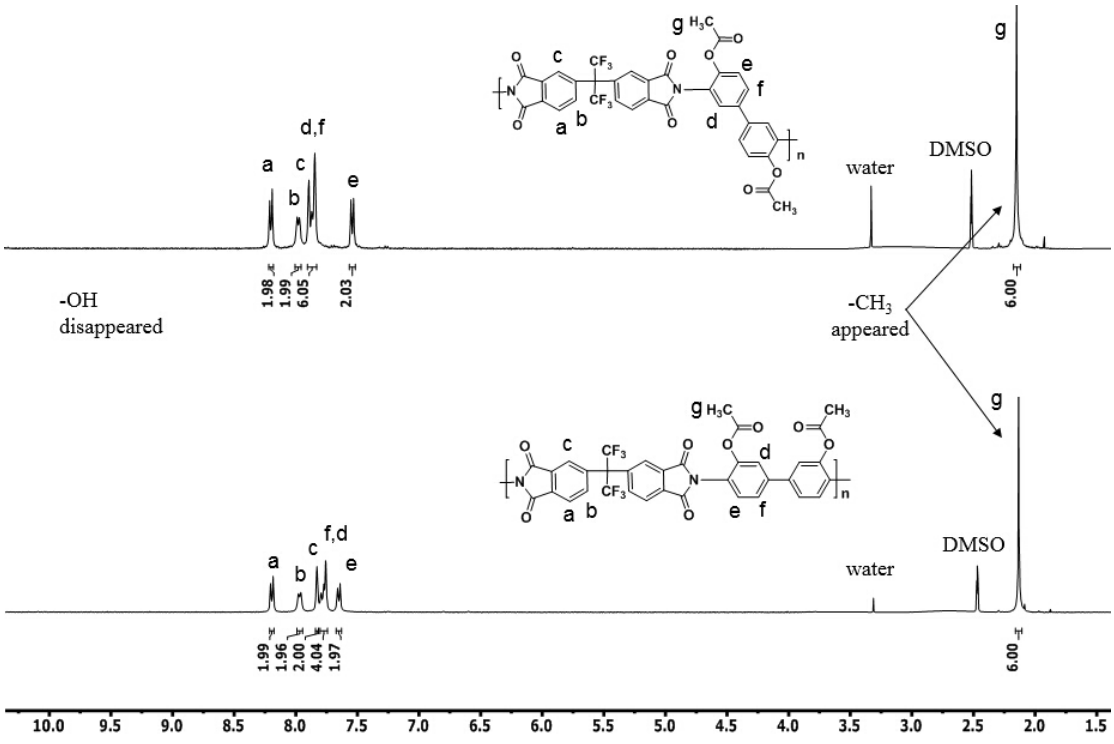

Figure 3.6. ^{1}H NMR spectra confirms the structures of meta and para HAB-6FDA-Ac polymers.

3.4.3. Thermal Analysis of isomeric TR precursors

TGA profiles (Figure 3.7) show similar two-step weight loss stages for the two isomeric polyhydroxyimides and their acetylated analogs in a nitrogen atmosphere. As reported previously,[14] the first weight loss corresponds to the thermal rearrangement process with loss of the by-products and the second depicts degradation of the polymers. The polyacetylimide precursors had earlier and more weight loss in the lower temperature region than the polyhydroxyimides, and this is in agreement with previous reports.[13] Theoretical mass losses for a 100% TR polybenzoxazole converted from the HAB-6FDA polyhydroxyimide and for a fully converted HAB-6FDA-Ac are 14.1 and 24.0% respectively. Figure 3.7 shows the weight losses observed upon heating those precursors in the TGA to be slightly lower than the theoretical values for full conversion. This may at least be partially attributable to the heating rates being too fast (10 °C/min) to allow the precursors to achieve full TR conversion before they underwent degradation as the temperature was eleva

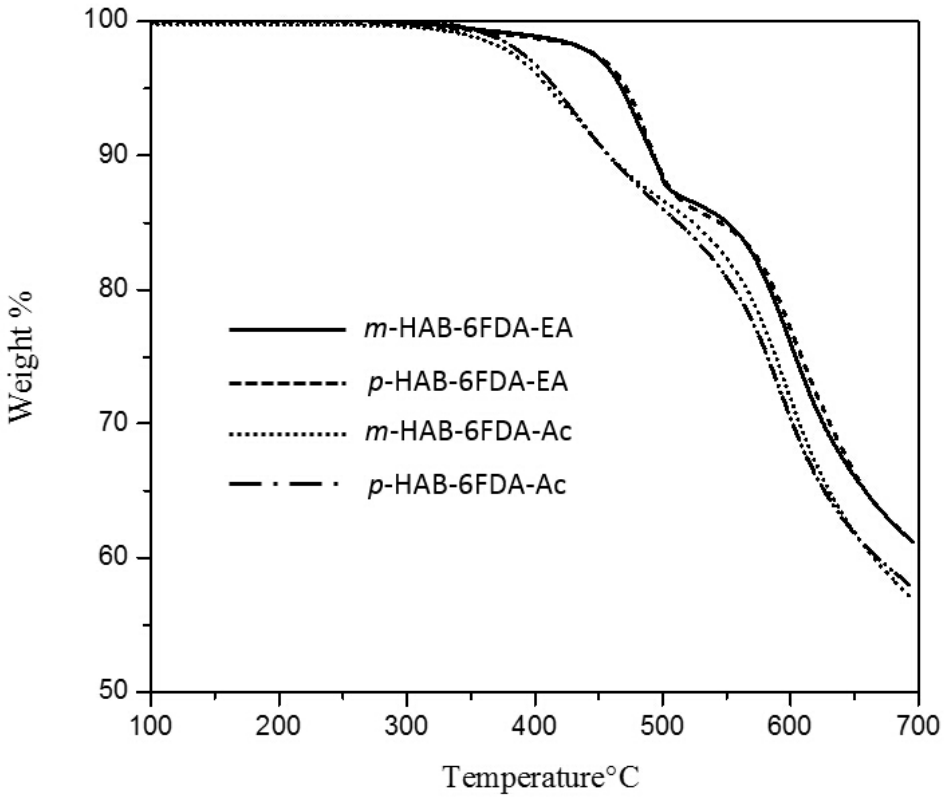

Figure 3.7. TGA profile of meta/para HAB-6FDA based polyimides. The sample was heat at 10°C/min from 25°C to 700°C under N2 atmosphere.

3.4.4. Structure characterization of TR precursors and TR polymers.

Structural changes that occurred upon conversion of the polyhydroxyimides to polyacetylimides and from the *ortho*-functional polyimide precursors to polybenzoxazoles during the thermal treatments were examined by ATR-FTIR. Figure 3.9 shows ATR-FTIR transmission spectra of *m*-HAB-6FDA, *m*-HAB-6FDA-Ac, *p*-HAB-6FDA and *p*-HAB-6FDA-Ac. Figures 3.10-11 show ATR-FTIR transmission spectra of the *m*-HAB-6FDA and *m*-HAB-6FDA-Ac polyimides and their corresponding TR polymers. Peak a (3500 cm^{-1}) represents the H-O stretch. Peaks b (1780 cm^{-1}) and c (1720 cm^{-1}) represent the symmetric and asymmetric imide carbonyl stretches, and peak d (1380 cm^{-1}) represents the imide C-N stretch. Peaks e (1560 cm^{-1}), f (1480 cm^{-1}) and g (1050 cm^{-1}) represent the benzoxazole ring stretches. As the

polyhydroxyimides were converted to polyacetylimides, the peak associated with the hydroxyl functional groups (peaks a, Figure 3.9) disappeared, which is a sign of complete acetylation. In Figures 3.10, as the polyhydroxyimides were exposed to different thermal treatments, the hydroxyl peak (a) and peaks associated with the polyimide structures (b, c and d) declined in intensity. Figure 3.11 shows the FTIR spectra of the polyacetylimides treated under different conditions. For the *m*-HAB-6FDA-Ac-TR350 polymer, a broad peak associated with the hydroxyl functionality was observed (peak a). The presence of the hydroxyl peak is a result of the loss of the acetate functional group and the formation of a hydroxyl group on the polyimide prior to the thermal rearrangement to form the polybenzoxazole. For *m*-HAB-6FDA-Ac-TR400 polymers, peaks (e, f, and g) began to develop that may be evidence of benzoxazole formation, but these peaks were very weak. Nevertheless, ATR-FTIR was a critical technique for monitoring the thermal rearrangement process from polyimides to polybenzoxazoles.

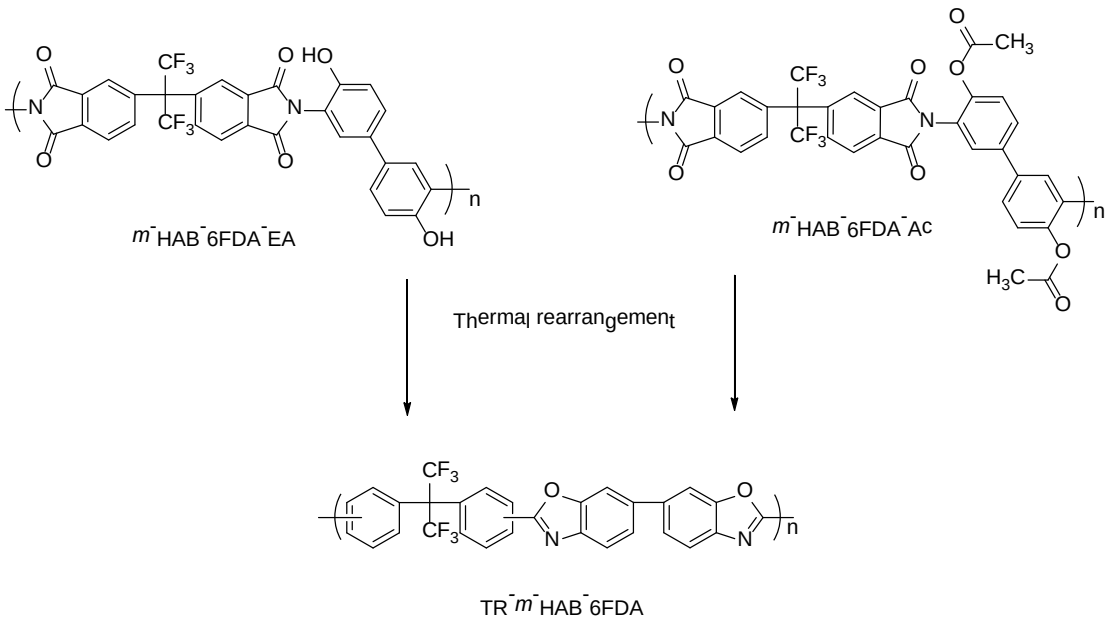

Figure 3.8. Thermal rearrangement of acetylated and non-acetylated m-HAB-6FDA polyimides

As polyimides undergo the TR process, their masses decrease. Therefore, conversion of the polyimides to TR polymers was quantified by weight loss using the following equation:[12]

$$Conversion\ (\%) = \frac{Actual\ Mass\ Loss}{Theoretical\ Mass\ Loss} \times 100$$

Table 3.2 shows the theoretical weight losses for the TR precursor polyimides, the measured losses due to thermal rearrangement after being heated at 400 °C for 60 min, and the percent conversion from the *ortho*-functional polyimides to the TR polymers. Thus, it appears that while the polyhydroxyimides convert almost quantitatively to polybenzoxazoles under these conditions, the efficiency of conversion of the acetylated polymers is rather low, even after treatment at 400 °C for 60 minutes.

Table 3.2. Thermal characters and TR conversions of meta/para HAB-6FDA based polymers.

Precursors	Theoretical weight loss (wt%)	Measured weight loss(wt%)	Conversion %
		TR400-60 min	
m-HAB-6FDA-EA	14.10%	13.0%	92%
p-HAB-6FDA-EA	14.10%	12.4%	88%
m-HAB-6FDA-Ac	24%	11.3%	47%
p-HAB-6FDA-Ac	24%	13.0%	54%

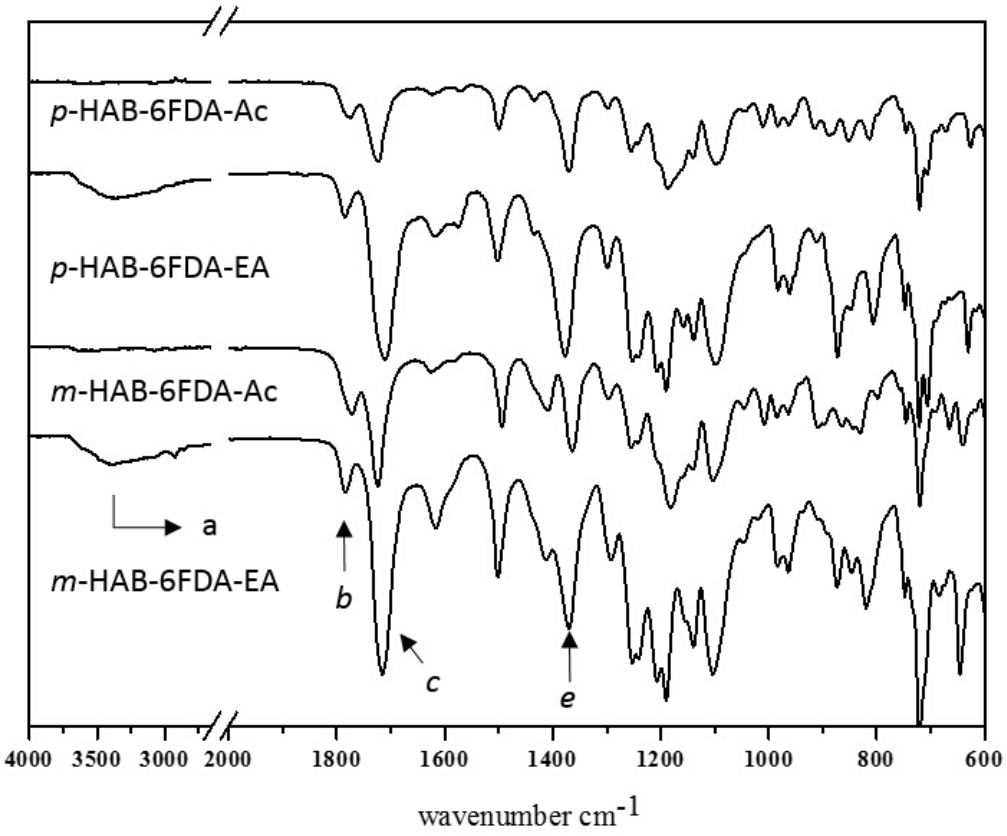

Figure 3.9. FT-IR spectra of meta/para HAB-6FDA based polyimide

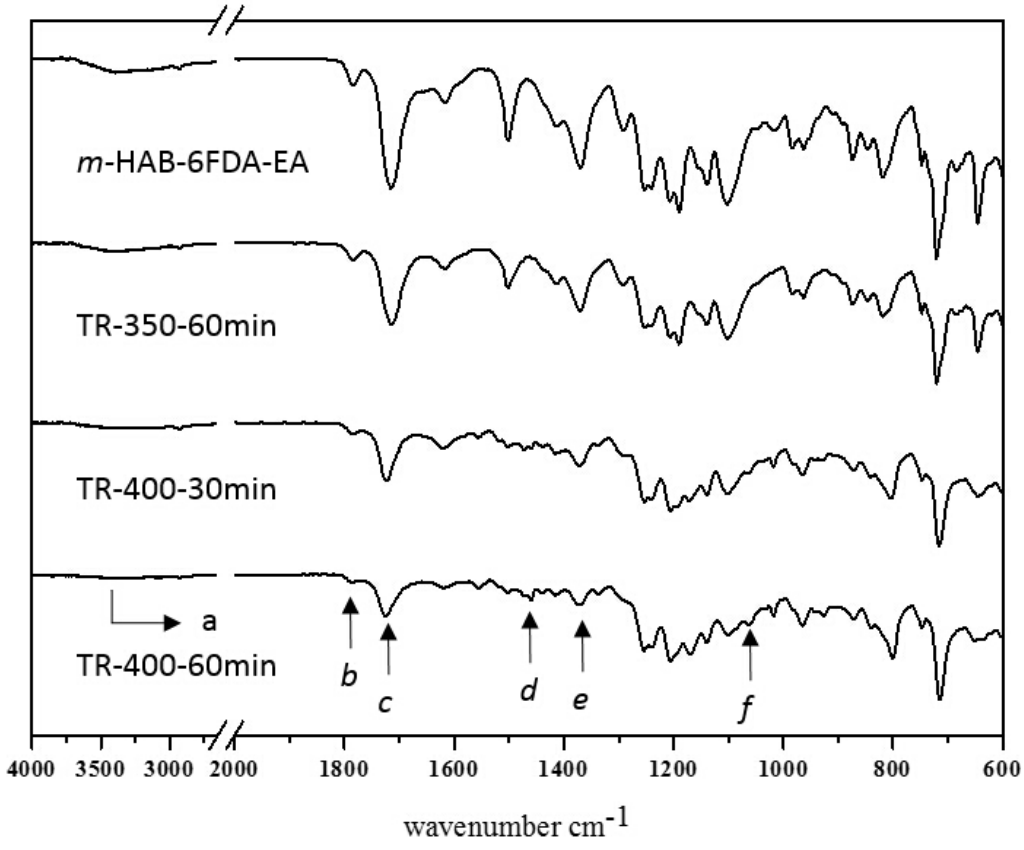

Figure 3.10. FT-IR spectra of m-HAB-6FDA-EA and its corresponding TR polymers

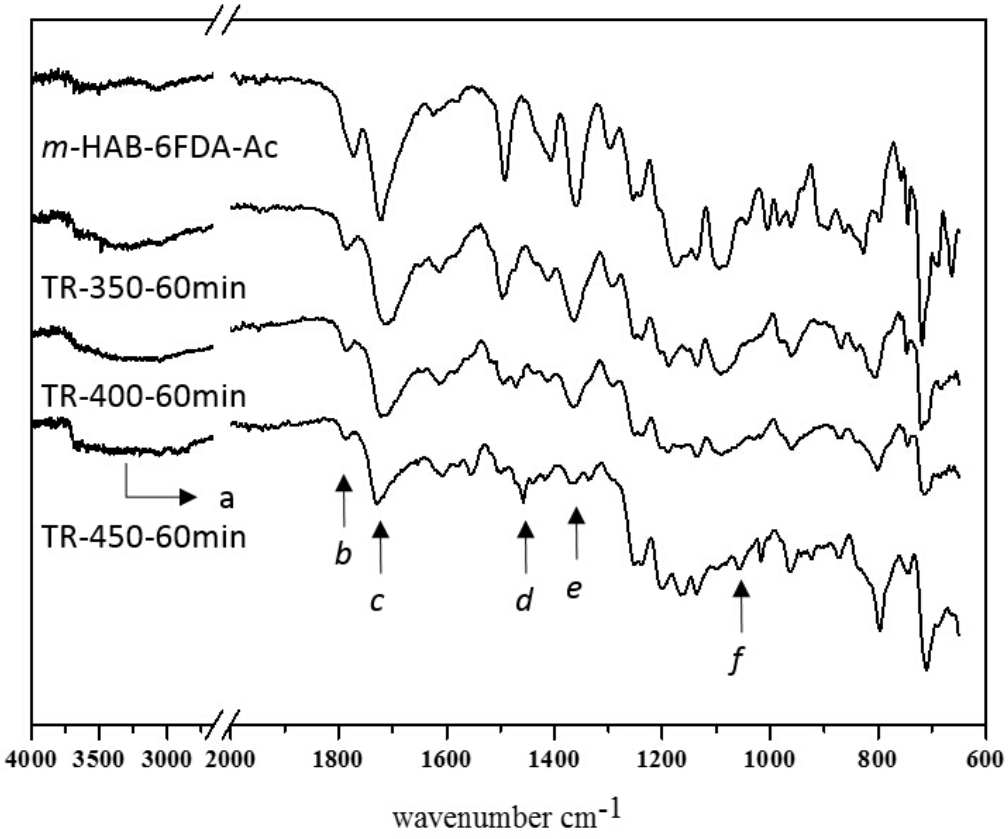

Figure 3.11. FT-IR spectra of m-HAB-6FDA-Ac and its corresponding TR polymers.

3.4.5. Initial gas transport results

Pure-gas permeation properties of H_2, O_2, N_2, CO_2, and CH_4 of the four *ortho*-functional polyimide precursors and their corresponding TR polymers were measured at 35 °C with an upstream pressure of 10 atm. Tables 3.3-4 show the gas permeation properties of the isomeric precursors with different *ortho*-functionalities and their corresponding TR polymers that were thermally treated at 400 °C for 60 minutes. Like other TR polymers, conversion of *ortho*-functional polyimides to polybenzoxazole TR polymers significantly improved the permeability coefficients of both *m*-HAB-6FDA and *p*-HAB-6FDA TR polymers.[23,24] The permeabilities of five common gases through the TR precursors and TR polymers are compared for *m*-HAB-6FDA and *p*-HAB-6FDA based structures (Tables 3.3 and 3.4). Upon thermal rearrangement at 400 °C for 60 minutes, all of the gas permeabilities increased. For example, permeability of O_2

for TR-*m*-HAB-6FDA-Ac and TR-*p*-HAB-6FDA-Ac increased by 400 and 936%, respectively, compared with those of their corresponding TR precursor polyimides. Additionally, the TR polymers derived from the polyacetylimide precursors had much higher gas permeabilities than the TR polymers derived from polyhydroxyimide precursors. For example, the permeability of CO_2 through the TR-*m*-HAB-6FDA-Ac was 75 Barrer whereas the permeability of CO_2 for TR-*m*-HAB-6FDA was only 57 Barrer. This phenomenon agrees with previous literature.[13,14,25]

Moreover, the TR polymers derived from *meta*- and *para*-oriented precursors also exhibited small differences in gas permeability. For example, the CH_4 gas permeability through TR400-*m*HAB-6FDA-Ac was 2.0 Barrer and that of TR400-*p*HAB-6FDA-Ac was 3.0 Barrer. There are two reasons for the small difference in gas permeability between the two isomers. First, the precursors have small differences in gas permeabilities between the *meta* and *para* isomers. These TR polymers could have two components depending on the percentage of conversion: unconverted polyimide with *ortho*-functional groups and rearranged polybenzoxazole. It was found that the permeability coefficients of the *meta* and *para* oriented polyhydroxyimides were not significantly different. Thus, the unconverted polyimide component may only contribute a small difference in gas permeabilities between the two isomeric TR polymers derived from the polyacetylimides. Second, unlike more conventional *meta*- or *para*-linked polymers, the benzoxazole structures in the isomeric TR polymers may not have significant differences in inter-segmental mobility (Figure 3.12). As a result, the TR polymer component derived from *meta* and *para* isomeric precursors also may only contribute small differences in gas permeability. So the simplicity of the *m*-HAB monomer synthetic route makes *meta*-oriented TR polymers an economically better option.

Table 3. 3. Ideal gas permeabilities for meta/para HAB-6FDA based polyimides and their corresponding TR polymers.

Samples	*Single Gas Permeabilities (Barrer)*					
	H_2		N_2		O_2	
	polyimide precursor	TR400-60 min	polyimide precursor	TR400-60 min	polyimide precursor	TR400-60 min
m-HAB-6FDA	33 ± 1	124 ± 4	0.23 ± 0.01	3.1 ± 0.1	1.7 ± 0.06	15 ± 0.5
p-HAB-6FDA	36 ± 2	147 ± 6	0.3 ± 0.02	3.7 ± 0.1	2.1 ± 0.1	18 ± 0.7
m-HAB-6FDA-Ac	43 ± 1	165 ± 7	0.7 ± 0.02	4.0 ± 0.2	4.0 ± 0.1	20 ± 0.8
p-HAB-6FDA-Ac	37 ± 2	237 ± 9	0.47 ± 0.02	6.0 ± 0.2	2.8 ± 0.1	29 ± 1

Table 3.4. Ideal gas permeabilities of CO2 and CH4 and ideal selectivity of CO_2/CH_4 for meta/para HAB-6FDA based polyimides and their corresponding TR polymers.

Samples	Single Gas Permeability (Barrer)				Selectivity	
	CO_2		CH_4		CO_2/CH_4	
	polyimide precursor	TR400-60 min	polyimide precursor	TR400-60 min	polyimide precursor	TR400-60 min
m-HAB-6FDA	5.9 ± 0.2	56 ± 2	0.065 ± 0.003	1.8 ± 0.06	91	31
p-HAB-6FDA	8.3 ± 0.5	73 ± 3	0.09 ± 0.006	2.2 ± 0.1	92	33
m-HAB-6FDA-Ac	15 ± 0.5	75 ± 3	0.39 ± 0.01	2.0 ± 0.08	39	38
p-HAB-6FDA-Ac	9.6 ± 0.5	115 ± 4	0.23 ± 0.01	3.0 ± 0.1	42	38

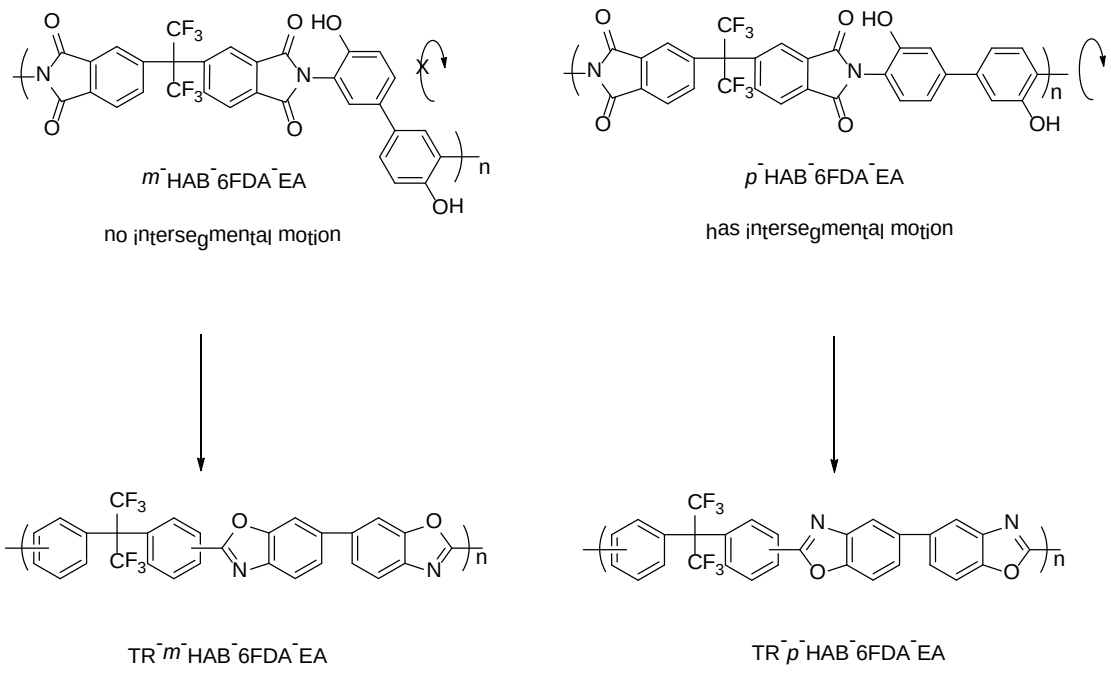

Figure 3.12. Comparison of meta and para HAB-6FDA polyimides and their corresponding TR polymers.

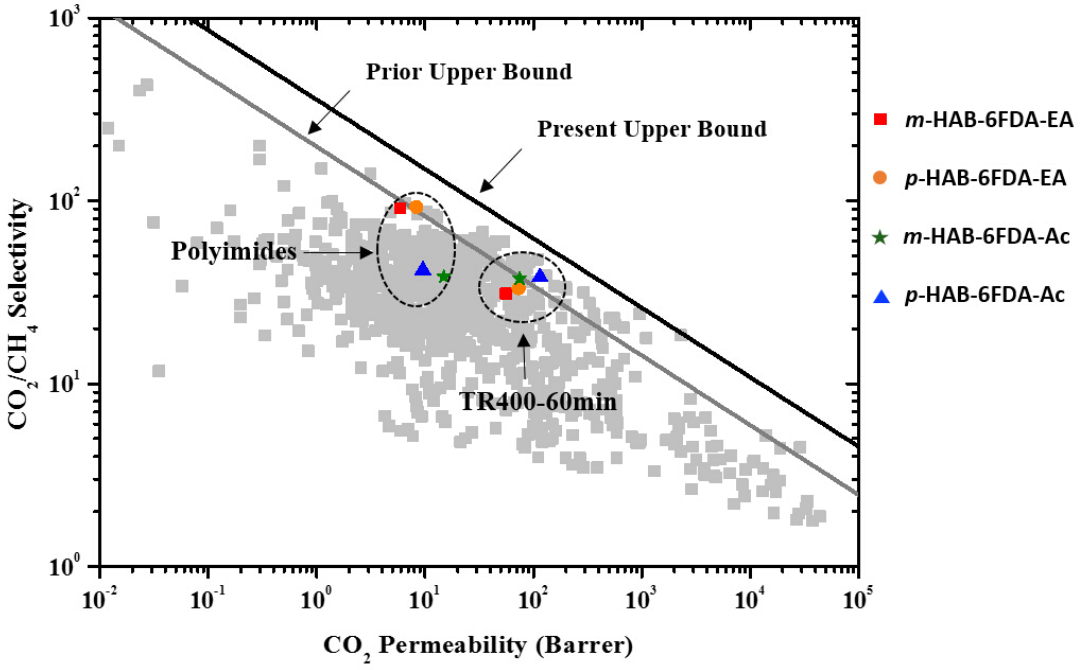

Figure 3.13. The upper bound plot of the CO2/CH4 gas pair.

Figure 3.13 illustrates a CO_2/CH_4 upper bound plot for *m*-HAB-6FDA, *p*-HAB-6FDA, *m*-HAB-6FDA-Ac, *p*-HAB-6FDA-Ac and their TR polymers. As a general observation, the polyhydroxyimides (*m*-HAB-6FDA and *p*-HAB-6FDA) have higher CO_2/CH_4 selectivities and lower CO_2 permeabilities than the polyacetylimides. The TR polymers derived from polyacetylimide precursors showed even greater CO_2 gas permeability and more competitive CO_2/CH_4 selectivity than the TR polymers derived from the polyhydroxyimide precursors. This may also be influenced by the fact that conversions of the TR-polyacetylimides were incomplete under the conditions imposed in this study, and thus, this aspect will require further investigation to fully understand. There are some trivial differences in the CO_2 gas permeability and the CO_2/CH_4 selectivity between *meta* and *para* oriented TR precursors and their corresponding TR polymers, and a detailed discussion of the differences in permeability between *meta* and *para* oriented TR precursors and TR polymers will be reported in a separate publication.[26] To this end, the *meta/para* oriented TR polymers do not have a substantial advantage over one another in CO_2/CH_4 gas separation but TR polymers derived from the partially-rearranged polyacetylimides demonstrate better CO_2/CH_4 gas separation properties than the TR polymers derived from the polyhydroxyimides (fully converted).

3.5. Conclusions

Meta and *para* oriented high molecular weight aromatic polyimides containing *ortho*-positioned hydroxyl groups were synthesized using a diester-diacid monomer to avoid possible reactions of the *ortho*-hydroxyl groups with the more reactive dianhydride monomer. Those polyhydroxyimides were post-modified to change the *ortho*-functional groups to acetates. Then the isomeric *ortho*-functional polyimides were converted to polymers with benzoxazole structures via thermal rearrangement

(TR). Mass measurements before and after conversion suggested strongly that thermally rearranging these polyimides at 400 °C for 60 minutes was efficient for conversion of the polyhydroxyimides but was insufficient for the corresponding polyacetylimides.

Gas transport measurements conducted on these isomeric polymer membranes confirmed the expected dramatic increases in permeabilities for all of these materials upon thermal rearrangement. Unlike traditional linear polymer membranes, the TR precursors had similar gas permeabilities between *meta* and *para* oriented isomers due to a possible dominating effect of the polar functional groups over the *meta/para* isomer effect. The TR polymers derived from *meta/para* oriented isomeric TR precursors also had similar gas separation properties, especially for CO_2/CH_4 separation, and it is hypothesized that this is due to a lack of intersegmental mobility distinction between the two isomeric TR polymers. Finally, the TR polymers derived from *meta/para* isomeric precursors had similar gas separation properties, but the TR polymers derived from the same backbone structure but with different *ortho*-functional groups had different gas separation properties.

Acknowledgments

The authors gratefully acknowledge the financial support of Air Products and Chemicals, Inc. and the National Science Foundation (Award Numbers DMR-1126564 and IIP-1237857).

3.6. Reference

(1) Baker, R. W.; Lokhandwala, K. Natural Gas Processing with Membranes: An Overview. *Ind. Eng. Chem. Res.* **2008**, *47*, 2109–2121.

(2) Sanders, D. F.; Smith, Z. P.; Guo, R.; Robeson, L. M.; McGrath, J. E.; Paul, D. R.; Freeman, B. D. Energy-Efficient Polymeric Gas Separation Membranes for a Sustainable Future: A Review. *Polymer.* **2013**, *54*, 4729–4761.

(3) Baker, R. W. Future Directions of Membrane Gas Separation Technology. *Ind. Eng. Chem. Res.* **2002**, *41*, 1393–1411.

(4) Freeman, B. D.; Pinnau, I.; Park, M. Polymeric Materials for Gas Separations. In *Polymer Membranes for Gas and Vapor Separation*; ACS Symposium Series 733; American Chemical Society: Washington, DC, **1999**; pp. 1–27.

(5) Yampolskii, Y. Polymeric Gas Separation Membranes. *Macromolecules* **2012**, *45*, 3298–3311.

(6) Stern, S. A. Polymers for Gas Separations: The next Decade. *J. Memb. Sci.* **1994**, *94*, 1–64.

(7) Wind, J. D.; Sirard, S. M.; Paul, D. R.; Green, P. F.; Johnston, K. P.; Koros, W. J. Carbon Dioxide-Induced Plasticization of Polyimide Membranes: Pseudo-Equilibrium Relationships of Diffusion, Sorption, and Swelling. *Macromolecules* **2003**, *36*, 6433–6441.

(8) Kanehashi, S.; Nakagawa, T.; Nagai, K.; Duthie, X.; Kentish, S.; Stevens, G. Effects of Carbon Dioxide-Induced Plasticization on the Gas Transport Properties of Glassy Polyimide Membranes. *J. Memb. Sci.* **2007**, *298*, 147–155.

(9) Park, H. B.; Jung, C. H.; Lee, Y. M.; Hill, A. J.; Pas, S. J.; Mudie, S. T.; Van Wagner, E.; Freeman, B. D.; Cookson, D. J. Polymers with Cavities Tuned for Fast Selective Transport of Small Molecules and Ions. *Science* **2007**, *318*, 254–258.

(10) Hodgkin, J. H.; Liu, M. S.; Dao, B. N.; Mardel, J.; Hill, A. J. Reaction Mechanism and Products of the Thermal Conversion of Hydroxy-Containing Polyimides. *Eur. Polym. J.* **2011**, *47*, 394–400.

(11) Jung, C. H.; Lee, J. E.; Han, S. H.; Park, H. B.; Lee, Y. M. Highly Permeable and Selective Poly(benzoxazole-Co-Imide) Membranes for Gas Separation. *J. Memb. Sci.* **2010**, *350*, 301–309.

(12) Han, S. H.; Lee, J. E.; Lee, K.-J.; Park, H. B.; Lee, Y. M. Highly Gas Permeable and Microporous Polybenzimidazole Membrane by Thermal Rearrangement. *J. Memb. Sci.* **2010**, *357*, 143–151.

(13) Guo, R.; Sanders, D. F.; Smith, Z. P.; Freeman, B. D.; Paul, D. R.; McGrath, J. E. Synthesis and Characterization of Thermally Rearranged (TR) Polymers: Influence of Ortho-Positioned Functional Groups of Polyimide Precursors on TR Process and Gas Transport Properties. *J. Mater. Chem. A* **2013**, *1*, 262-272.

(14) Smith, Z. P.; Sanders, D. F.; Ribeiro, C. P.; Freeman, B. D.; Paul, D. R.; Mcgrath, J. E.; Swinnea, S. Gas Sorption and Characterization of Thermally Rearranged Polyimides Based on 3,3'-dihydroxy-4,4'-diamino-biphenyl (HAB) and 2,2'-bis-(3,4-dicarboxyphenyl) hexafluoropropane dianhydride (6FDA). *J. Memb. Sci.* **2012**, *415-416*, 558-567.

(15) Guo, R.; Sanders, D. F.; Smith, Z. P.; Freeman, B. D.; Paul, D. R.; McGrath, J. E. Synthesis and Characterization of Thermally Rearranged (TR) Polymers: Influence of Ortho-Positioned Functional Groups of Polyimide Precursors on TR Process and Gas Transport Properties. *J. Mater. Chem. A* **2013**, *1*, 262–272.

(16) Aitken, C. L.; Koros, W. J.; Paul, D. R. Effect of Structural Symmetry on Gas Transport Properties of Polysulfones. *Macromolecules* **1992**, *25*, 3424–3434.

(17) Coleman, M. R.; Koros, W. J. Isomeric Polyimides Based on Fluorinated Dianhydrides and Diamines for Gas Separation Applications. *J. Memb. Sci.* **1990**, *50*, 285–297.

(18) Comesaña-Gándara, B.; Calle, M.; Jo, H. J.; Hernández, A.; de la Campa, J. G.; de Abajo, J.; Lozano, A. E.; Lee, Y. M. Thermally Rearranged Polybenzoxazoles Membranes with Biphenyl Moieties: Monomer Isomeric Effect. *J. Memb. Sci.* **2014**, *450*, 369–379.

(19) Mi, Y.; Stern, S. A.; Trohalaki, S. Dependence of the Gas Permeability of Some Polyimide Isomers on Their Intrasegmental Mobility. *J. Memb. Sci.* **1993**, *77*, 41–48.

(20) Xu, Y.; Fei, F.; Zhao, J.; Yu, X. Preparation and Characterization of Novel Polyimides with Hydroxyl Groups. *J. Macromol. Sci. Part B* **2011**, *50*, 2090–2102.

(21) Moy, T. M.; DePorter, C. D.; McGrath, J. E. Synthesis of Soluble Polyimides and Functionalized Imide Oligomers via Solution Imidization of Aromatic Diester-Diacids and Aromatic Diamines. *Polymer.* **1993**, *34*, 819–824.

(22) Guo, R.; Mcgrath, J. E. Aromatic Polyethers, Polyetherketones, Polysulfides, and Polysulfones. In *Polymer Science:A Comprehensive Reference*; Matyjaszewski, K.; Möller, M., Eds.; Elsevier B.V., **2012**; Vol. 5, pp. 377–430.

(23) Calle, M.; Lozano, A. E.; Lee, Y. M. Formation of Thermally Rearranged (TR) Polybenzoxazoles: Effect of Synthesis Routes and Polymer Form. *Eur. Polym. J.* **2012**, *48*, 1313–1322.

(24) Park, H. B.; Han, S. H.; Jung, C. H.; Lee, Y. M.; Hill, A. J. Thermally Rearranged (TR) Polymer Membranes for CO_2 Separation. *J. Memb. Sci.* **2010**, *359*, 11–24.

(25) Sanders, D. F.; Smith, Z. P.; Ribeiro, C. P.; Guo, R.; McGrath, J. E.; Paul, D. R.; Freeman, B. D. Gas Permeability, Diffusivity, and Free Volume of Thermally Rearranged Polymers Based on 3,3′-Dihydroxy-4,4′-Diamino-

Biphenyl (HAB) and 2,2′-Bis-(3,4-Dicarboxyphenyl) Hexafluoropropane Dianhydride (6FDA). *J. Memb. Sci.* **2012**, *409-410*, 232–241.

(26) Liu, Q.; Borjigin, H.; Paul, D. R.; Riffle, J. S.; McGrath, J. E.; Freeman, B. D. Gas Transport Properties of Thermally Rearranged (TR) Isomers and Their Aromatic Polyimide Precursors. *Submitt. to Membr. Sci.* **2015**.

Chapter 4: Synthesis and Characterization of Polybenzimidazoles derived from Tetraaminodiphenylsulfone for High Temperature Gas Separation Membranes

Hailun Borjigin, [a] *Kevin Stevens,* [b] *Ran Liu,* [a] *Joshua Moon,* [b] *Andrew Shaver,* [a] *Benny D. Freeman,* [b] *J. S. Riffle*[*a] *and James E. McGrath* [a]

[a] Macromolecules and Interfaces Institute, Virginia Tech, Blacksburg, VA 24061, USA

[b] Department of Chemical Engineering, Center for Energy and Environmental Resources, The University of Texas at Austin, Austin, TX, 78758, USA

[*] To whom correspondence should be addressed, judyriffle@aol.com

Keywords: polybenzimidazole, gas separation, gas transport

From Polymer. 2015, 71, 135-142. Used with permission of Elsevier, 2015.

4.1. Abstract

A series of polybenzimidazoles containing sulfonyl groups were synthesized in Eaton's reagent for high temperature H_2/CO_2 separation membranes. The key monomer, 3,3',4,4'-tetraaminodiphenylsulfone, was prepared via a novel and economical synthetic route starting from 4,4'-dichlorodiphenylsulfone. These polybenzimidazoles with sulfonyl moieties had enhanced solubilities in dipolar aprotic solvents relative to the commercial Celazole® that is prepared from diaminobenzidine. Thermal gravimetric analysis showed that the materials were stable at elevated temperatures with 5% weight loss values of at least 485°C in either air or N_2. Glass transition temperatures of 3 polybenzimidazoles in this series were ascertained by dynamic mechanical analysis to be 438-480°C. These sulfonyl-containing polybenzimidazoles exhibited excellent gas separation properties for H_2/CO_2. Polymers from tetraaminodiphenylsulfone and either terephthalic or isophthalic acid crossed Robeson's upper bound for H_2/CO_2.

4.2. Introduction

Polymeric membranes for gas separation have become an important technology for various industrial refinery processes. In contrast to traditional separation technologies such as cryogenic distillation, pressure swing adsorption and chemical absorption, membrane separations offer several advantages, including lower energy consumption, lower capital investment and ease of operation.[1] Due to a significant growth in interest over the last ~30 years, numerous polymers have been developed as membranes for a variety of gas separations.[2] An inherent trade-off relationship between permeability and gas selectivity based on empirical observations of available gas transport data has been reported by Robeson,[3-5] and the theory behind this phenomenon was described by Freeman.[6] Most of the available gas transport data on polymeric membranes from research laboratories have been measured in the temperature range of 25-35^{o}C. However, for many industrial applications, the ideal operating temperature may vary significantly from ambient conditions. For example, a high operation temperature (150-300^{o}C) is required to improve the thermal efficiency for H_2 separation from pre-combustion syngas in the *Integrated Gasification Combustion Cycle* (IGCC) system for electricity production.[7,8] These harsh conditions eliminate most polymer membranes from consideration due to thermal instabilities that lead to degradation and loss of mechanical properties.[9]

Polybenzimidazoles (PBIs), initially developed by Marvel, are well known for their outstanding thermal stability, often exhibiting glass transition temperatures greater than 400^{o}C as well as flame retardance and chemical stability.[10,11] Due to these characteristics, they are promising candidates for gas separation membranes that can be used at high temperatures. Membranes prepared from a commercial polybenzimidazole, Celazole®, have been shown to have attractive gas transport

properties.[12,13] Celazole® (sometimes referred to as *m*-PBI in the literature)[7,12] is prepared from 3,3'-diaminobenzidine and isophthalic acid. However, polybenzimidazoles based on the 3,3'-diaminobenzidine monomer have very limited solubilities in common solvents due to their rigid rod structures and intermolecular hydrogen bonding.[15] For instance, *m*-PBI is only partially soluble in dimethylacetamide and insoluble in other common solvents, and PBIs based on 3,3'-diaminobenzidine and terephthalic acid are insoluble in common organic solvents.[11] Structural modification of polymer backbones to include flexible linkages usually increase the solubility of PBIs.[16] However, a reduction in rigidity causes a decrease in the glass transition temperature, thus compromising the high temperature properties of these glassy polymers.[17]

This work describes the synthesis and characterization of the sulfonyl-containing tetraamine monomer, 3,3'-4,4'-tetraaminodiphenylsulfone (TADPS), and of a series of PBIs containing this monomer. This tetraamine monomer was prepared via a novel synthetic route from the economical reagent 4,4'-dichlorodiphenylsulfone. Due to the sulfonyl linkage between the two diaminophenyl groups, tetraaminodiphenylsulfone has a bent structure compared to diaminobenzidine with a linear structure. We hypothesized that the kinked structure introduced by the sulfonyl linkages in the PBI backbones would reduce the chain packing efficiency and therefore enhance the gas transport properties of the PBIs. Initial investigations of pure gas transport properties are also discussed herein.

4.3. Experimental

4.3.1. Materials

4,4’-Dichlorodiphenylsulfone (DCDPS) was kindly provided by Solvay and recrystallized from toluene before use. Isopropanol, acetic acid, ammonium hydroxide solution (29%), nitric acid (69.3%) and sulfuric acid were purchased from Spectrum Chemicals and used as received. Hydrazine hydrate, palladium on carbon, sodium bicarbonate and 4,4’-oxybis(benzoic acid) were purchased from Sigma-Aldrich and used as received. Dimethylsulfoxide (DMSO), dimethylacetamide (DMAc) and *N*-methyl-2-pyrrolidone (NMP) were purchased from Fisher and used as received. Eaton’s Reagent was purchased from Alfa Aesar. Celite was purchased from EMD Chemicals. Isophthalic acid was provided by Amoco and recrystallized from methanol before use. Terephthalic acid was provided by Eastman and recrystallized from methanol before use.

4.3.2. Synthesis of the 3,3’,4,4’-tetraaminodiphenylsulfone monomer (TADPS)

4.3.2.1. Synthesis of 3,3’-dinitro-4,4’-dichlorodiphenylsulfone (DNDCDPS)

Excess 4,4’-dichlorodiphenylsulfone (100.5 mmol, 28.75 g) and 290 mL of 96% H_2SO_4 were added to a 500-mL three-necked flask equipped with a condenser, mechanical stirrer and addition funnel. The reaction mixture was stirred at room temperature until the 4,4’-dichlorodiphenylsulfone completely dissolved. Nitric acid (69.3%) (201.0 mmol, 18.28 g) was added dropwise via the addition funnel. Upon completion of addition, the solution was stirred for 6 h at room temperature. The final heterogeneous solution containing a pale yellow precipitant was poured into 2 L of deionized water, and $NaHCO_3$ was added until the solution reached a pH of 7. Then the crude product was filtered and dried in *vacuo* at 100°C. The product was recrystallized

from acetic acid to obtain a 92% yield. ^{1}H NMR (d_6-DMSO): δ8.70 (d, 2H), δ 8.32 (d, 2H), δ 8.29 (dd, 2H), δ 8.05 (d, 2H).

4.3.2.2. Synthesis of 3,3'-dinitro-4,4'-diamino diphenyl sulfone (DNDADPS)

3,3'-Dinitro-4,4'-dichlorodiphenylsulfone (125.1 mmol, 21.80 g), NH_4OH (312.7 mmol, 43.6 mL) and 300 mL of DMSO were added into a 500-mL pressure reactor equipped with heating coils and an overhead stirrer. The reactor was pressurized to 60 psi with nitrogen then heated to 140°C. After 16 h, the reaction mixture was cooled and precipitated in deionized water. The yellow precipitant was filtered, washed with copious amounts of water and dried in *vacuo* at 80°C. A 90% yield of product was obtained. ^{1}H NMR (d_6-DMSO): δ8.42 (d, 2H), δ 8.04 (bs, 4H), δ 7.75 (dd, 2H), δ 7.10 (d, 2H).

4.3.2.3. Synthesis of 3,3',4,4'-tetraaminodiphenylsulfone

3,3'-Dinitro-4,4'-diaminodiphenylsulfone (30.9 mmol, 10.46 g), 1.05 g Pd/C and 700 mL of isopropanol were added to a 1000-mL three-necked flask equipped with a condenser, mechanical stirrer and addition funnel. The reaction mixture was heated in a thermocouple-regulated oil bath set at 100°C and stirred. Hydrazine hydrate (10.2 mL, 216.4 mmol) was added dropwise through the addition funnel. After complete addition, the solution was stirred and refluxed for 12 h in the 100°C oil bath. The reaction mixture was hot-filtered through Celite. The product started to crystallize from the filtrate upon cooling. The light grey lustrous crystals were filtered and washed with water. The monomer product was dried in *vacuo* at 100°C overnight to afford a 62% yield. Melting point: 176°C.

4.3.3. Synthesis of tetraaminodiphenylsulfone-isophthalic acid polybenzimidazole (TADPS-IPA)

The TADPS-IPA polymer was synthesized by direct polycondensation of the tetraamine and dicarboxylic acid in Eaton's reagent (PPMA) which served as both a condensing agent and solvent. This polymerization procedure was modified from previous literature.[18] TADPS (11.6 mmol, 3.2200 g), IPA (11.6 mmol, 1.9220 g) and Eaton's reagent (22 mL) were added to a 100-mL three-necked flask equipped with a mechanical stirrer, nitrogen inlet, and a condenser. A stirred, thermocouple-regulated oil bath was used to heat the reaction to 145°C. After refluxing for 24 h, the hot viscous solution was poured into 1 L of a stirring saturated $NaHCO_3$ solution to precipitate a highly fibrous solid. The solid was filtered again on an aspirator and then boiled in 500 mL of deionized water for 2 h (repeated 4 times with new DI water each time) to remove any residual salts. The solid polymer was finally dried at 150°C in *vacuo* for 24 h. Yield was 95%.

4.3.4. Synthesis of tetraaminodiphenylsulfone-terephthalic acid polybenzimidazole (TADPS-TPA) and tetraaminodiphenylsulfone-oxy bis(benzoic acid) polybenzimidazole (TADPS-OBA)

The TADPS-TPA and TADPS-OBA polymers were synthesized in the exact manner as the TADPS-IPA polymer, except TPA (11.6 mmol, 3.2200 g) or OBA (11.6 mmol, 2.9854 g) were used instead of IPA. Yields were 96 and 95% respectively.

4.3.5. Structural Characterization

^{1}H NMR analysis was performed on a Varian Inova spectrometer operating at 400 MHz. All spectra were obtained from 15% (w/v) 1-mL solutions in DMSO-d_6.

Size exclusion chromatography (SEC) was conducted on the TADPS-IPA, TADPS-TPA and TADPS-OBA polybenzimidazoles to measure molecular weight

distributions. The solvent was DMAc that was distilled from CaH_2 and that contained dry LiCl (0.1 M). The column set consisted of 3 Agilent PLgel 10-μm Mixed B-LS columns 300x7.5 mm (polystyrene/divinylbenzene) connected in series with a guard column having the same stationary phase. The column set was maintained at 50 °C. An isocratic pump (Agilent 1260 infinity, Agilent Technologies) with an online degasser (Agilent 1260), autosampler and column oven was used for mobile phase delivery and sample injection. A system of multiple detectors connected in series was used for the analyses. A multi-angle laser light scattering (MALLS) detector (DAWN-HELEOS II, Wyatt Technology Corp.), operating at a wavelength of 658 nm, a viscometer detector (Viscostar, Wyatt Technology Corp.), and a refractive index detector operating at a wavelength of 658 nm (Optilab T-rEX, Wyatt Technology Corp.) provided online results. The system was corrected for interdetector delay and band broadening. Data acquisition and analysis were conducted using Astra 6 software from Wyatt Technology Corp. Validation of the system was performed by monitoring the molar mass of a known molecular weight polystyrene sample by light scattering. The accepted variance of the 21,000 g/mole polystyrene standard was defined as 2 standard deviations (11.5% for M_n and 9% for M_w) derived from a set of 34 runs.

4.3.6. Membrane preparation

For each polymer, 0.5 g of polymer was weighed into a scintillation vial, 10 mL of DMAc was added, and the mixture was stirred until a homogeneous solution was obtained. The solution was syringe-filtered through a 0.45 μm PTFE filter into a new vial. Each vial was sonicated for 30 min to remove dissolved gases. A 10x10 cm^2 glass plate was cleaned with acetone and dried before use. The solution was cast on the glass plate on a leveled casting surface in the vacuum oven and allowed to dry under full

vacuum at room temperature overnight. The temperature was then increased to 60°C under full vacuum for 4 h. The temperature was increased to 100°C for another 1 h under full vacuum. The film was removed from the glass plate with the aid of water and treated in boiling water for 4 h to remove remaining solvent. The following day the film was dried in the oven at 140°C under full vacuum.

4.3.7. X-ray diffraction

Powder X-ray diffraction (PXRD) was performed using a Scintag X-1 theta-theta diffractometer, with a Cu X-ray source and a Si(Li) solid state detector tuned to Cu Kα radiation of 1.54 Å wavelength to characterize the amorphous nature of the PBIs in this study.

4.3.8. Solubility

Solubilities of the PBIs were determined by stirring 0.5 grams of polymer powder in 10 mL of solvent for 24 h at room temperature or 100 ^{o}C. The solvents were NMP, DMAc, DMSO and THF.

4.3.9. Water uptake

The membrane water uptake was determined by the weight difference between dry and wet membranes. Membranes (~0.2 grams) that had been vacuum-dried at 120 ^{o}C for 24 h were weighed (W_{dry}) and then immersed in deionized water at room temperature for 24 h. The wet membrane was blotted dry and immediately weighed again (W_{wet}). The water uptake of the membranes was calculated according to Equation 1. The water uptake measurements of the membranes were carried out in triplicate

independently with different pieces of membranes to check the reproducibility of the results.

$$(1)\ \text{Water Uptake}\ (\%) = \frac{W_{wet} - W_{dry}}{W_{wet}} \times 100$$

4.3.10. Thermal analysis

The TADPS-based PBIs were characterized by thermogravimetric analysis (TGA) and dynamic mechanical analysis (DMA). TGA scans were conducted using a TA Instruments Q5000 thermogravimetric analyzer under nitrogen and air atmospheres. A heating rate of 10°C min^{-1} was employed from 25 to 700°C. Dynamic mechanical analysis was performed using a TA Instruments Q800 configured in tensile geometry. Storage modulus (E') and tan δ were measured in a temperature sweep mode (1 Hz, 2 °C min^{-1}) at temperatures ranging from 150 to 550 °C under a N_2 atmosphere.

4.3.11. Gas transport

Pure gas permeabilities of H_2, He, O_2 and CO_2 (UHP grade, Airgas, Radnor, Pennsylvania, USA) through the TADPS-based PBIs were measured via a constant-volume, variable-pressure method.[19] The upstream pressure was measured by a Honeywell Super TJE transducer (Honeywell Sensotec, Columbus, Ohio, USA) with a 1500 psig range. The downstream pressure was maintained under vacuum and measured by an MKS Baratron 626B (MKS Instruments, Andover, Massachusetts, USA). Coupons of each film were masked to a metal disk with a pre-machined hole using Master Bond EP46HT-2 epoxy (Master Bond Inc., Hackensack, New Jersey, USA), and the exposed film area was measured. Prepared samples were stored in a dessicator prior to placement in the pressure cell to reduce exposure to moisture. Mounted membrane samples were placed in a 47-mm high-pressure filter holder

(Millipore, Billerica, Massachusetts, USA) and degassed at 35°C overnight. The downstream pressure rise was measured over a range of upstream pressures, and the calculated permeabilities are reported herein at 10 atm and 35°C.

4.4. Results and Discussion

4.4.1. Synthesis and Characterization of the 3,3'-4,4'-Tetraaminodiphenylsulfone Monomer (TADPS)

A synthesis procedure for the TADPS monomer has been previously reported as a four-step method starting from 4,4'-diaminodiphenylsulfone (DDS).[20] We developed a three-step synthetic route to make polymer-grade TADPS monomer starting with dichlorodiphenylsulfone (DCDPS), which is a widely used monomer for polysulfone synthesis (Figure 4.1).

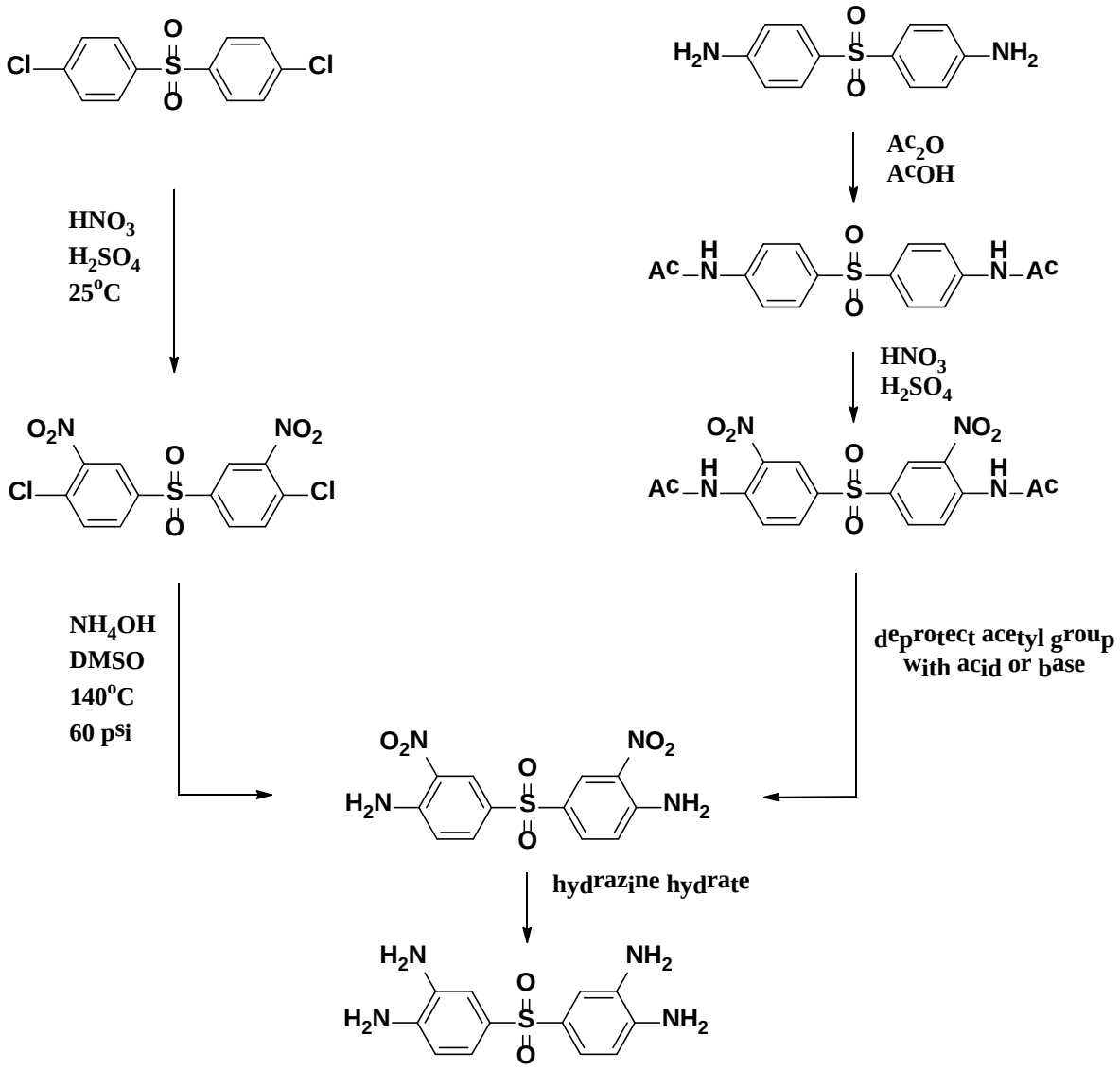

Figure 4.1. Two possible routes for TADPS synthesis

TADPS is the key monomer in these PBIs. The SO_2 linkage was introduced to provide a bend in the structure to increase solubility of the PBIs (Figure 4.2). In the previously-reported synthetic route, protection and deprotection of the amino groups from DDS were required before and after nitration.[20] As a result, synthesis of TADPS via this method consisted of more synthetic steps, which contributed to inefficiency and increased cost. In this study, nitration of DCDPS was conducted first to activate the sites with the chlorine substituents toward amination by nucleophilic substitution with

ammonium hydroxide. Finally TADPS was achieved by reducing the nitro groups to amines. This method also produced an overall yield of 57% which is higher than the reported yield (34%) of TADPS derived from DDS.[20]

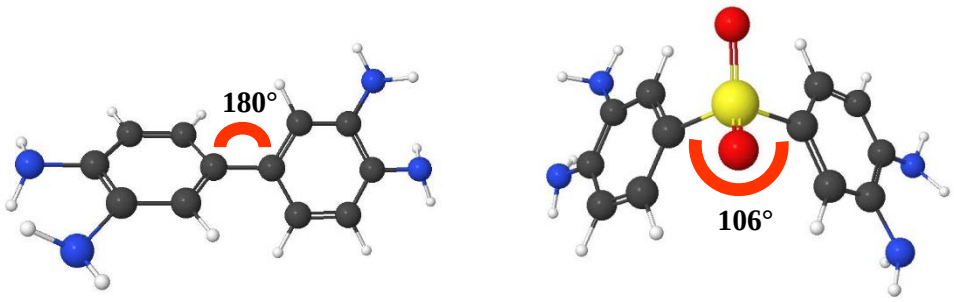

Figure 4.2. 3,3'-diaminobenzidine molecule (left) vs. TADPS (right) molecules

The ^{1}H NMR spectrum of TADPS is shown in Figure 4.3. All of the peaks integrate appropriately to confirm the molecular structure. The ^{1}H NMR spectrum was also free of "extra" peaks that would correspond to organic side products or contaminants. The melting point of the recrystallized product was in good agreement with the reported value.[20]

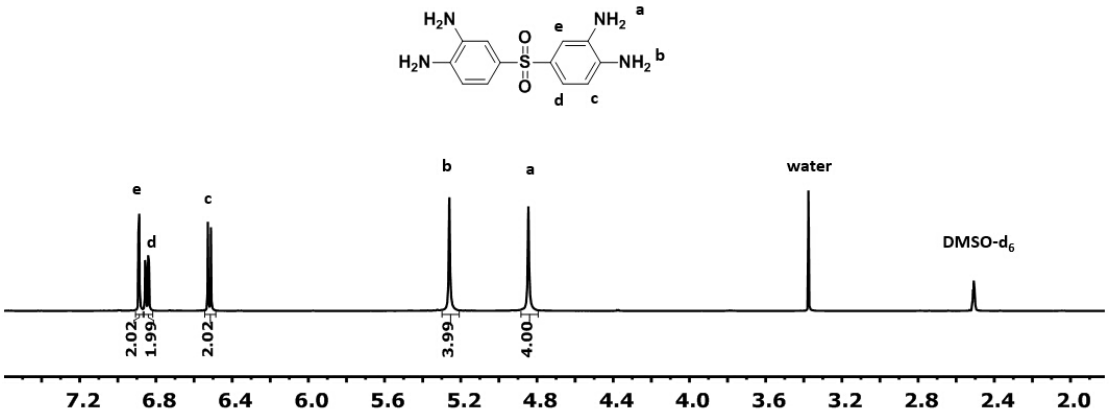

Figure 4.3. ^{1}H-NMR spectrum of the TADPS monomer

4.4.2. Synthesis and Characterization of Polybenzimidazoles derived from TADPS

The TADPS-based PBIs in this study were synthesized by direct polycondensation using Eaton's reagent as both a solvent and condensing agent (Figure 4.4).[18] PBI synthesis in acid solution was originally carried out in poly(phosphoric acid) (PPA), which is a beneficial method for preparing acid-doped PBI fuel cell membranes.[21] However, using Eaton's reagent as a reaction solvent has some obvious advantages for general PBI synthesis. First, Eaton's reagent is much less viscous than PPA and thus it is easier to handle. Secondly, the method conducted in Eaton's reagent can be accomplished at a lower temperature (135-145°C) than that required in PPA (180-200°C). Finally, Eaton's reagent is easier to remove than PPA once the polymerization is completed.[22]

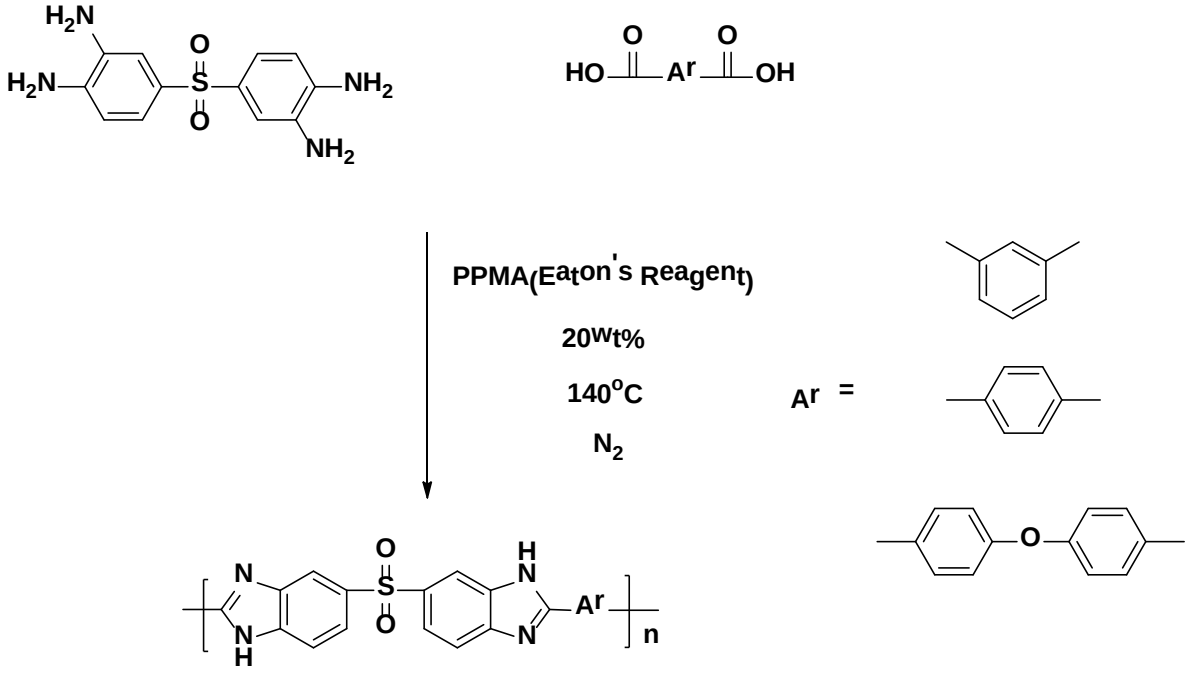

Figure 4.4. Synthesis of polybenzimidazole using Eaton's reagent as a solvent

After polymer isolation and drying, the TADPS-based PBIs were characterized by NMR spectroscopy. The ^{1}H NMR spectra shown in Figure 4.5 confirm the expected polymer structures and show that the solvent was effectively removed. The integral values were consistent with the expected chemical structures and no extraneous peaks were observed in the spectra.

The TADPS-based PBIs were sufficiently high molecular weight to form transparent and ductile films. SEC of the PBIs quantitatively substantiated the molecular weights (Figure 4.6 and Table 4.1). The chromatograms of the polymers showed a monomodal Gaussian distribution with reasonable polydispersities. It is noted that the polydispersities in Table 4.1 are somewhat lower than the value of two that is expected for polymers prepared by polycondensation. The reported molecular weights were measured by static light scattering in the SEC which directly measures weight average molecular weight. Thus, the M_w values may be more accurate than the M_n values that were calculated from the software.

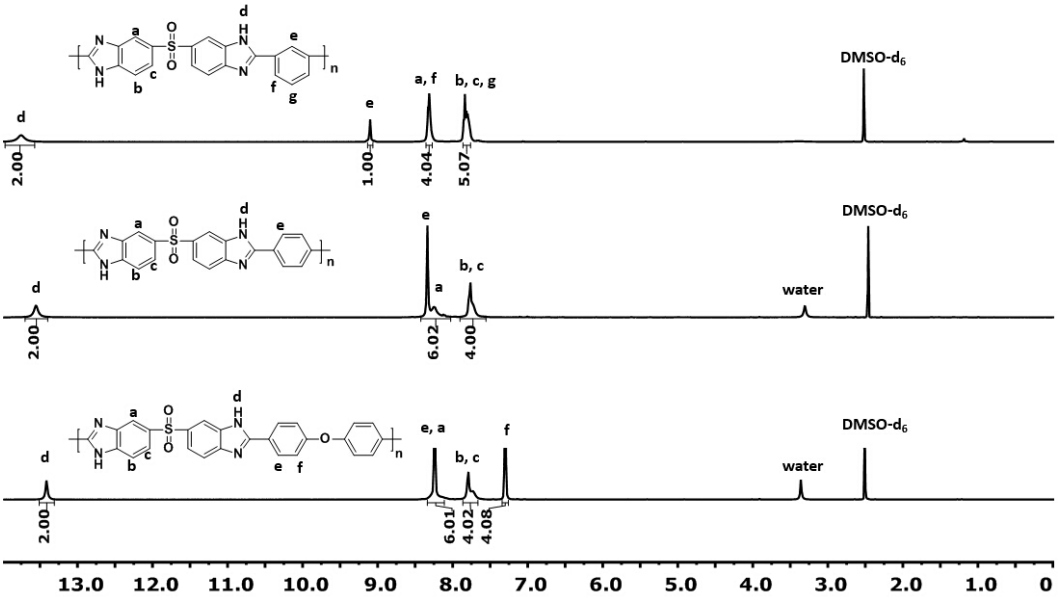

Figure 4.5. ^{1}H-NMR spectra of TADPS based polybenzimidazoles

Table 4.1. Molecular weights by SEC of TADPS based polybenzimidazoles

	Mn (kDa)	Mw (kDa)	PDI	dn/dc (mL/g)
TADPS-TPA	20	31	1.5	0.31
TADPS-IPA	18	29	1.6	0.28
TADPS-OBA	35	63	1.8	0.30

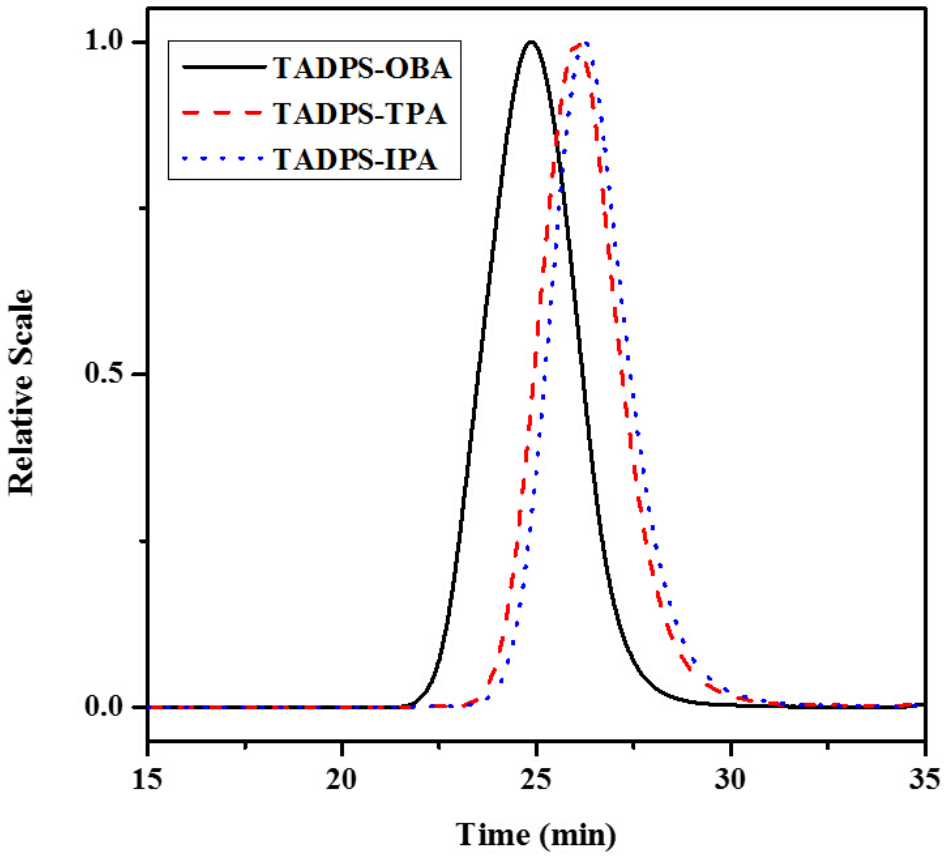

Figure 4.6. Light scattering SEC chromatograms of TADPS based polybenzimidazoles

4.4.3. X-Ray diffraction

XRD was used to probe whether any regions of crystallinity existed in these sulfonyl-containing PBI membranes. As shown in Figure 4.7, the broad amorphous halos observed for all three of the polymers confirmed that they were completely amorphous. This can be desirable for gas separation membranes since crystalline domains reduce both gas diffusivity and solubility resulting in a reduction in permeability.[23]

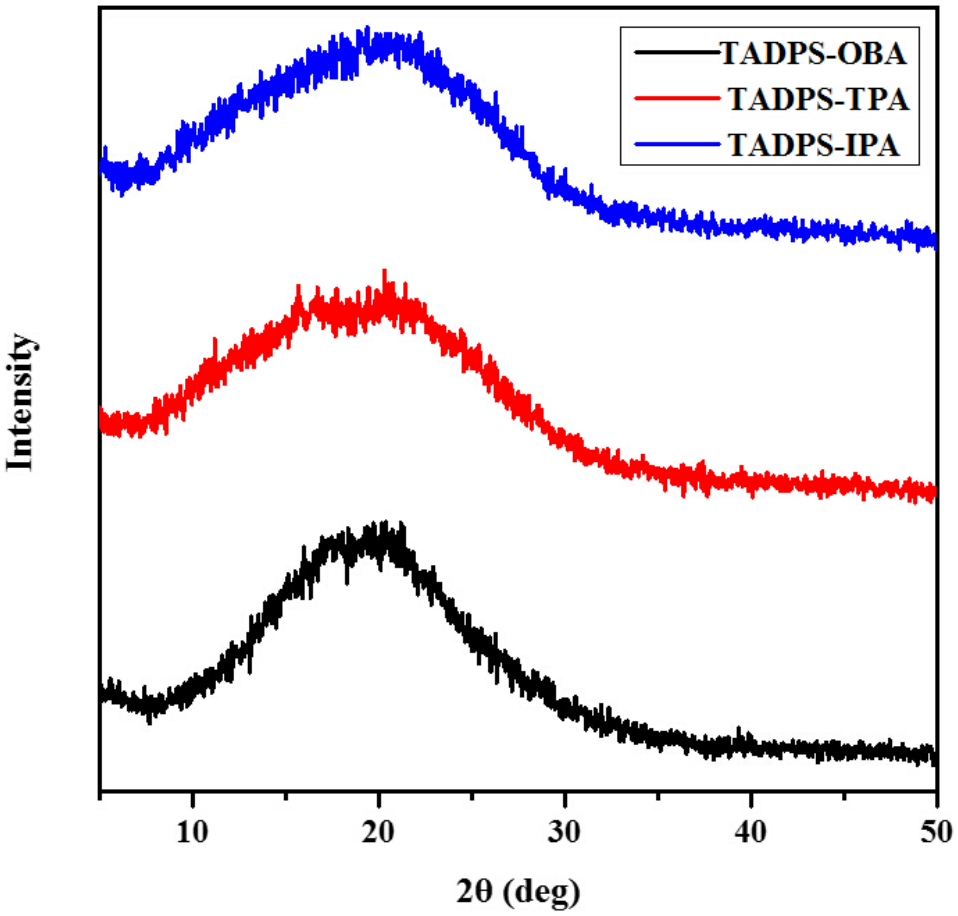

Figure 4.7. XRD of the TADPS based polybenzimidazoles

4.4.4. Solubility and water uptake

The low solubility of PBIs often limits their processibility by solvent-casting to form thin membranes. The solubilities in various solvents and water uptake of these

PBIs are listed in Table 4.2. With introduction of sulfonyl linkages into the PBI chains, their solubilities were significantly enhanced compared to poly-[2,2'-(*m*-phenylene)-5,5'-bisbenzimidazole], the commercial polybenzimidazole (Celazole®, *m*-PBI). All three of the TADPS-based PBIs were completely soluble in common dipolar aprotic solvents at a 5.0 wt% polymer concentration, which is in the range of concentrations for solution processing to form thin membranes. As expected, all of these polymers were still insoluble in common organic solvents such as THF and methanol.

PBIs, in general, have high water uptake due to the hydrophilicity of the imidazole ring.[24] All of these sulfonyl-containing PBIs exhibited high hydrophilicity, with TADPS-TPA showing a water uptake of 25 wt%.

Table 4.2. Solubility in common solvents at 25°C and water uptake of polybenzimidazoles

	NMP	**DMAc**	**DMSO**	**THF**	**Water Uptake**
TADPS-IPA	++	++	++	-	18%
TADPS-TPA	+	++	++	-	25%
TADPS-OBA	++	++	+	-	12%
m*-PBI	+	+	++	-	15%

++: Soluble at room temperature; +: Partially soluble at room temperature and fully soluble at refluxing temperature; -: Insoluble
*The data of *m*-PBI is reported from previous literature.[166,165]

4.4.5. Thermal Gravimetric Analysis

PBIs are renowned for their excellent thermal stability.[11,14] Introduction of the SO_2 linkage into the polymer chain resulted in polymers that did not show any weight loss before 400°C in either air or N_2 (Figure 4.8-9). The 5% weight loss temperatures are listed in Table 4.3. It was observed that all of the TADPS-based PBIs exhibited lower decomposition temperatures than *m*-PBI, and this was likely due to the introduction of the relatively less stable sulfonyl groups. Overall, the high thermal stabilities of all three TADPS-based PBIs make them potential candidates for high temperature membrane separations.

Table 4.3. Thermal properties of polybenzimidazoles

	Tg	**5% weight loss in N_2**	**5% weight loss in Air**
TADPS-OBA	428 °C	485 °C	510 °C
TADPS-TPA	480 °C	499 °C	525 °C
TADPS-IPA	447 °C	503 °C	532 °C
***m*-PBI**	417 °C*	576 °C*	-

* The reported data for *m*-PBI (Celazole®) is from previous literature [26]

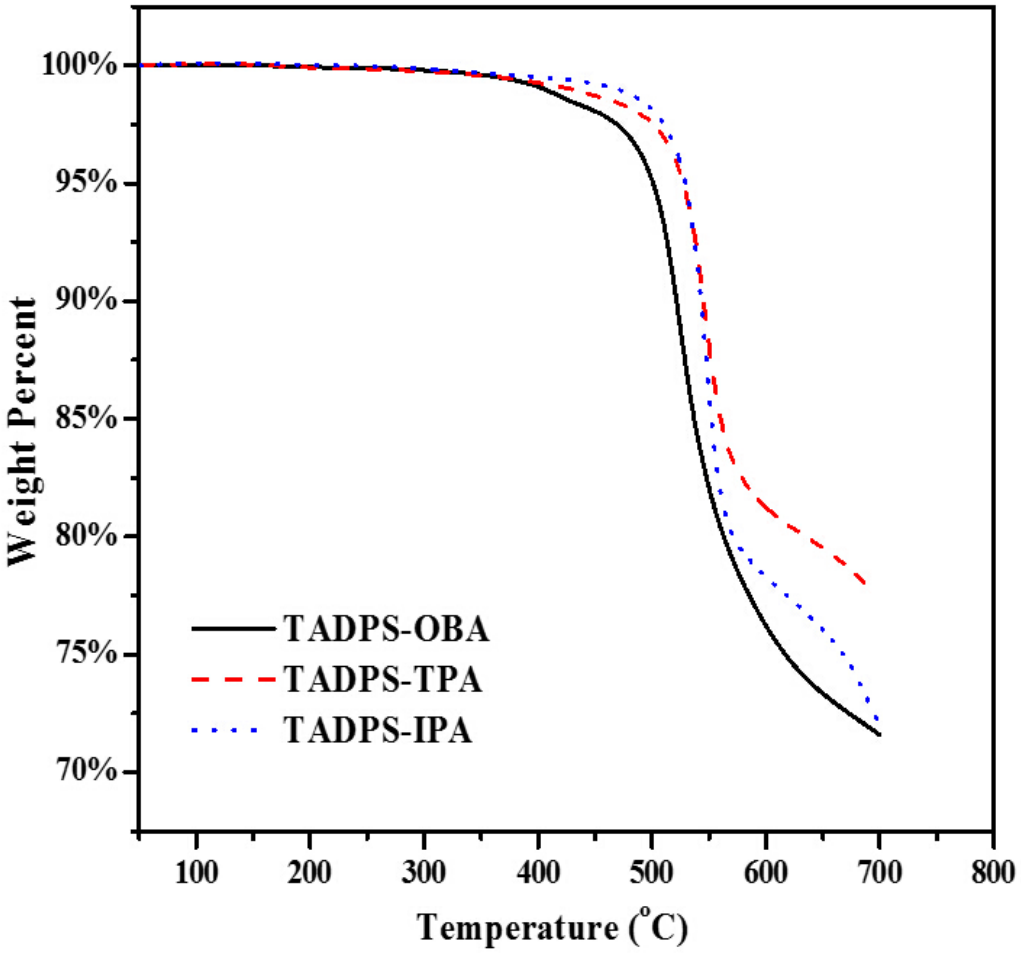

Figure 4.8. Thermal gravimetric analysis of TADPS based polybenzimidazoles under N_2

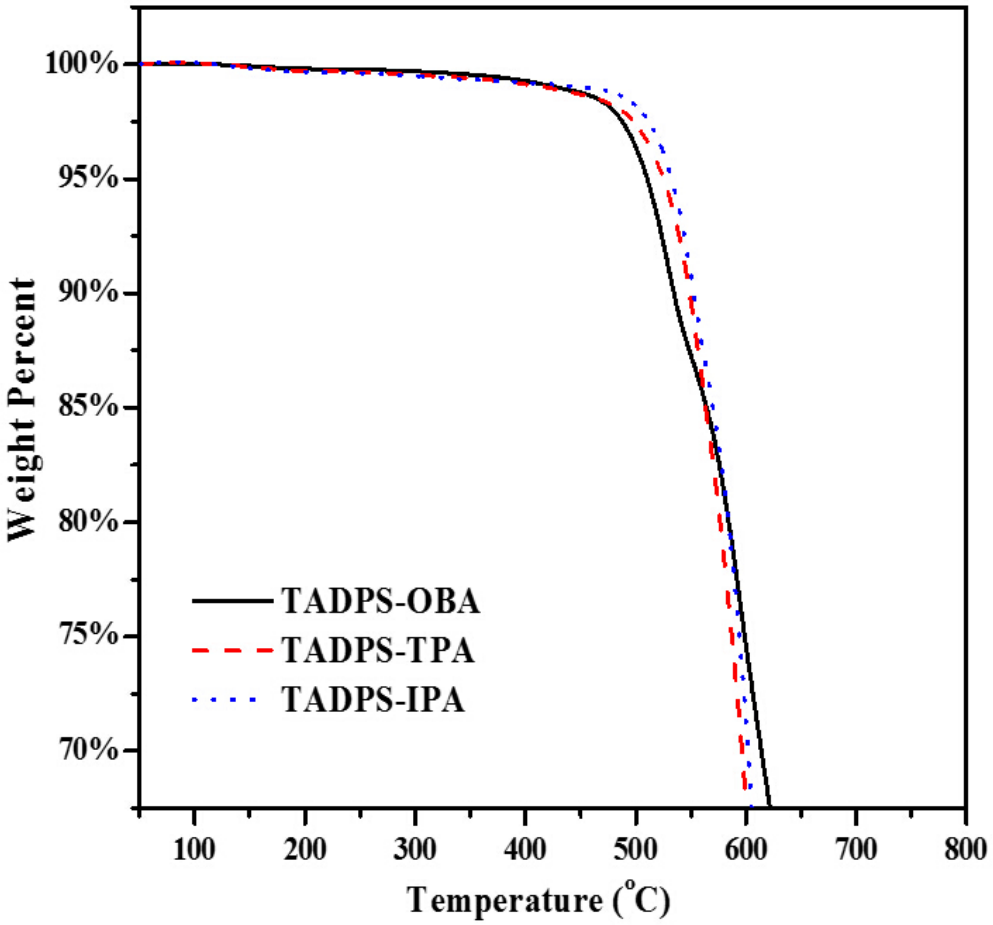

Figure 4.9. Thermal gravimetric analysis of sulfonyl-containing polybenzimidazoles in air

4.4.6. Dynamic Mechanical Analysis

DMA results for the series of TADPS-based PBIs under N_2 are shown in Figure 4.10-11. These samples were treated with boiling water for 4 hours and then dried in *vacuo* at 180°C for at least 24 hours before DMA testing. Two motional relaxation processes were observed with increasing temperature (designated β and α), consistent with results reported for other PBIs such as *m*-PBI.[26] Here, the β processes correspond to localized sub-glass transition motions of limited range, while the α process corresponds to the glass-rubber relaxation.

Storage moduli (Figure 4.11) reveal that all three of these sulfonyl-containing PBIs maintain a stable plateau up to at least 230 °C. Up to this temperature, TADPS-TPA, TADPS-IPA and TADPS-OBA maintain a storage modulus of 3.5, 2.6 and 2.1 GPa, respectively. Above that temperature, the storage moduli of these PBIs started to decrease slowly as the temperature was increased up to 430, 397 and 371°C respectively. The initial reductions in storage moduli corresponded to the *beta* relaxations of these polymers.[26] Afterwards, a large drop in storage modulus was observed for all three of the polymers which corresponds to the glass transition. The storage modulus curves indicated that the TADPS-based PBIs are high-temperature amorphous polymers that maintain their structural stiffness up to 430, 397 and 371°C respectively. For all three of these materials, at temperatures beyond 496, 481 and 456°C respectively (very close to the 5% weight loss values in N_2 from TGA), a stiffening occurs that is likely associated with degradation by *in-situ* crosslinking.

In comparison with *m*-PBI, the three TADPS-based PBIs had higher glass transition temperatures, which is likely due to the enhanced rigidity imparted by the double bond feature of the C-S linkage.[27] Similar glass transition temperature enhancements in polymers have been observed with comparisons between poly(arylene ether) and poly(arylene ether sulfone).[9] The TADPS-OBA PBI had a lower glass transition temperature than the other two polymers. This can be attributed to the flexible ether linkages in the TADPS-OBA PBI that reduces the rigidity of the polymer chain.

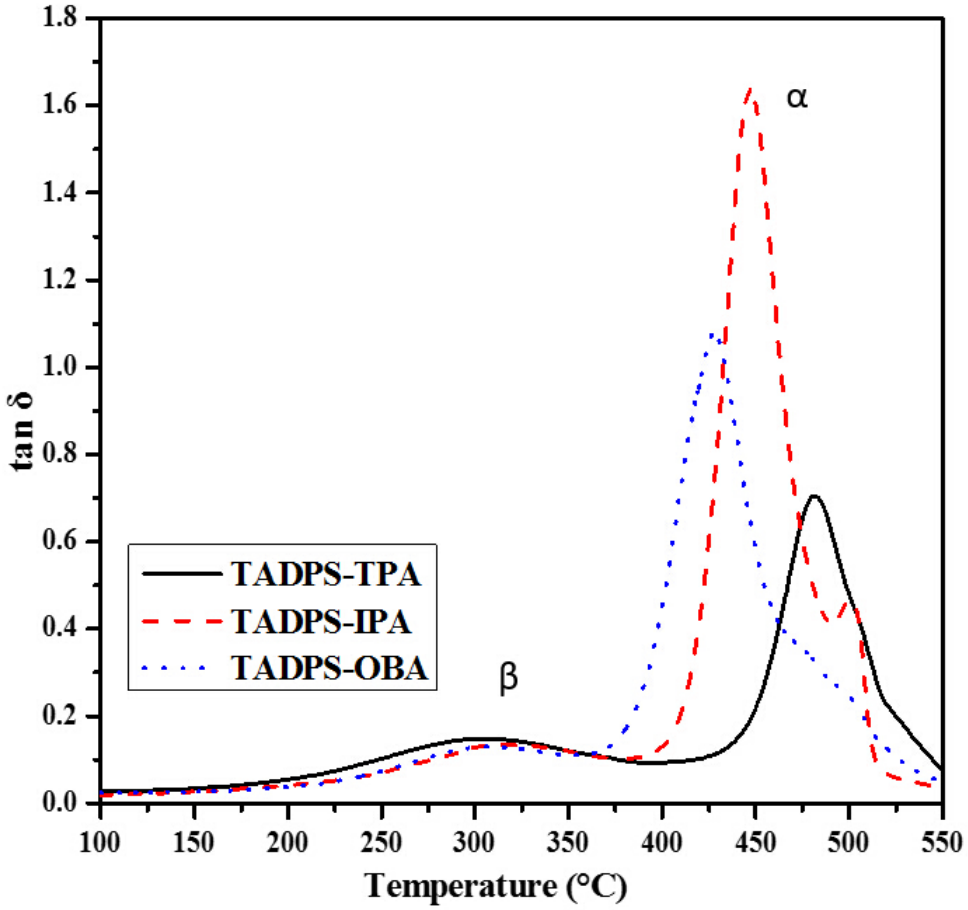

Figure 4.10. Dynamic mechanical analysis (tan δ vs temperature) of TADPS based polybenzimidazoles under N_2

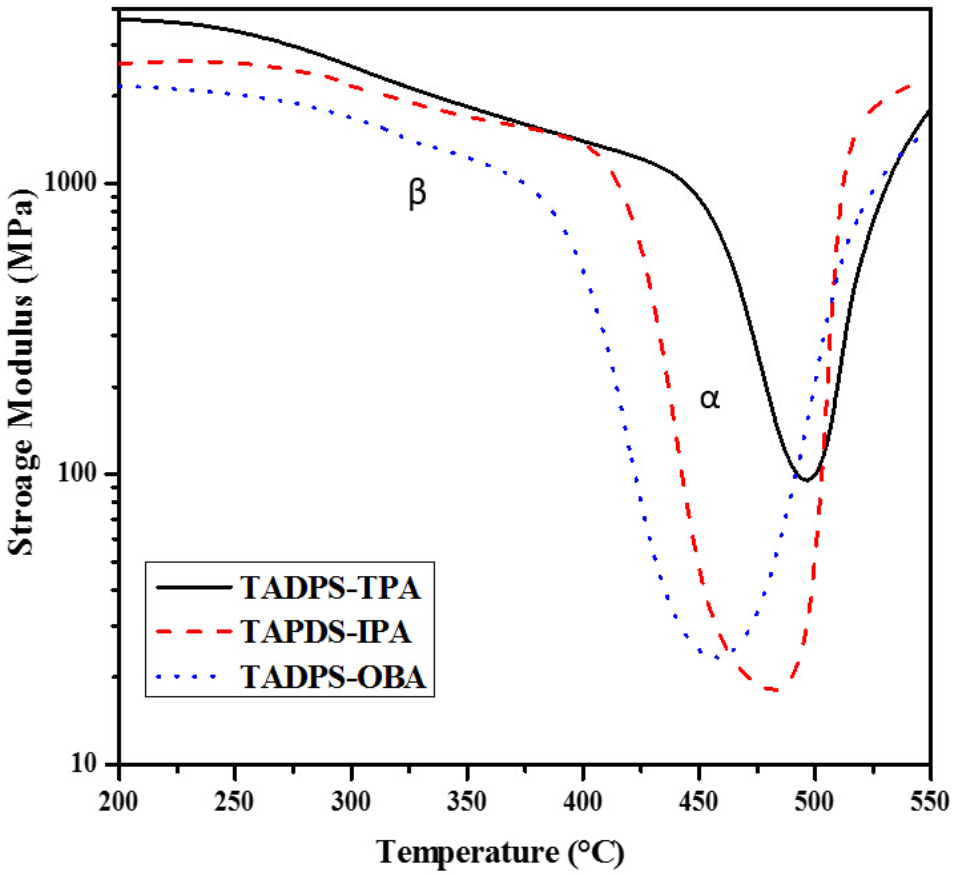

Figure 4.11. Dynamic mechanical analysis (storage modulus vs temperature) of TADPS based polybenzimidazoles under N_2

4.4.7. Gas transport Properties

Gas permeation properties of four gases (H_2, He, O_2 and CO_2) through the three sulfonyl-containing PBIs were measured at 35°C by single gas permeation experiments. Tables 4.4-5 show the permeabilities and ideal selectivities of these materials. The permeability coefficients for TADPS-OBA were higher than those of TADPS-IPA and TADPS-TPA and increased from TADPS-IPA to TADPS-TPA to TADPS-OBA. For example, permeability of CO_2 was 0.11 Barrer for TADPS-IPA, 0.28 Barrer for TADPS-IPA, and 0.56 Barrer for TADPS-OBA. The ether linkages in TADPS-OBA introduce additional kinks in the polymer backbone that disrupt chain packing, leading

to higher gas permeability coefficients relative to those for the TADPS-TPA and TADPS-IPA polymers. This same phenomenon has also been observed for aromatic polyimides.[28,29] Permeability measurements of slower gases (N_2, CH_4) were attempted, but the estimated permeabilities were below the detection limit of the instrument. Further work with thinner films will be necessary to measure accurate permeabilities of these species at 35°C and will be pursued as part of a future study.

Table 4.4. Ideal gas permeabilities for TADPS based polybenzimidazoles tested at 35°C and 10 atm.

Samples	Pure Gas Permeabilities (Barrer)			
	H_2	He	O_2	CO_2
TADPS-OBA	5.71	6.65	0.17	0.56
TADPS-TPA	5.45	6.67	0.08	0.28
TADPS-IPA	3.61	5.10	0.05	0.11

The TADPS-IPA and TADPS-TPA PBIs are *meta*- and *para*-linked isomers. Generally, *para*-linked linear aromatic polymers pack less efficiently and have more segmental mobility than *meta*-oriented aromatic polymers.[30] Thus, higher fractional free volumes and higher permeabilities for *para*-oriented aromatic polymers are often observed.[31,32] TADPS-based PBIs follow this meta/para isomer effect.[30,31] Furthermore, whereas the permeabilities increase from TADPS-IPA to TADPS-TPA to TADPS-OBA, the selectivities decrease as expected. For TADPS-OBA, the H_2/CO_2 selectivity was 10.1, which increased to 19.5 for TADPS-TPA and 32.2 for TADPS-IPA. A high H_2/CO_2 selectivity coupled with a H_2 permeability only moderately lower than those of TADPS-TPA and TADPS-OBA causes TADPS-IPA to cross both the

prior H_2/CO_2 upper bound (initially reported in 1994)[5] and the present upper bound (revised in 2008).[4]

Table 4.5. Ideal gas selectivities for TADPS based polybenzimidazoles tested at 35°C and 10 atm.

Samples	Ideal Gas Selectivity				
	He/H_2	H_2/O_2	He/O_2	H_2/CO_2	CO_2/O_2
TADPS-OBA	1.16	32.7	38.1	10.1	3.23
TADPS-TPA	1.22	64.5	78.9	19.5	3.30
TADPS-IPA	1.41	66.8	94.3	32.2	2.08

As discussed previously, H_2/CO_2 separation was the focus for these PBIs. In Figure 4.12, the TADPS-based PBIs are plotted with the H_2/CO_2 upper bound to compare with *m*-PBI and other PBI derivatives reported by the Benicewicz group at near-ambient temperature (30-43°C).[33] By introduction of fluorinated bulky linkages from the diacid monomers into the PBI backbone, the PBI derivatives had much higher H_2 permeabilities than *m*-PBI.[33] However, the H_2/CO_2 selectivities of these PBI derivatives were substantially lower than the *m*-PBI. As a result, the PBI derivatives still fell below the prior upper bound. Adding sulfonyl rather than fluorinated linkages in the tetraamine monomer did not significantly improve H_2 permeabilities compared with *m*-PBI. The TADPS-OBA polymer also shows a lower H_2/CO_2 selectivity, but the selectivities of TADPS-TPA and TADPS-IPA were enhanced.

The upper bounds reported by Robeson were based on experimental results of gas transport properties of existing polymers measured at ambient temperature (25-35°C). Freeman later provided the fundamental theory of the upper bound which agreed well with empirical observations.[6] Both Freeman et al.[6] and Robeson[3,34] showed that

the slope of the upper bound is related to the ratio of the penetrant diameters and is unlikely to change as the state of the art develops.[6]. As mentioned by Robeson,[4] limited data are available at the low-permeability limit of the H_2/CO_2 upper bound. A more complete structure-property study of PBIs could contribute to this region of the upper bound plot.

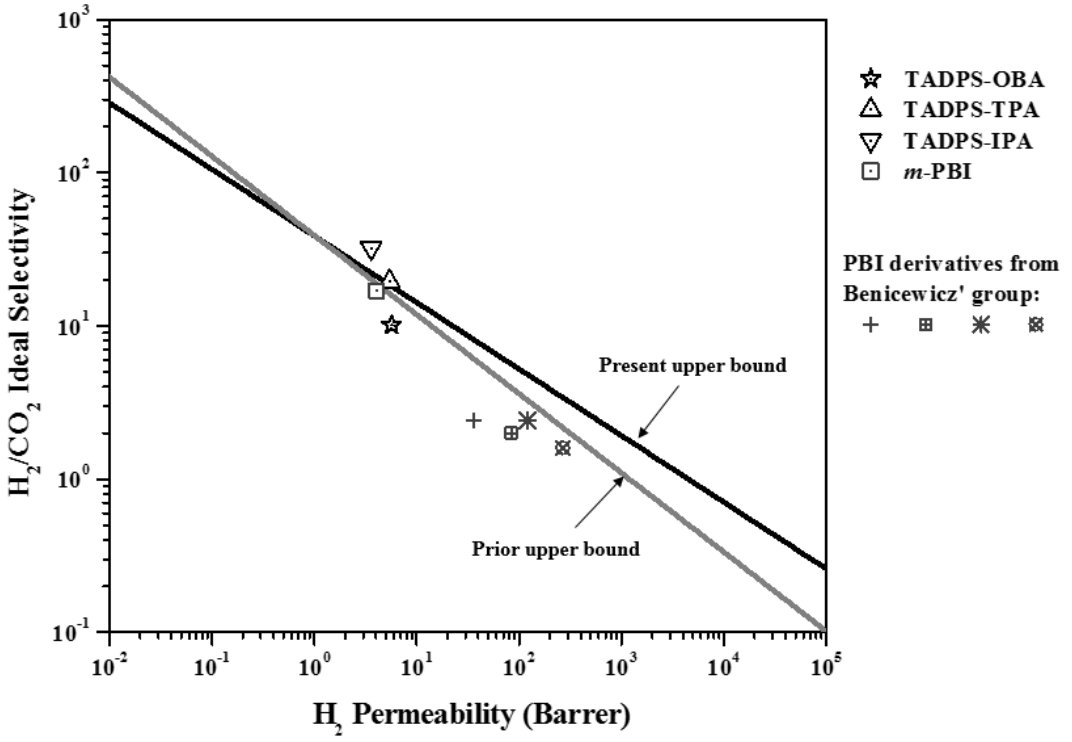

Figure 4.12. H2/CO2 upper bound plot comparison of TADPS based polybenzimidazoles with other PBIs. (The gas transport data is reported by Li. et al.29 m-PBI was measured at 43°C and other PBI derivatives were measured at different temperatures in a range of 30 -41°

It would be desirable to operate H_2/CO_2 separations at elevated temperatures for H_2 production from pre-combustion syngas.[7,12] TADPS-based PBIs are potential candidates for high temperature gas separation in part due to their thermal stabilities. Permeability obeys an Arrhenius-van't Hoff relation with temperature.[23] For H_2/CO_2 separation, Li et al. demonstrated that PBIs and their derivatives move toward the upper

right and cross the upper bound as temperature increases.[33] We expect that the TADPS-based PBIs will show a similar behavior with temperature to achieve even better gas separation properties. The study of temperature-dependent gas separation properties of TADPS-based PBIs will be the focus of a future publication.

4.5. Conclusions

3,3',4,4'-Tetraaminodiphenylsulfone was synthesized via a novel route with fewer overall steps and improved yield relative to previously-reported methods, starting from an economical commercial monomer (dichlorodiphenylsulfone). A series of high molecular weight PBIs based on the 3,3',4,4'-tetraaminodiphenylsulfone monomer were synthesized by solution polymerization in Eaton's Reagent and their properties were compared to the commercial *m*-PBI (Celazole®) and other PBI derivatives for H_2/CO_2 gas separation. The TADPS-based PBIs had increased glass transition temperatures and better organo-solubilities compared to *m*-PBI. These TADPS-based PBIs were fabricated into films by solution casting for gas transport measurements at 35°C. These TADPS-based PBIs exhibited good gas separation properties for H_2/CO_2 separation. TADPS-IPA and TADPS-TPA demonstrated a significant enhancement on the upper bound graph compared with *m*-PBI, and TADPS-IPA crossed both the prior and present upper bounds. Based on their attractive H_2/CO_2 transport properties, TADPS-based PBIs are promising candidates for further study.

Acknowledgements

The authors gratefully acknowledge the support of the National Science Foundation under grant numbers DMR-1126564 and AIR-1237857.

4.6. Reference

(1) Stern, S. A. Polymers for Gas Separations: The next Decade. *J. Memb. Sci.* **1994**, *94*, 1–64.

(2) Baker, R. W. Future Directions of Membrane Gas Separation Technology. *Ind. Eng. Chem. Res.* **2002**, *41*, 1393–1411.

(3) Robeson, L. M. Correlation of Separation Factor versus Permeability for Polymeric Membranes. *J. Memb. Sci.* **1991**, *62*, 165–185.

(4) Robeson, L. M. The Upper Bound Revisited. *J. Memb. Sci.* **2008**, *320*, 390–400.

(5) Robeson, L. M.; Burgoyne, W. F.; Langsam, M.; Savoca, a. C.; Tien, C. F. High Performance Polymers for Membrane Separation. *Polymer.* **1994**, *35*, 4970–4978.

(6) Freeman, B. D. Basis of Permeability/Selectivity Trade-off Relations in Polymeric Gas Separation Membranes. *Macromolecules.* **1999**, 32, 375–380.

(7) Merkel, T. C.; Zhou, M.; Baker, R. W. Carbon Dioxide Capture with Membranes at an IGCC Power Plant. *J. Memb. Sci.* **2012**, *389*, 441–450.

(8) O'Brien, K. C.; Krishnan, G.; Berchtold, K. A.; Blum, S.; Callahan, R.; Johnson, W.; Roberts, D.-L.; Steele, D.; Byard, D.; Figueroa, J. Towards a Pilot-Scale Membrane System for Pre-Combustion CO_2 Separation. *Energy Procedia* **2009**, *1*, 287–294.

(9) Robeson, L. M.; Farnham, A. G.; McGrath, J. E. Synthesis and Dynamic Mechanical Characteristics of Poly(Aryl Ethers). *Appl. Polym. Symp.* **1975**, *26*, 375–385.

(10) Ueda, M.; Sato, M.; Mochizuki, A. Synthesis by Direct Reaction of Diacids and Tetramine. *Macromolecules*. **1985**, 18, 2723–2726.

(11) Vogel, H.; Marvel, C. S. Polybenzimidazoles, New Thermally Stable Polymers. *J. Polym. Sci.* **1961**, *50*, 511–539.

(12) Berchtold, K. A.; Singh, R. P.; Young, J. S.; Dudeck, K. W. Polybenzimidazole Composite Membranes for High Temperature Synthesis Gas Separations. *J. Memb. Sci.* **2012**, *415-416*, 265–270.

(13) Pesiri, D. R.; Jorgensen, B.; Dye, R. C. Thermal Optimization of Polybenzimidazole Meniscus Membranes for the Separation of Hydrogen, Methane, and Carbon Dioxide. *J. Memb. Sci.* **2003**, *218*, 11–18.

(15) Li, X.; Qian, G.; Chen, X.; Benicewicz, B. C. Synthesis and Characterization of a New Fluorine-Containing Polybenzimidazole (PBI) for Proton-Conducting Membranes in Fuel Cells. *Fuel Cells* **2013**, 13, 832–842.

(16) Kumbharkar, S. C.; Liu, Y.; Li, K. High Performance Polybenzimidazole Based Asymmetric Hollow Fibre Membranes for H_2/CO_2 Separation. *J. Memb. Sci.* **2011**, *375*, 231–240.

(17) Kumbharkar, S. C.; Karadkar, P. B.; Kharul, U. K. Enhancement of Gas Permeation Properties of Polybenzimidazoles by Systematic Structure Architecture. *J. Memb. Sci.* **2006**, *286*, 161–169.

(18) Ueda, M.; Sato, M.; Mochizuki, A. Poly(benzimidazole) Synthesis by Direct Reaction of Diacids and Tetramine. *Macromolecules* **1985**, 18, 2723–2726.

(19) Lin, H.; Freeman, B. D. Permeation and Diffusion. In *Springer-Handbook of Materials Measurement Methods*; Czichos, H.; Smith, L.; Saito, T., Eds.; Springer, **2006**; pp. 371–387.

(20) Lakshmi Narayan, T. V.; Marvel, C. S. Polybenzimidazoles. VI. Polybenzimidazoles Containing Aryl Sulfone Linkages. *J. Polym. Sci. Part A-1 Polym. Chem.* **1967**, *5*, 1113–1118.

(21) Mader, J. A.; Benicewicz, B. C. Sulfonated Polybenzimidazoles for High Temperature PEM Fuel Cells. *Macromolecules* **2010**, *43*, 6706–6715.

(22) Jouanneau, J.; Gonon, L.; Cedex, G. Synthesis of Sulfonated Polybenzimidazoles from Functionalized Monomers : Preparation of Ionic Conducting Membranes. **2007**, 40, 983–990.

(23) Ghosal, K.; Freeman, B. D. Gas Separation Using Polymer Membranes : An Overview. *Polym. Adv. Techologies* **1994**, *5*, 673–697.

(24) Brooks, N. W.; Duckett, R. A.; Rose, J.; Ward, I. M.; Clements, J. An NMR Study of Absorbed Water in Polybenzimidazole. *Polymer.* **1993**, *34*, 4038–4042.

(25) Klaehn, J. R.; Luther, T. A.; Orme, C. J.; Jones, M. G.; Wertsching, A. K.; Peterson, E. S. New Soluble N-Substituted Polybenzimidazoles by Post-Polymerization Modification. *Polym. Prepr.* **2005**, *46*, 708–709.

(26) Menczel, J. D. Thermal Measurements on Poly[2,2'-(m-Phenylene)-5,5'-Bibenzimidazole] Fibers. *J. Therm. Anal. Calorim.* **2000**, *59*, 1023–1027.

(27) Guo, R.; Mcgrath, J. E. Aromatic Polyethers, Polyetherketones, Polysulfides, and Polysulfones. In *Polymer Science:A Comprehensive Reference*; Matyjaszewski, K.; Möller, M., Eds.; Elsevier B.V., **2012**; Vol. 5, pp. 377–430.

(28) Tanaka, K.; Kita, H.; Okamoto, K. Permeability and Permselectivity of Gases in Fluorinated Polyimides. *Polymer.* **1992**, *33*, 585–592.

(29) Tanaka, K.; Masaki, O.; Toshino, H.; Kita, H.; Okamoto, K. Effect of Methyl Substituents on Permeability and Permselectivity of Gases in Polyimides

Prepared from Methyl-Substituted Phynylenediamines. *J. Polym. Sci. Part B Polym. Phys.* **1992**, *30*, 907–914.

(30) Mi, Y.; Stern, S. A.; Trohalaki, S. Dependence of the Gas Permeability of Some Polyimide Isomers on Their Intrasegmental Mobility. *J. Memb. Sci.* **1993**, *77*, 41–48.

(31) Coleman, M. R.; Koros, W. J. Isomeric Polyimides Based on Fluorinated Dianhydrides and Diamines for Gas Separation Applications. *J. Memb. Sci.* **1990**, *50*, 285–297.

(32) Borjigin, H.; Liu, Q.; Zhang, W.; Gaines, K.; Riffle, J. S.; Paul, D. R.; Freeman, B. D.; McGrath, J. E. Synthesis and Characterization of Thermally Rearranged (TR) Polybenzoxazoles: Influence of Isomeric Structure on Gas Transport Properties. *Submitted to Polymer* **2015**.

(33) Li, X.; Singh, R. P.; Dudeck, K. W.; Berchtold, K. A.; Benicewicz, B. C. Influence of Polybenzimidazole Main Chain Structure on H_2/CO_2 Separation at Elevated Temperatures. *J. Memb. Sci.* **2014**, *461*, 59–68.

(34) Robeson, L. M.; Freeman, B. D.; Paul, D. R.; Rowe, B. W. An Empirical Correlation of Gas Permeability and Permselectivity in Polymers and Its Theoretical Basis. *J. Memb. Sci.* **2009**, *341*, 178–185.

Chapter 5. Conclusion and Recommended Future Research

5.1. Conclusion for High Performance Polymers for Gas Separation Membrane Research

Results from this dissertation have defined some important structure-property relationships for high performance polymer membrane gas separations. Polyimides, TR polybenzoxazoles and polybenzimidazoles were synthesized and investigated. Relationships among meta/para isomer effect with gas transport property, polymer backbone structures with gas transport properties and the way to achieve outstanding gas separation properties were the focus of this dissertation.

Investigation of *meta/para* orientated TR procurers, polyhydroxyimides\polyacetylimides, and TR polybenzoxazoles for CO_2/CH_4 gas separation membranes revealed the relationship between the gas transport properties and the *meta/para* orientated isomers, as well as how the TR polybenzoxazole membranes were prepared. The permeability of the *para* oriented TR precursor polyhydroxyimide does show higher gas permeability coefficients than that of *meta*-linked analogs However, the differences in permeability of these TR precursor polyhydroxyimide are not as substantial as that of the traditional aromatic polyimides reported in previous literatures due to the polar groups on the TR precursor polyhydroxyimide. Interestingly, after acetylation of the polyhydroxyimides, the permeability coefficients of *para*/*meta* linked the polyacetylimide contradict from the permeability coefficients of traditional *meta/para* linked polyimides. We hypothesize that the presence of bulky groups at the *ortho*-position, in this case the acetate groups, can cause steric hindrance and inhibit the phenylene “ring flip” effect of the *para* isomer. Consequently, the acetate groups diminish the *para*/*meta* isomer effect and greater permeability coefficients of *meta* linked polyacetylimide are observed than that

of *para* linked polyacetylimide. The TR polybenzoxazoles derived from *para* oriented isomeric TR precursors had slightly higher gas permeability coefficients than the *meta* orientated analogues, and it is hypothesized that the small distinction is due to a lack of intersegmental mobility distinction between the two isomeric TR polymers. However, TR polybenzoxazoles derived from the same backbone structure but with bulky *ortho*-functional groups had significant higher gas permeability coefficients than the one derived from the same backbone structure with *ortho* hydroxyl functional groups.

Incorporation of sulfonyl linkages into polybenzimidazole backbone by using 3,3',4,4'-tetraaminodiphenylsulfone (TADPS) monomers significantly enhanced solubilities of the polymer in common organic solvents. The enhanced solubilities of these TADPS based polybenzimidazoles would increase the processibility of them. Investigation of *meta/para* orientated polybenzimidazoles for gas separation membranes reveals the relationship between the gas transport properties and the *meta/para* orientated isomeric polybenzimidazoles. TADPS-based PBIs follow the *meta/para* isomer effect on gas transport properties like other linear aromatic step-growth polymers.[147,170] These TADPS based polybenzimidazoles are good candidates for high temperature gas separation application such as H_2/CO_2 syngas separation, due to their good thermal stabilities and excellent gas separation properties. The TADPS-TPA polymer crossed the prior upper bound for H_2/CO_2 while the TADPS-IPA crossed both prior and present upper bound for H_2/CO_2 at 35°C. The excellent H_2/CO_2 gas separation properties of these polybenzimidazoles catches people's interest to find out the gas separation properties of the materials at elevated temperatures. A detailed study of temperature-dependent gas separation properties of TADPS-based PBIs will be the focus of a future publication.

5.2. Recommended Direction for Future Gas Separation Membrane Research

5.2.1. Synthesis of UV crosslink-able polybenzimidazoles for gas separations membranes

One of the intriguing approach to improve the properties of gas separation ("beat the upper bound") is to crosslink them under the glass transition temperature of the material.[173] Both Hays et al. and our group have demonstrated that UV crosslinking of aromatic polyimides enhanced the gas selectivity coefficients substantially than their linear analogues and the UV crosslinked materials crossed the upper bounds. Therefore, I propose that incorporating UV sensitive functional groups into polybenzimidazoles could be one of the directions for beating the upper bound. The UV crosslinked polybenzimidazoles could be achieved by a variety of methods, discussed below.

Incorporating carbonyl groups and benzylic methyl groups into polymer structures is one of the effective methods to UV crosslink polymers under Tg, which have been extensively applied into poly(arylene ether)s and polyimides in our group.[174] However, adding these functional groups into polybenzimidazoles has not been done in previous literatures.

Polybenzimidazoles are usually polymerized via polycondensation reactions by a tetraamino monomer and a diacid monomer, so ketone and benzylic methyl functional groups could be incorporated into either tetraamino or diacid monomers to achieve UV crosslink-able polybenzimidazoles. One if the strategies is to polymerize ketone containing tetraamine with methylated diacid. Synthesis of 3,3',4,4'-tetraaminobenzophenone monomer could successfully add ketone group in the PBI from the tetraamine monomer. The 3,3',4,4'-tetraaminobenzophenone (TABP) monomer could be synthesized using the synthetic route for 3,3',4,4'-

tetraaminodiphenlsulfone in Chapter 4. The synthetic scheme for TABP is showed in Figure 5.1. The synthesis of methylated diacid monomer is describe in Thomas et al.[175] Consequently, UV crosslink-able polybenzimidazole can be made via polycondensation in Eaton's reagent (Figure 5.2). Thus a UV crosslink-able polybenzimidazoles could be prepared and UV crosslinking would be happened after exposure of the PBI under UV radiation.

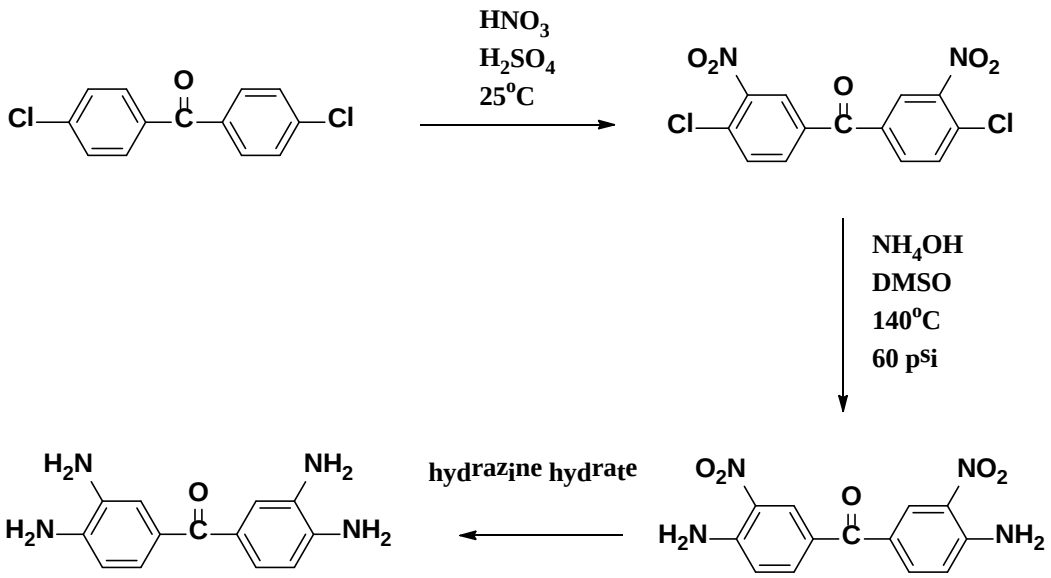

Figure 5.1. Synthesis of 3,3',4,4'-tetraaminobenzophenone

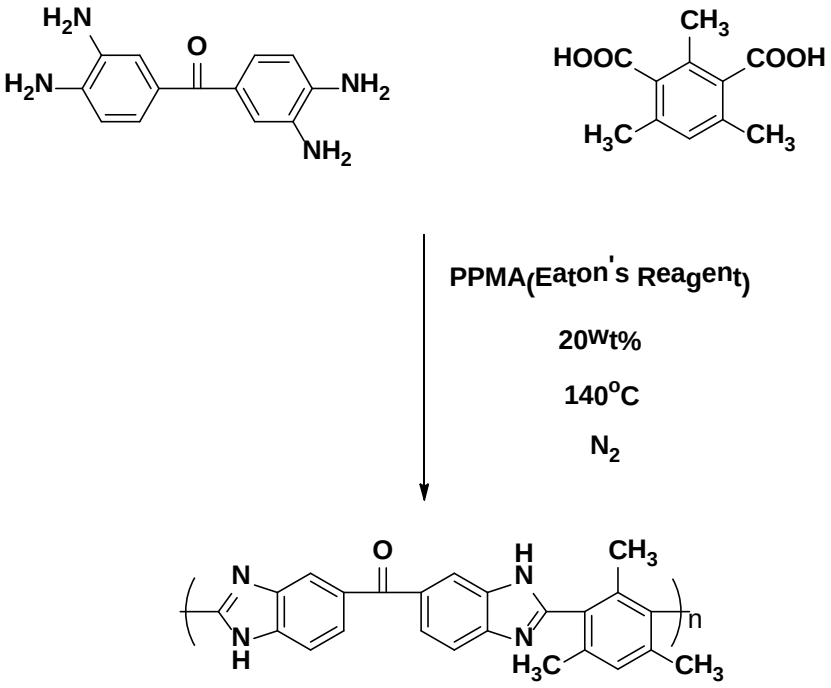

Figure 5.2. Synthesis of a UV crosslink-able polybenzimidazole

5.2.2. Post modification of polybenzimidazoles for gas separation membranes

A Patent was recently filed by Zheng et al. of Air Products and Chemicals that proposed a method for preparing polymeric membranes.[176] In this method, the polymeric materials including at least one polymer and one at least porogen are treated to degrade the porogenic part thermally, chemically, electrically and/or by radiation at a temperature smaller than the glass transition temperature of the polymer materials. This method is one of the method to surpass the upper bound introduced by Robeson in his lecture that insert labile groups in high T_g polymers and degrade below the Tg. Therefore, I propose to synthesize a polymer material that has high T_g polybenzimidazoles as the polymer backbone with labile groups (such as low molecular weight polypropylene oxide) grafted on the backbone. The polypropylene are lack of thermal stability and usually would achieve 99% volatilization upon exposure at 330°C for 30 minutes.[177] The thermal degradation temperature is lower than the Tg of PBIs(greater than 400°C), so the thermal treatment at 330°C will not achieve an

equilibrium state of the PBI to affect the free volume that generated by the PBI. However the high temperature will degrade the polypropylene oxide to create more free volumes. Therefore, a combination of polypropylene oxide and polybenzimidazole would be a good candidate for fabrications into a membranes as the Zheng et al.[176] described.

The post-modification of polybenzimidazoles to add side substituents have been demonstrated in several pervious literatures. Generally the PBIs are depronated by a strong base such NaH to form a macroinitiator for anionic polymerizations. Then monomers such as propylene oxide can be added to from grafted polybenzimidazoles. The number of repeating unit of polypropylene oxide can be controlled by adjusting the ratio of propylene oxide amount and macroinitiator amount. A synthetic scheme for synthesis of polypropylene oxide grafted PBI is shown in Figure 5.3.

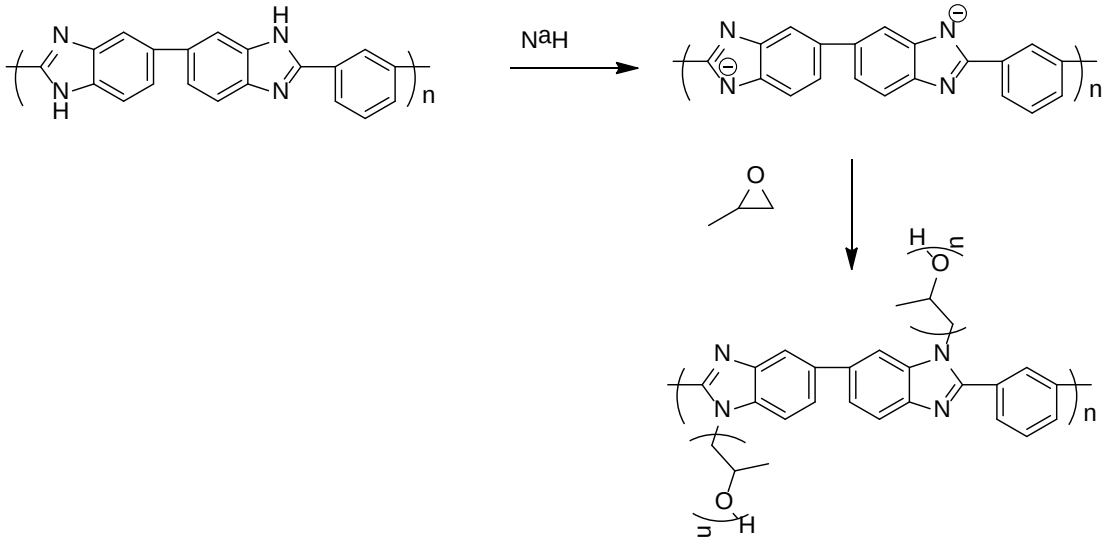

Figure 5.3. Synthesis of polypropylene oxide grafted polybenzimidazoles

The polypropylene oxide may also be grafted on PBIs using epoxy end capped polypropylene oxide. Yang et al. demonstrated a membrane fabrication method to make a crosslinked PBI membrane for fuel cell membrane application.[178] In this method, the

PBI polymer and difunctional epoxy end capped polyethylene oxide mixture solution was prepared and cast into a film. The film was treated at 120°C for 8 hours during the film casting process, and a crosslinked film was formed. This film casting process might be very useful for gas separation membrane. The crosslinked structure for PBI will increase the material rigidity therefore increase the glass transition temperature of the material (Figure 5.4). If the crosslinker is short chain polypropylene oxide or polyethylene oxide which would be labile groups, a post thermal treatment will degrade the crosslinker and achieve more free volume and increase the permeability coefficients of the polymer.

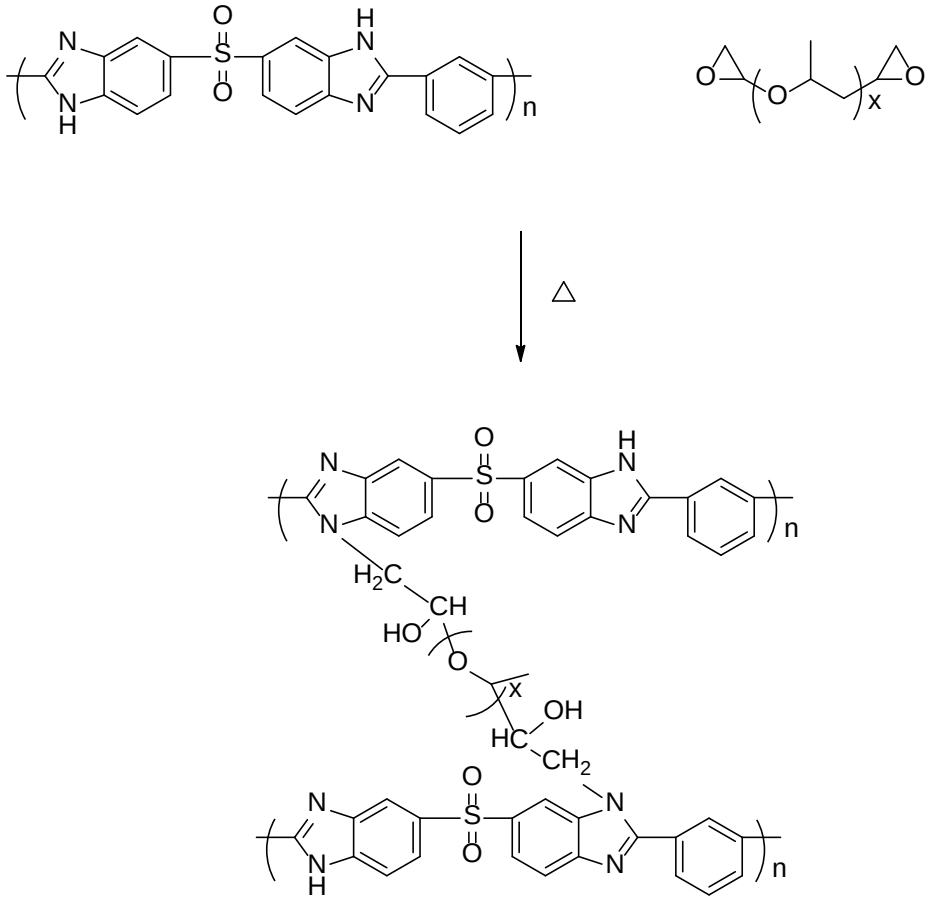

Figure 5.4. Preparation of crosslinked polybenzimidazoles using epoxy end capped polypropylene oxide

5.3. Reference

(1) Coleman, M. R.; Koros, W. J. Isomeric Polyimides Based on Fluorinated Dianhydrides and Diamines for Gas Separation Applications. *J. Memb. Sci.* **1990**, 50, 285–297.

(2) Borjigin, H.; Liu, Q.; Zhang, W.; Gaines, K.; Riffle, J. S.; Paul, D. R.; Freeman, B. D.; McGrath, J. E. Synthesis and Characterization of Thermally Rearranged (TR) Polybenzoxazoles: Influence of Isomeric Structure on Gas Transport Properties. *Submitted to Polymer* **2015**.

(3) Robeson, L. M. Lecture 3. Membrane Separation of Gases and Liquid. Lect. Slides, *Macro Lab Course* Virginia Tech **2015**, 44.

(4) Sundell, B. J.; Shaver, A. T.; Liu, Q.; Nebipasagil, A.; Pisipati, P.; Mecham, S. J.; Riffle, J. S.; Freeman, B. D.; McGrath, J. E. Synthesis, Oxidation and Crosslinking of Tetramethyl Bisphenol F (TMBPF)-Based Polymers for Oxygen/nitrogen Gas Separations. Polymer. **2014**, 55, 5623–5634.

(5) Thomas, O. D.; Soo, K. J. W. Y.; Peckham, T. J.; Kulkarni, M. P.; Holdcroft, S. A Stable Hydroxide-Conducting Polymer. **2012**, 134, 10753–10756.

(6) Zheng, S.; Robeson, L. M.; Murphy, M. K.; Quay, J. R. Polymers, Polymer Membranes and Methods of Producing the Same. US 8,926,733 B2, **2015**.

(7) Madorsicy, S. L.; Straus, S. Thermal Degradation of Polyethylene Oxide and Polypropylene Oxide. J. Polym. Sci. **1959**, 36, 183–194.

(8) Yang, J.; Xu, Y.; Liu, P.; Gao, L.; Che, Q.; He, R. Epoxides Cross-Linked Hexafluoropropylidene Polybenzimidazole Membranes for Application as High Temperature Proton Exchange Membranes. Electrochim. Acta **2015**, 160, 281–287.